論文 / 著書情報
Article / Book Information

題目(和文)	制御理論に基づいた進化的に発展するネットワークシステムの性能解析
Title(English)	Performance Analysis of Evolving Dynamical Network systems Based on Control Theory
著者(和文)	浦田賢吾
Author(English)	Kengo Urata
出典(和文)	学位:博士(工学), 学位授与機関:東京工業大学, 報告番号:甲第11419号, 授与年月日:2020年3月26日, 学位の種別:課程博士, 審査員:井村 順一,藤田 政之,三平 満司,山北 昌毅,早川 朋久
Citation(English)	Degree:Doctor (Engineering), Conferring organization: Tokyo Institute of Technology, Report number:甲第11419号, Conferred date:2020/3/26, Degree Type:Course doctor, Examiner:,,,,
学位種別(和文)	博士論文
Type(English)	Doctoral Thesis

Tokyo Institute of Technology

Doctoral Thesis

Performance Analysis of Evolving Dynamical Network Systems Based on Control Theory

---

Author:
Kengo Urata

Supervisor:
Prof. Jun-ichi Imura

Tokyo Institute of Technology
School of Engineering
Department of Systems and Control Engineering

December, 2019

Abstract

This thesis addresses performance analysis of evolving dynamical network systems, which are constructed by the connection of multiple dynamical subsystems in a step-by-step manner. First, we propose an index of localizability on the basis of the retrofit controller. The retrofit controller enables the distributed design of a local controller such that the entire network system is kept stable for any variations of the other neighboring subsystems excluding the subsystem of interest. The localizability index measures the degree of the performance invariance for the variation of neighboring subsystems excluding the subsystem of interest, rather than conventional robust performance evaluated by the worst-case performance. Subsequently, the performance improvement problem for the evolving network system is addressed; the L_2-gain of the entire network system is reduced as the number of subsystems increases. We assume that each subsystem has passivity property, which is characterized by two matrix parameters. The parameters contribute to evaluate the L_2-gain of the model set, which is defined as the L_2-gain of the worst-case system for all dynamical systems satisfying parameter-integrated passivity. We find a class of subsystems, i.e., conditions on the passivity parameters of subsystems to achieve the performance improvement of the feedback system. Moreover, we address the performance improvement problem for homogeneous network systems, where multiple identical subsystems are interconnected. In this analysis, each identical subsystem is described by a sub-network system involving multiple dynamical components, each of which includes a single integrator. Then, we find a class of the network structure to achieve the performance improvement; the disturbance sensitivity of the entire network system, evaluated by the $\mathcal{H}_\infty$-norm, is reduced as the number of the components inside each subsystem increases.

Contents

Chapter 1

Introduction

1.1 Background

Analysis and synthesis of large-scale dynamical network systems have been developed in much literature [1–12]. Throughout this thesis, we explicitly focus on the fact that actual network systems generally *evolve* as involving additional subsystems. A typical example is a power system with a large number of renewable energy (RE) resources, such as photovoltaic (PV) and wind-turbine generators. As illustrated in Fig. 1.1, let us consider an existing power system including thermal and nuclear power generators. This power system is supposed to be incrementally updated by installing some renewable energies and renewable energy farms into the existing power system. In such a situation, the respective renewable energies are not installed into the existing power system at once, but gradually installed. Under these installation, the entire power system must stably maintain a desired constant power frequency in power supply and demand. As shown in this example, practical large-scale network systems tend to vary its composition because multiple subsystems are connected to a baseline system in a step-by-step manner. Motivated by this fact, such a network system is referred to as an *evolving* network system in this thesis. We need to develop a suitable design strategy that achieves the desired specification of the entire network system at any stage of the subsystem addition, such as the stability, consensus, synchronization, sufficient control performance, and so on.

One naive approach to achieve the desired specification of the entire network system at every stage of subsystem addition is to design one feedback controller in a centralized manner. However, it is not easy to design and implement such a centralized controller due to obtaining the resultant high dimensional controller. To explicitly address this issue, there have been developed decentralized and distributed control methods for general network

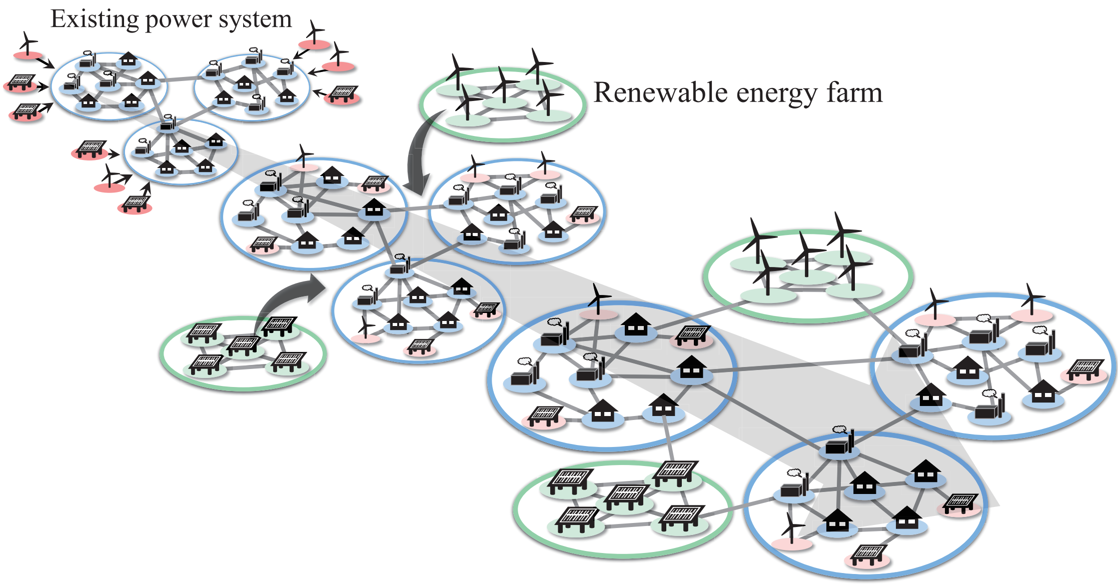

Figure 1.1: Evolving power system. Renewable energies, such as photovoltaic and wind turbine generators, are gradually installed in an existing power system composed of thermal and nuclear generators.

systems [13–16]. In the notion of the decentralized and distributed control, the entire network system is stabilized by multiple controllers, each of which utilizes only the local measurement of each subsystem and is implemented to the subsystem, rather than a single controller in a centralized manner. In most decentralized and distributed control methods [13–16], the local controller design is based on the premise that the information of the whole system model is available. From a practical viewpoint, not only the implementation of the local controller but also its design should be performed in a distributed manner [17] (this is also called *modularized* manner [18]); each local controller (subsystem) is designed independently of the others except for their brief specification. Under the modularized design as well as the decentralized and distributed control, our final goal of this thesis is to develop a design strategy of the evolving network system, in particular, the local specification for subsystems and a suitable connection rule among subsystems, to achieve the stability and the sufficient control performance. It should be emphasized here that the design strategy should achieve not only the stability and sufficient control performance of the "present" network system but also those of the "future" network system that evolves by gradual subsystem addition.

System design and control problems to guarantee the stability of the evolving network system have been studied on the basis of various concepts; see e.g., expanding construction [13], plug and play control [19], and compositional stabilization [20]. Furthermore, passivity, or more generally, dissipativity [21–23] is one of the key properties to preserve the stability of the evolving network system. As stated in the passivity theorem [24], the feedback system composed of passive subsystems is kept stable and also passive. On the basis of the passivity property, the evolving network system guarantees the stability as long as each subsystem has the passivity property and the subsystems are interconnected under a specific connection rule. In fact, there have been studied in many papers; e.g., cooperative control [25–28], synchronization problem [29], various application such as power network systems [30–32] and biological network analysis [33]. In addition to guaranteeing the entire stability, there have been some studies addressing the performance analysis of the evolving network systems; see e.g., optimal controller design in a distributed manner [34], the dissipativity-based analysis [35], and the passivity-index based analysis [36, 37]. We note that these papers provide the controller design and the dissipativity conditions for each subsystem that guarantee the robust performance of the entire network system evaluated by e.g., the *worst-case* performance. On the premise that the composition of the entire network system may be change by connection of additional subsystems, it is also important to suppress the degree of the performance deterioration in addition to the certification of the worst-case performance. Furthermore, it is desire to *improve* the entire control performance by the evolution of the network system, rather than *preserving* or *not deteriorating* the stability and the control performance.

1.2 Contribution of Thesis

With the background as stated in Section 1.1, this thesis addresses the quantitative performance analysis of the evolving network system toward the development of the design strategy. In particular, we focus on the two new types of performance specifications for the evolving network system, rather than conventional robust performance evaluated by the worst-case performance. One is *localizability* for the distributed design of the controller, which is a new performance measure and is proposed in Chapter 2. To explain the concept of the localizability, we extract the subsystem of interest from the entire network system. Then, the entire network system is described by the standard feedback system composed of the subsystem of the interest and the other subsystems excluding the subsystem of interest. Under such a situation, we consider the local controller design for the subsystem of interest. The model parameters and system structure in the other subsystems are assumed to be may change due to the redesign of local controllers in the subsystems and the new subsystem addition. In the framework of the conventional robust controller design [38], the variation of the other subsystems is described by the uncertainty with a norm constraint. Then, the robust performance, which is defined as the worst-case performance of the entire network system for all uncertainties satisfying the norm constraint, is well-utilized for the controller design. However, such a norm constraint in the uncertainty cannot be practically estimated in prior to analysis or controller design of the evolving network system. Motivated by this fact, we propose an index of the localizability, which is defined for the uncertainty feedback system *without* the norm constraint on the basis of the retrofit control method [39–41]. The retrofit control method enables the distributed design of the local controller that guarantees the stability of the entire network system for any variation in the unbounded uncertainty part, i.e., the other subsystems excluding the subsystem of interest, as long as the entire system before implementing the retrofit controller is stable. The localizability measures the degree of the invariance of the control performance for any variation belonging to the uncertainty set, rather than the worst-case performance.

Another specification for the evolving network system discussed in this thesis is the *performance improvement*; the control performance of the entire network system, evaluated by e.g., L_2-gain, is reduced as the number of subsystems increases. We first focus on the local specification, namely, *model set* for subsystems to achieve the performance improvement. In addition, the network structure in the evolving network system is confined to the standard feedback connection. Each subsystem is described by model sets, rather than detailed models such as the state-space representation or transfer function. To describe the model set, we integrate two matrix parameters into the passivity. The matrix parameters enable a more flexible description of the model set than the scalar parameters introduced in the precious works; e.g., passivity indices [36, 37] and γ-passivity [42]. We define the L_2-gain of "the model set" as the L_2-gain of the worst-case system belonging to the model set. Then, the matrix parameters characterizing the subsystems enables to evaluate the L_2-gain of the model set describing a feedback system composed of two passive subsystems. It should be noted that the detailed model is not required for the performance analysis. Then, we find conditions on the matrix parameters to achieve the performance improvement, i.e., the L_2-gain of the model set describing the feedback system is strictly reduced to that describing the disconnected subsystem. The performance improvement problem concerning general feedback system is extended to that concerning an iterative feedback system, which expresses a special class of the evolving network systems. The performance improvement problem for the feedback system is discussed in Chapter 3.

Subsequently, we address the performance improvement problem for the homogeneous network system, where multiple identical subsystems are interconnected. In this analysis, the network structure to achieve the performance improvement is focused on, rather than the local specification for subsystems discussed in Chapter 3. The analysis of the network structure to achieve the performance improvement has been studied for some papers [7–9]. However, we note that the analyses in the conventional works are valid for only consensus network systems in which each subsystem is described by a single integrator. In this thesis, each subsystem in the network system is described by a sub-network system, referred as to a cluster, which is composed of multiple distinct nodes. In addition, each node is described by a dynamical system including a single integrator. The description is general in the sense of expressing, e.g., a single integrator and a second-order oscillator in the first- and second-order consensus network systems employed in [5–12]. In this analysis, we pay attention to the network structure among clusters and that among nodes inside each cluster, referred respectively as to external and internal network structure. Through numerical and theoretical analyses, we find that the external and internal network structures tend to be sparse and dense such that the performance improvement is achieved: the $\mathcal{H}_\infty$-norm of the network system is strictly reduced as the number of subsystems increases. In particular, in the theoretical analysis, it is shown that in the limit of sufficient large number of nodes, the evolving network system achieves the minimum $\mathcal{H}_\infty$-norm, evaluated by the maximum eigenvalue associated with the external network if the internal structure is described by the complete graph.

The main contributions of this thesis are twofold. One is to propose the concept of localizability, which measures the degree of the performance invariance for any variation in the unbounded uncertainty. This is discussed in Chapter 2. Another contribution is find a solution to the local specification for subsystems and the network structure such that the performance improvement is achieved for a special class of the evolving network systems, which is discussed in Chapter 3 and 4.

1.3 Organization

The remainder of this thesis is organized as follows. In Chapter 2, we propose an index of the localizability for the distributed controller design. To define the localizability, the retrofit control system is introduced. Then, the localizability is defined as the $\mathcal{H}_\infty$-norm of the error system based on the isolation of the subsystem of interest extracted from the entire control system. In the end of this chapter, the retrofit controller placement problem for a PV-integrated power system is analyzed by using the proposed localizability. Chapter 3 addresses the performance improvement problem for feedback systems. To formulate the problem, we illustrate an example to motivate the performance improvement problem through the frequency control of power system with RE farms. First, the general problem setting is formulated. To provide a solution to the problem, we define the parameter-integrated passivity describing a model set. With the model set, a solution to the problem is provided, i.e., conditions on the parameters to achieve the performance improvement is derived. Finally, the frequency control of the power system is analyzed based on the performance improvement analysis. In Chapter 4, we analyze the disturbance sensitivity of the homogeneous network system that has two specific network structures, evaluated by $\mathcal{H}_\infty$-norm. In the analysis, we numerically and theoretically find suitable network structures to achieve the performance improvement. Finally, Chapter 5 concludes this thesis.

NOTATION: The following notation is to be used throughout this thesis.

$\mathbb{R}$	the set of all real numbers
$\mathbb{R}_+$	the set of all nonnegative real numbers
$\mathbb{C}$	the set of all complex numbers
$\mathbb{L}_2^n$	the L_2-space, i.e., the set of all square integrable functions
$\mathcal{R}^{n\times m}$	the set of all real and rational $n \times m$ transfer matrices
$\mathcal{RP}^{n\times m}$	the set of all proper transfer matrices in $\mathcal{R}^{n\times m}$
$\mathcal{RH}_\infty^{n\times m}$	the set of all stable transfer matrices in $\mathcal{RP}^{n\times m}$
$\mathrm{col}(x_i)_{i\in\mathcal{I}}$	the vector where a scalar x_i for $i \in \mathcal{I}$ are arranged in vertical
e_i	the unit vector where the only ith entry is one, while the others are zero
$\mathbf{1}_n$	the n-dimensional vector where all entries are one
I_n	the $n \times n$ identity matrix
O_n	the $n \times n$ square matrix where all entries are zero
$\{M\}_{ij}$	the (i, j) entry of a mtrix M
$M^\top$	the transpose of a matrix M
M^{-1}	the inverse of a matrix M
$M^\dagger$	a generalized inverse of M satisfying $MM^\dagger M = M$
$\mathrm{Im}\, M$	the image of a matrix M
$\mathrm{Ker}\, M$	the kernel of a matrix M
$\mathrm{M} \otimes N$	the Kronecker product of matrices M and N
$\underline{\lambda}(M)$	the minimum eigenvalue of a real symmetric matrix M
$\bar{\lambda}(M)$	the maximum eigenvalue of a real symmetric matrix M
$\bar{\sigma}(M)$	the maximum singular value of a matrix M
$\mathrm{diag}(X_1, X_2, \ldots, X_n)$	the diagonal matrix in which diagonal elements consist of complex-valued matrices $X_k, k \in \{1, 2, \ldots, n\}$, simply denoted by $\mathrm{diag}(X_k)$
$\underline{\mathbb{V}}(M)$	the eigenspace corresponding to $\underline{\lambda}(M)$

In what follows, the subscript n is often omitted for notational simplicity, e.g., employing $\mathbb{L}_2$ instead of $\mathbb{L}_2^n$. In addition, we distinguish the notation of the system description and that of its transfer matrix. For example, let us denote the system by G. Then, its transfer matrix is denoted by $G(s)$. Let us define the truncation operator as

$$(P_T f)(t) := \begin{cases} f(t) & t \in [0, T) \\ 0 & \text{otherwise.} \end{cases}$$

Then, the extended L_2-space is defined as

$$\mathbb{L}_{2e} := \{v | P_T v \in \mathbb{L}_2, \ \forall T \in [0, \infty)\}.$$

For $v \in \mathbb{L}_{2e}$ and $T \in \mathbb{R}_+$, the finite time L_2-nor is defined as

$$\|v\|_{L_2,T} := \left(\int_0^T \|v(\tau)\|^2 d\tau \right)^{\frac{1}{2}}.$$

In addition, for $v \in \mathbb{L}_2$, the L_2-norm is defined as

$$\|v\|_{L_2} := \left(\int_0^\infty \|v(\tau)\|^2 d\tau \right)^{\frac{1}{2}}.$$

For a causal and L_2-stable system Σ with the input u and output y, the L_2-gain of the system is defined as

$$\|\Sigma\|_{L_2} := \sup_{u \in \mathbb{L}_2 \setminus \{0\}} \frac{\|y\|_{L_2}}{\|u\|_{L_2}}.$$

Letting be $\Sigma(s)$ be the transfer function of Σ, we define the $\mathcal{H}_\infty$-norm of the system Σ as

$$\|\Sigma\|_\infty := \sup_{\omega \in \mathbb{R}} \bar{\sigma}(\Sigma(j\omega))$$

The matrix M is said to be irreducible if it cannot be conjugated into block triangular form by a permutation matrix P, i.e., there does not exist P that

$$PMP^\top = \begin{bmatrix} M_{11} & M_{12} \\ 0 & M_{22} \end{bmatrix},$$

where M_{11} and M_{22} are square matrices. Two linear spaces $\mathcal{X}$ and $\mathcal{Y}$ are said to be disjoint if $\mathcal{X} \cap \mathcal{Y} = \{0\}$ holds. The matrix M is said to be an M-matrix if it has nonpositive off-diagonal entries and all real parts of the eigenvalues of M are positive [43]. Then, the symbol $\mathbb{M}$ denotes the set of all M-matrices. For a matrix $M \in \mathbb{R}^{m \times n}$ and a causal operator $\mathcal{F} : \mathbb{L}_{2e} \to \mathbb{L}_{2e}$, their direct product is defined as

$$M \otimes \mathcal{F} := \begin{bmatrix} \{M\}_{11}\mathcal{F} & \cdots & \{M\}_{1n}\mathcal{F} \\ \vdots & & \vdots \\ \{M\}_{m1}\mathcal{F} & \cdots & \{M\}_{mn}\mathcal{F} \end{bmatrix}.$$

Let M be a complex-valued matrix partitioned as

$$M := \begin{bmatrix} M_{11} & M_{12} \\ M_{21} & M_{22} \end{bmatrix} \in \mathbb{C}^{(p_1+p_2)\times(q_1+q_2)}$$

and let $N_\ell \in \mathbb{C}^{q_2\times p_2}$ and $N_\mathrm{u} \in \mathbb{C}^{q_1\times p_1}$ be two other matrices. Suppose that there exist $(I_{p_2} - M_{22}N_\ell)^{-1}$ and $(I_{p_1} - M_{11}N_\mathrm{u})^{-1}$. Then, the lower linear fractional transformation (LFT) [38] with respect to N_ℓ is defined as

$$\mathcal{F}_\ell(M, N_\ell) := M_{11} + M_{12}N_\ell(I_{p_2} - M_{22}N_\ell)^{-1}M_{21}.$$

The upper LFT with respect to N_u is defined as

$$\mathcal{F}_u(M, N_\mathrm{u}) := M_{22} + M_{21}N_\mathrm{u}(I_{p_1} - M_{11}N_\mathrm{u})^{-1}M_{12}.$$

We use $\mathcal{G} = \{\mathcal{V}, \mathcal{E}\}$ to denote an unweighted undirected graph where $\mathcal{V}$ is the set of vertices and $\mathcal{E}$ is the set of edges, in other words, $(v_i, v_j) \in \mathcal{E}$ if and only if v_i and v_j are interconnected. For the undirected graph $\mathcal{G}$, we define the graph Laplacian matrix $\mathcal{L}$ where the the (v_i, v_j)th entry is equal to -1 if $(v_i, v_j) \in \mathcal{E}$ holds and is zero otherwise, and diagonal entries satisfies $\{\mathcal{L}\}_{ii} = -\sum_{j\neq i}\{\mathcal{L}\}_{ij}$. For matrices A, B, C, and D, we use the following notation of

$$\left[\begin{array}{c|c} A & B \\ \hline C & D \end{array}\right] := C(sI - A)^{-1}B + D.$$

Chapter 2

Quantitative Analysis of Controller Design Localizability

2.1 Introduction

This chapter proposes a new performance measure, which is called by *localizabity*, on the basis of the retrofit control [39–41]. The retrofit controller is a plug-in type local controller such that the stability of the resultant feedback system is preserved for any variation of neighboring subsystems other than the subsystem of interest as long as the feedback system before implementing the retrofit controller is stable. It should be noted that the design of the retrofit controller requires only a model of the subsystem of interest. Then, we define the localizability index as the $\mathcal{H}_\infty$-norm of an error system defined based on the isolation of the subsystem of interest from the entire system. The localizability index measures the degree of the performance deterioration for any variation of neighboring subsystems other than the subsystem of interest. It is shown that the localizability index requires only the model parameters of the subsystem of interest in the upper bound evaluation. Finally, we illustrate a numerical analysis of retrofit controller placement problems for power systems by using the localizability index.

This remainder of chapter is organized as follows. In Section 2.2, the retrofit control is introduced. In Section 2.3, the localizability index is defined for the feedback system to which the retrofit control is implemented. Then, it is shown that the localizability is evaluated by only the model of the subsystem of interest. On the basis of the localizability index proposed in Section 2.3, we numerically analyze the placement problem of teh retrofit controller in a PV-integrated power system.

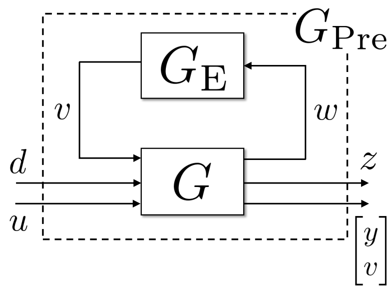

Figure 2.1: Preexisting system G_{Pre} composed of a local system G and an environment G_{E}

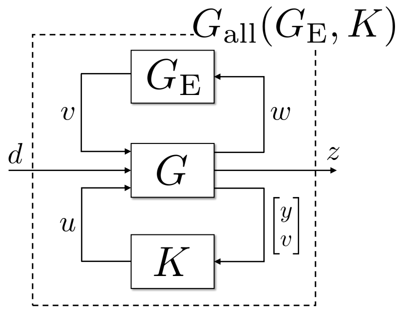

Figure 2.2: Control system $G_{\mathrm{all}}(G_{\mathrm{E}}, K)$

2.2 Preliminary: System Description and Retrofit Controller Design

2.2.1 System Description

We consider an interconnected system G_{Pre} composed of two dynamical systems G and G_{E} as illustrated in Fig. 2.1. The interconnected system G_{Pre} is assumed to be a stably operated system, which has been already controlled by some preexisting controllers. From this fact, the interconnected system G_{Pre} is called by a preexisting system in this chapter. From the preexisting system G_{Pre}, we extract the subsystem of interest, which is called by a local system G. On the other hand, a part of subsystems other than the local system is called by an environment G_{E}. Towards further improvement of the local control performance, we implement a local controller K, which utilizes a local measurement, to the local system G, as illustrated in Fig. 2.2.

The local system G is described by

$$\begin{bmatrix} w \\ z \\ y \\ v \end{bmatrix} = \begin{bmatrix} G_{wv} & G_{wd} & G_{wu} \\ G_{zv} & G_{zd} & G_{zu} \\ G_{yv} & G_{yd} & G_{yu} \\ I & 0 & 0 \end{bmatrix} \begin{bmatrix} v \\ d \\ u \end{bmatrix} := G \begin{bmatrix} v \\ d \\ u \end{bmatrix}, \tag{2.1}$$

where $w \in \mathbb{R}^r$ and $v \in \mathbb{R}^s$ denote the interconnection signals from G and G_{E}, respectively. The symbols $z \in \mathbb{R}^p$ and $d \in \mathbb{R}^q$ denote the control output and the disturbance input, respectively, and $y \in \mathbb{R}^\ell$ and $u \in \mathbb{R}^m$ denote the measurement output and the control input, respectively. The symbol $G_{\bullet *}$ denotes the transfer function matrix from the signal $*$ to the signal $\bullet$. In the following, we utilize the same notation as the system description G, G_{E}, and K for the notation of its transfer function. From (2.1), we see that the interconnection signal v from G_{E} is included in the output signal of G. This implies that the interconnection signal v is measurable in addition to the signal y. On the other hand, the environment G_{E} is described by

$$v = G_{\mathrm{E}} w. \tag{2.2}$$

The preexisting system G_{Pre} is described by

$$\begin{bmatrix} z \\ y \\ v \end{bmatrix} = G_{\mathrm{Pre}} \begin{bmatrix} w \\ u \end{bmatrix}, \tag{2.3}$$

where $G_{\mathrm{Pre}} \in \mathbb{C}^{(\ell+p+s)\times(q+r)}$ is described by

$$G_{\mathrm{Pre}} := \mathcal{F}_{\mathrm{u}}(G, G_{\mathrm{E}}).$$

The local controller K is described by

$$u = K \begin{bmatrix} y \\ v \end{bmatrix}.$$

Then, the control system $G_{\mathrm{all}}(G_{\mathrm{E}}, K)$ in Fig. 2.2 is described by

$$z = G_{\mathrm{all}}(G_{\mathrm{E}}, K) d,$$

where $G_{\rm all}(G_{\rm E}, K) \in \mathbb{C}^{p\times q}$ is described by

$$G_{\rm all}(G_{\rm E}, K) := \mathcal{F}_{\ell}(\mathcal{F}_u(G, G_{\rm E}), K).$$

In the following discussion, we assume that both local system and preexisting system are internally stable, i.e., G and $\mathcal{F}_{\rm u}(G, G_{\rm E})$ are stable. For simplicity of notation, the set of environment $G_{\rm E}$ that is allowed in this problem setting is denoted as

$$\mathcal{S}_{\rm E} := \{G_{\rm E} | \mathcal{F}_{\rm u}(G, G_{\rm E}) \in \mathcal{RH}_\infty\}.$$

Furthermore, we assume to design the local controller K in a distributed manner; for the local controller design, only the model parameters of G are assumed to be known, while those of the environment $G_{\rm E}$ are unknown.

2.2.2 Retrofit Controller

Most of conventional robust control problems [44] impose some norm-bounded condition with respect to the environment $G_{\rm E}$ (the uncertainty part), e.g., for some constant μ, $\|G_{\rm E}\|_\infty \le \mu$ holds. The problem setting in this chapter imposes the internal stability of the preexisting system $G_{\rm Pre}$, while it does not explicitly impose the norm-bounded condition with respect to $G_{\rm E}$. This premise of new robust control finds out a specific structure in the local controller, which reflects only the model parameter of the local system. This implies that the local contrller is designable in a distributed manner. Such a special local controller is called by a *retrofit controller* [39–41]. The retrofit controller K enables to guarantee the internal stability of the control system $G_{\rm all}(G_{\rm E}, K)$ for any $G_{\rm E} \in \mathcal{S}_{\rm E}$.

Let us consider the local controller given by

$$K := \hat{K} \begin{bmatrix} I_\ell & -G_{yv} \end{bmatrix}, \tag{2.4}$$

where $\hat{K} \in \mathbb{C}^{m\times \ell}$ is the transfer function such that $\hat{K}(I_\ell - G_{yu}\hat{K})^{-1} \in \mathcal{RH}_\infty$ holds, i.e., $\hat{K}$ is a stabilizing controller for the local system G isolated from the environment $G_{\rm E}$. For simplicity of notation, we denote the set of all stabilizing controllers $\hat{K}$ as

$$\mathcal{S}_K := \{\hat{K} | \hat{K}(I_\ell - G_{yu}\hat{K})^{-1} \in \mathcal{RH}_\infty\}.$$

In the following proposition, we provide the stability of the control system with the local controller in the form of (2.4).

Proposition 1. Suppose that G is internally stable and G_{wu} is left invertible. Then, the control system $G_{\rm all}(G_{\rm E}, K)$ is internally stable for any $G_{\rm E} \in \mathcal{S}_{\rm E}$ if and only if K has the form of (2.4) with $\hat{K} \in \mathcal{S}_K$.

The proof of Proposition 1 is omitted in this thesis; see e.g., [40, 41].

Proposition 1 characterizes the class of all local controllers such that the control system $G_{\rm all}(G_{\rm E}, K)$ is internally stable for any $G_{\rm E} \in \mathcal{S}_{\rm E}$. The local controller given by the form of (2.4) is called by a *retrofit controller* [39–41]. From (2.4), the retrofit controller consists of a part G_{yv} of the model parameter G and the controller $\hat{K} \in \mathcal{S}_K$ that stabilizes the local system G_{yu}. This implies that the retrofit controller design requires only the model parameter of G, not that of $G_{\rm E}$. The retrofit controller given by (2.4) is a simplified version. More general form of the retrofit control without the measurement of the interconnection signal v is also proposed in [39–41].

2.3 Quantitative Analysis of Localizability for Retrofit Controller Design

As stated in Proposition 1, the retrofit controller enables to guarantee the internal stability of the control system $G_{\rm all}(G_{\rm E}, K)$ for any $G_{\rm E} \in \mathcal{S}_{\rm E}$. In the control performance, it is desirable to have high robustness in the sense that the local control performance $\|G_{\rm all}(G, K)\|_\infty$ is kept invariant for any variation in the environment $G_{\rm E}$. In this chapter, such robustness is called by the *localizability* for the distributed design of the local controller. In this section, confining our attention of the local controller to the retrofit controller, we give the quantitative analysis of the localizability for the retrofit controller design.

We assume that the environment $G_{\rm E}$ is changed to $\tilde{G}_{\rm E}$ due to adding the perturbation Δ to $G_{\rm E}$. Then, the perturbated environment is described by

$$\tilde{G}_{\rm E} := \mathcal{F}_{\rm u}(G_{\rm E}, \Delta).$$

Because the perturbation Δ is assumed to be changed such that the preexisiting $G_{\rm Pre}$ is kept stable, the set of all admissible perturbation Δ is described by

$$\mathcal{S}_\Delta := \{\Delta | \mathcal{F}_{\rm u}(G_{\rm E}, \Delta) \in \mathcal{S}_{\rm E}\}.$$

We define an error system between the retrofit control system with Δ and that without Δ as

$$\hat{z} = G_{\rm er}(\Delta, K)w, \tag{2.5}$$

where the transfer matrix $G_{\rm er}(\Delta, K) \in \mathbb{C}^{p\times q}$ is given by

$$G_{\rm er}(\Delta, K) := G_{\rm all}(\tilde{G}_{\rm E}, K) - G_{\rm all}(G_{\rm E}, K). \tag{2.6}$$

Using the error system (2.5), the localizability index for the retrofit controller design is defined as follows.

Definition 1. *Consider the control system $G_{\rm all}(G_{\rm E}, K)$ with the retrofit controller (2.4). Then,*

$$f(\Delta, K) := \|G_{\rm er}(\Delta, K)\|_\infty$$

is said to be a localizability index for the distributed design of the local controller.

The localizability index $f(\Delta, K)$ is defined as the $\mathcal{H}_\infty$-norm of the error system $G_{\rm er}(\Delta, K)$. To give an interpretation of $f(\Delta, K)$, we consider $f(\Delta, K) = 0$. Then, it follows that $\|G_{\rm all}(\tilde{G}_{\rm E}, K)\|_\infty = \|G_{\rm all}(G_{\rm E}, K), K)\|_\infty$. This implies that the local control performance $\|G_{\rm all}(G_{\rm E}, K)\|_\infty$ is invariant for any variation in the environment $G_{\rm E}$. From this fact, we see that the value of $f(\Delta, K)$ assesses the influence of the environment $G_{\rm E}$ to the local control performance $\|G_{\rm all}(G_{\rm E}, K)\|_\infty$, in other words, the degree of the deterioration of the control performance for any variation of the environment.

In the following discussion, we state how to calculate the localizability index $f(\Delta, K)$. Note that it is impossible to directly calculate $f(\Delta, K)$ because the model parameters of the environment $G_{\rm E}$ are assumed to be unknown. Instead of the direct calculation, we develop an estimation method of $f(\Delta, K)$ based on its upper or lower bound. To this end, we first provide the upper bound of $f(\Delta, K)$ in the following theorem.

Theorem 1. Consider the control system $G_{\rm all}(G_{\rm E}, K)$ with the retrofit controller (2.4). Then, for any $\Delta \in \mathcal{S}_\Delta$, it follows that

$$f(\Delta, K) \le \alpha\varepsilon(\hat{K}), \tag{2.7}$$

where nonnegative constants are given by

$$\alpha := \|G_{zv}(\tilde{Q}_{\rm E} - Q_{\rm E})\|_\infty,$$
$$\varepsilon(\hat{K}) := \|\mathcal{F}_\ell(\Pi, \hat{K})\|_\infty,$$

and the transfer matrices $\tilde{Q}_{\rm E}$, $Q_{\rm E} \in \mathbb{C}^{s\times r}$, and $\Pi \in \mathbb{C}^{(r+\ell)\times(q+m)}$ is described by

$$\tilde{Q}_{\rm E} := \tilde{G}_{\rm E}(I_r - G_{wv}\tilde{G}_{\rm E})^{-1}, \tag{2.8}$$

$$Q_{\rm E} := G_{\rm E}(I_r - G_{wv}G_{\rm E})^{-1}, \tag{2.9}$$

$$\Pi := \begin{bmatrix} G_{wd} & G_{wu} \\ G_{yd} & G_{yu} \end{bmatrix}. \tag{2.10}$$

Proof. Let us consider $G_{\rm all}(G_{\rm E}, K)$ with the retrofit controller (2.4). Letting $Q_K \in \mathbb{C}^{m\times\ell}$ be

$$Q_K = \hat{K}(I_\ell - G_{yu}\hat{K})^{-1}, \tag{2.11}$$

we have

$$\begin{aligned}
G_{\rm all}(G_{\rm E}, K) &= \mathcal{F}_\ell\left(\mathcal{F}_u\left(\left[\begin{array}{c|cc} G_{wv} & G_{wd} & G_{wu} \\ \hline G_{zv} & G_{zd} & G_{zu} \\ G_{yv} & G_{yd} & G_{yu} \\ I & 0 & 0 \end{array}\right], G_{\rm E}\right), K\right) \\
&= \mathcal{F}_u\left(\mathcal{F}_\ell\left(\left[\begin{array}{cc|c} G_{wv} & G_{wd} & G_{wu} \\ G_{zv} & G_{zd} & G_{zu} \\ \hline G_{yv} & G_{yd} & G_{yu} \\ I & 0 & 0 \end{array}\right], K\right), G_{\rm E}\right) \\
&= \mathcal{F}_u\left(\begin{bmatrix} G_{wv} & G_{wd} + G_{wu}Q_K L_{yd} \\ G_{zv} & G_{zd} + G_{zu}Q_K L_{yd} \end{bmatrix}, G_{\rm E}\right) \\
&= G_{zd} + G_{zu}Q_K G_{yd} + G_{zv}Q_{\rm E}(G_{wd} + G_{wu}Q_K G_{yd}).
\end{aligned} \tag{2.12}$$

Note that $Q_{\rm E} = 0$ holds if $G_{\rm E} = 0$ holds. Then, from (2.6), we show that $G_{\rm er}(\Delta, K)$ is equivalent to

$$G_{\rm er}(\Delta, K) = G_{zv}(\tilde{Q}_{\rm E} - Q_{\rm E})(G_{wd} + G_{wu}Q_K G_{yd}). \tag{2.13}$$

It follows that

$$\begin{aligned}
f(\Delta, K) &= \|G_{zv}(\tilde{Q}_{\rm E} - Q_{\rm E})(G_{wd} + G_{wu}Q_K G_{yd})\|_\infty \\
&\le \|G_{zv}(\tilde{Q}_{\rm E} - Q_{\rm E})\|_\infty \|G_{wd} + G_{wu}Q_K G_{yd}\|_\infty.
\end{aligned} \tag{2.14}$$

Let us consider a feedback system composed of

$$\begin{bmatrix} w \\ y \end{bmatrix} = \Pi \begin{bmatrix} d \\ u \end{bmatrix}, \tag{2.15}$$

and $u = \hat{K}y$. Then, its transfer function $\mathcal{F}_\ell(\Pi, \hat{K})$ is equivalent to

$$\mathcal{F}_\ell(\Pi, \hat{K}) = G_{wd} + G_{wu}Q_K G_{yd}. \tag{2.16}$$

From (2.14) and (2.16), we show that, for any $\Delta \in \mathcal{S}_\Delta$, (2.7) holds. □

As stated in Theorem 1, the localizability index $f(\Delta, K)$ is bounded by $\alpha\varepsilon(\hat{K})$, which is the product of the unknown parameter α and the known parameter $\varepsilon(\hat{K})$. Then, $\varepsilon(\hat{K})$ is described by the $\mathcal{H}_\infty$-norm of the feedback system composed of

$$\begin{bmatrix} w \\ y \end{bmatrix} = \Pi \begin{bmatrix} d \\ u \end{bmatrix}$$

and $u = \hat{K}y$. This implies that the value of $\varepsilon(\hat{K})$ assesses the control performance from the disturbance d injected into G to the interconnection signal w.

As shown in Theorem 1, the localizability index $f(\Delta, K)$ is bounded from above by a product of the unknown parameter α and the known parameter $\varepsilon(\hat{K})$. This implies that the localizability $f(\Delta, K)$ can be estimated in the sense of the upper bound. To give a meaning of the known parameter $\varepsilon(\hat{K})$, we consider a feedback system $\mathcal{F}_\ell(\Pi, \hat{K})$ composed of Π and $\hat{K}$, which is the stabilizing controller for the local system. We see that the value of $\varepsilon(\hat{K})$ is equivalent to the $\mathcal{H}_\infty$-norm of $\mathcal{F}_\ell(\Pi, \hat{K})$. This means that the value of $\varepsilon(\hat{K})$ assesses the suppression performance of the system with the disturbance, which is injected into G, and the signal w that injects into the environment G_{E}.

Furthermore, we consider the retrofit controller design to minimize the ocalizability index $f(\Delta, K)$. In the retrofit control problem, the model of G_{E} is not assumed to be available for the controller design. Due to this fact, we cannot directly find the retrofit controller K to minimize the value of $f(\Delta, K)$. To overcome this issue, Theorem 1 is utilized for the retrofit controller design problem to minimize the value of $f(\Delta, K)$ without the model information about G_{E}. From (2.7), the minimum value of $f(\Delta, K)$ with respect to K is bounded from above by the product of α and the minimum value of $\varepsilon(\hat{K})$ with respect to $\hat{K}$. Note that the minimization problem of $\varepsilon(\hat{K})$ is reduced to that of the $\mathcal{H}_\infty$-norm of the feedback system $\mathcal{F}_\ell(\Pi, \hat{K})$. This implies the minimization problem corresponds to the design problem of the optimal $\mathcal{H}_\infty$ controller for Π.

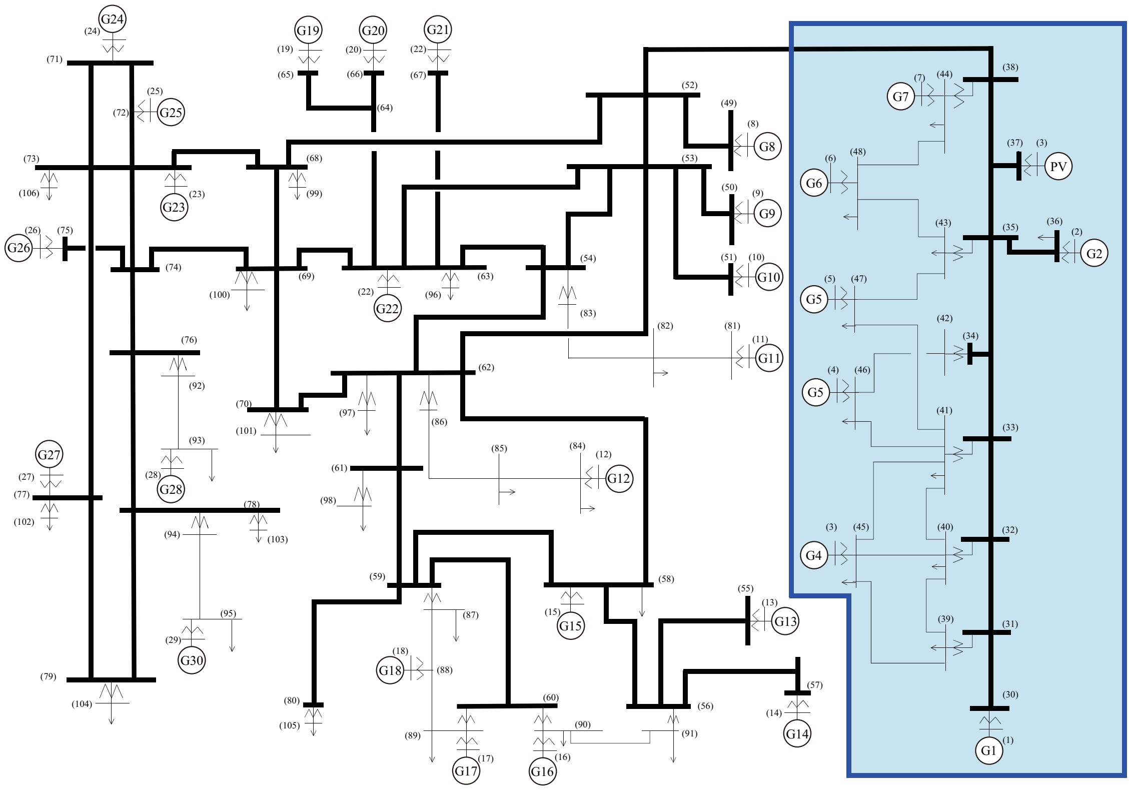

Figure 2.3: PV-integrated IEEJ EAST 30-machine model. In the model, one generator is replaced with one PV plant. In the figure, synchronous generators and loads are represented by the circles and arrows, repectively, and the buses indicates the bold lines. In the figure, the blue colored region depicts the local system.

2.4 Application to Placement of Retrofit Controller in Power Systems

In this section, the placement problem of the retrofit controller is addressed through an example of power systems. Then, the result is analyzed by the localizability index.

2.4.1 Power System Model

As illustrated in Fig. 2.3, the power system model is based on the IEEE EAST 30-machine power model in which one generator is replaced with one PV plant. The IEEE EAST 30-machine power model [45] represents the power system in the eastern half of Japan. The power system model is composed of 29 generators, 31 loads, 108 buses, and one PV plant. The local system, which is illustrated in the blue colored region in Fig. 2.3, includes

7 generators and one PV plant. The local system G linearized around an equilibrium point is described by

$$G : \begin{cases} \dot{x} = Ax + B_v v + Bu + B_d d, \\ w = C_w x + D_v v, \\ z = C_z x, \\ y = Cx + Dv, \end{cases} \tag{2.17}$$

where $x \in \mathbb{R}^{91}$ is the state of generators in the local system. Each generator has the state with 13 dimensions, which includes the rotor angle, frequency deviation, magnetic flux of an excitation system, and so on. The symbol $v \in \mathbb{R}$ denotes the voltage at the bus in the environment which is connected to G. Let $u := [\, u_1 \ u_2 \ \ldots \ u_7 \,]^\top \in \mathbb{R}^7$ and $y := [\, y_1 \ y_2 \ \ldots \ y_7 \,]^\top \in \mathbb{R}^7$. Then, u_i and $y_i \in \mathbb{R}, i \in \{1, 2, \ldots, 7\}$ denote the input injected into the excitation system and the frequency deviation in each generator, respectively. The symbol $z \in \mathbb{R}$ denotes the average of all frequency deviations in G. In addition, the symbol $d \in \mathbb{R}$ denotes the disturbance and is assumed to be injected into all generators in G.

2.4.2 Problem Setting and Solution for Retrofit Controller Placement

Let us implement one retrofit controller to only the ith generator. Then, (2.17) is rewritten as

$$G : \begin{cases} \dot{x} = Ax + D_v v + BE_i u + B_d d, \\ w = C_w x + D_v v, \\ z = C_z x, \\ y = E_i Cx + Dv, \end{cases} \tag{2.18}$$

where the matrix $E_i := e_i e_i^\top \in \mathbb{R}^{7\times 7}$ represents the selection of the ith generator to which the retrofit controller is implemented. The stabilizing controller $\hat{K}$ in the retrofit controller is designed as the $\mathcal{H}_\infty$ controller that minimizes the $\mathcal{H}_\infty$-norm of the system with the input d and the output w.

The aim of this section is to provide the placement of the retrofit controller that minimizes the localizability of the control system. In this chapter, the localizability means the robustness in the sense that the control performance with respect to the frequency deviation average in the local system is kept invariant to some extent for any variation of the model parameters of the generators in the power system excluding the local system. To provide a solution for the controller placement problem, we utilize the localizability index

Table 2.1: Localizability index and controllability Gramian for each controller port selection. This table cites from [46].

i	$\min_{\hat{K}} \varepsilon_i(\hat{K})$	W_i
1	◯12.8	242.8
2	21.7	192.2
3	20.2	◯262.4
4	15.0	194.6
5	18.3	150.8
6	31.5	159.2
7	44.7	169.2

$f(\Delta, K)$, in particular, the value of $\varepsilon(\hat{K})$. Let us consider the transfer function $\Pi_i \in \mathbb{C}^{8\times 14}$ described by

$$\Pi_i := \begin{bmatrix} \Gamma(sI-A)^{-1}B_d & \Gamma(sI-A)^{-1}BE_i \\ E_iC(sI-A)^{-1}B_d & E_iC(sI-A)^{-1}BE_i \end{bmatrix}.$$

Then, the optimal controller placement $i_{\rm op}$ is given by

$$i_{\rm op} = \arg\min_i \min_{\hat{K}} \varepsilon_i(\hat{K}), \text{ s.t. } \hat{K} \in \mathcal{S}_K,$$

where $\varepsilon_i(\hat{K}) \in \mathbb{R}$ is given by

$$\varepsilon_i(\hat{K}) = \|\mathcal{F}_\ell(\Pi_i, \hat{K})\|_\infty.$$

2.4.3 Numerical Experiment

Table 2.1 illustrates the value of $\min_{\hat{K}} \varepsilon_i(\hat{K})$ in the case that the retrofit controller is implemented to the ith generator. To compare the controller placement method based on the controllability Gramian, Table 2.1 also illustrates the trace of the controllability Gramian, which is defined as

$$W_i := \int_0^\infty e^{A\tau} BE_iE_iB^\top e^{A^\top \tau} d\tau.$$

From Table 2.1, we see that it is optimal to implement to the 1st generator in the sense of the localizability index. On the other hand, in the sense of the controllability Gramian, it

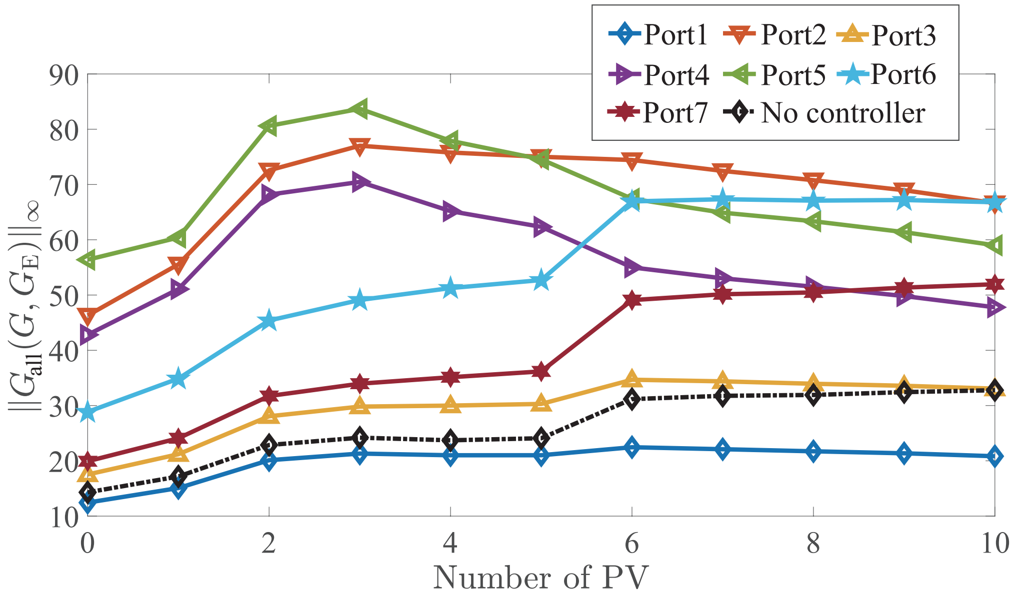

Figure 2.4: $\mathcal{H}_\infty$-norm of the control system $G_{\rm all}(G_{\rm E}, K)$ versus the number of PVs. This table cites from [46].

is optimal to implement to the 3rd generator. Figure 2.4 shows Figure 2.4 shows the $\mathcal{H}_\infty$-norm of the control system under the variation of $G_{\rm E}$. The power system in next generation is supposed to be gradually reduce its inertia because PVs are replaced with existing synchronous generators. Due to this fact, the deterioration of the control performance with respect to the frequency deviation in the entire power system is concerned. Motivated by this fact, the variation of is expressed by replacing generators in $G_{\rm E}$ with PVs In addition, in Fig. 2.4, we assume that $G_{\rm E}$ continue to be changed until all 50% of, i.e., 11 synchronous generators in the environment $G_{\rm E}$ are completely replaced with PVs. From Fig. 2.4, the variation of the $\mathcal{H}_\infty$-norm of $G_{\rm all}(G_{\rm E}, K)$ is minimum for the variation of $G_{\rm E}$ in the case of the implementation to the 1st generator. This fact shows the effectiveness of the controller placement based on the localizability index. Furthermore, we see that the $\mathcal{H}_\infty$-norm of $G_{\rm all}(G_{\rm E}, K)$ is also minimum in the case of the implementation to the 1st generator in spite of theoretically not being guaranteed. This fact indicates that the localizability index is also related to the local control performance.

Through the numerical experiment as illustrated in Fig. 2.4, we show that the variation of $\|G_{\rm all}(G_{\rm E}, K)\|_\infty$ is minimum for the variation of $G_{\rm E}$ in the case of the implementation to the 1st generator. However, focusing on the other cases of the implementation to the other generators in Table 2.1 and Fig. 2.4, we see that there are not necessarily correlations

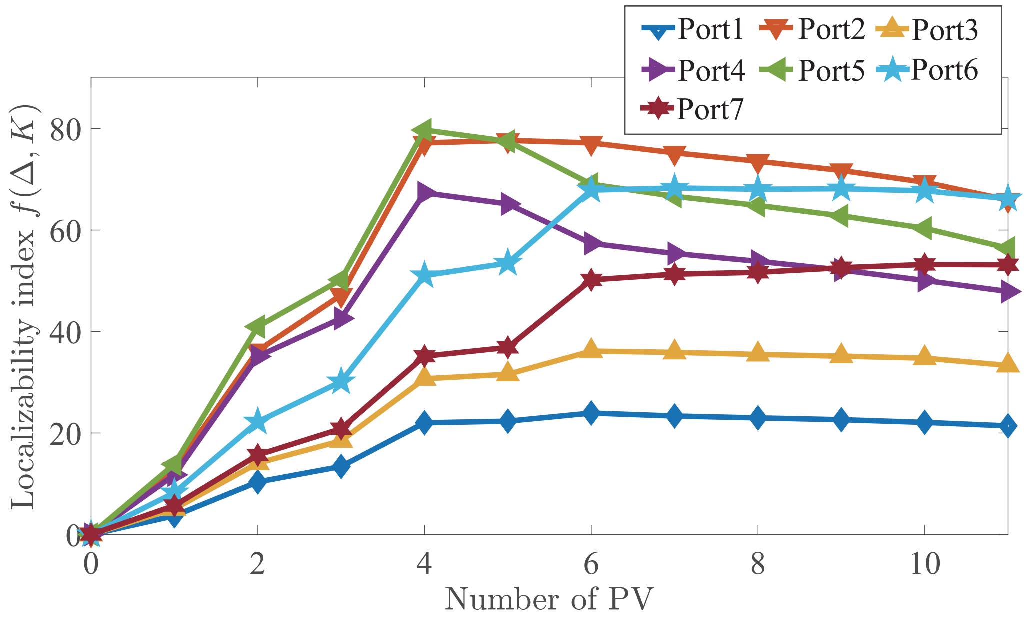

Figure 2.5: Localizability index $f(\Delta, K)$ versus the number of PVs. This table cites from [46].

between the value of $\min_{\hat{K}} \varepsilon_i(\hat{K})$ and the degree of the variation of $\|G_{\mathrm{all}}(G_{\mathrm{E}}, K)\|_\infty$. This comes from the conservativeness of the evaluation $\alpha\varepsilon(\hat{K})$ in the sense of upper bound. In other words, there is a limit in the estimation of the localizability index under using only the available local information without using the model of G_{E}. Figure 2.5 shows the actual value of $f(\Delta, K)$ when G_{E} is changed. As seen in Fig. 2.4 and Fig. 2.5, we see that the evaluation of $f(\Delta, K)$ by $\alpha\varepsilon(\hat{K})$ is conservative because there are some correlations between the actual value of $f(\Delta, K)$ and the variation of $\|G_{\mathrm{all}}(G_{\mathrm{E}}, K)\|_\infty$. On possible way to reduce such conservativeness in the evaluation is that the identified environment model G_{E} is utilized for the estimation of $f(\Delta, K)$, in particular, the value of α. In fact, the paper [47] has proposed the retrofit control method into which the modeling technique for the environment is integrated. In this chapter, the model of G_{E} is not assumed to be available for the estimation of $f(\Delta, K)$. However, under the assumption of obtaining the interconnection signal v from G_{E}, the model of G_{E} can be identified by using some closed-loop identification techniques. The identified environment model contributes to provide a less conservative estimation of $f(\Delta, K)$.

2.5 Chapter Summary

In this chapter, we proposed the localizability index for the feedback system to which the retrofit controller is implemented. The localizability index was defined as the $\mathcal{H}_\infty$-norm of the error system between the control system with and without the environment. The proposed index measured the degree of the performance invariance for any variation in the environment, in other words, that how much the control performance of the local system is kept invariant with respect to the variation of the environment. Then, it was shown that the estimation of the localizability index requires only the model parameters of the local system in the sense of the upper bound. Through an example of PV-integrated power systems, we analyze the retrofit controller placement problem and show the effectiveness of the placement based on the localizability index.

Chapter 3

Performance Improvement via Iterative Connection of Passive Systems

3.1 Introduction

In this chapter, the problem of the *performance improvement* is addressed for a feedback system composed of two passive systems. We employ a model set description for each subsystem: each subsystem is assumed to be passivity property that is characterized by two matrix parameters. The parameters are utilized for the evaluation of L_2-gain of the model set, which is defined as the worst-case system in the model set. The feedback system composed of the performance-integrated passive systems is also passive. In addition, the parameters characterizing the model set describing the feedback system is given as the parameter transition. Then, we derive conditions on the passivity parameters such that the performance improvement is achieved; the L_2-gain of the model set describing the feedback system is strictly reduced as compared to that describing the subsystems. In the above discussion, only parameters characterizing the model set of subsystems is not required for the L_2-gain evaluation of the feedback system. In this sense, the problem addressed in this paper is referred to as the *model-set-based* analysis. Subsequently, the model-set-based analysis of the feedback system is extended to that of an *iterative* feedback system, which is a special class of the evolving network system as shown in Fig. 3.1. Then, conditions on the passivity parameters to achieve the gradual improvement are derived.

The remainder of this chapter is organized as follows. In order to motivate the model-set based analysis, Section illustrates an example of the frequency control of power systems

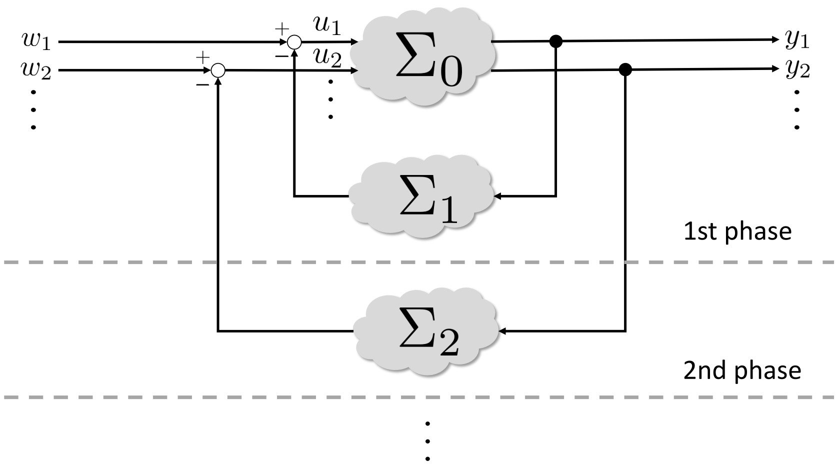

Figure 3.1: Evolution of a baseline system Σ_0 by gradually connecting multiple subsystems Σ_i in a step-by-step manner.

involving a large number of RE resources. We formulate the general model-set-based quantitative analysis, in particular, performance improvement problem in Section 3.3.1. Then, the performance-integrated passivity is defined. Under the preliminary in Section 3.3.1, a solution to the performance improvement problem for general feedback and iterative feedback systems are presented in Section 3.4. In other words, we derive a condition on model set of subsystems to achieve the performance improvement. Based on the model-set-based analysis in 3.4, we perform the analysis of the frequency control of the power system in 3.5. Finally, Section 3.6 concludes this chapter.

3.2 Motivating Example

3.2.1 Nonlinear Power System Model

As illustrated in Fig. 3.2, a power network system that is constructed by installing some RE farms in a baseline power system. The RE farms are composed of a large number of RE resources and the baseline power system is composed of N_{G} generators, N_{L} loads, and N_{B} buses. In addition, N_{R} RE farms are connected to some fixed buses in the baseline power system. We suppose that there are no isolated buses in the baseline power system;

The contents of Sections 3.2, 3.3, and 3.4 and Figures 3.2, 3.3, 3.4, and 3.5 in this chapter cite from the following reference: ©2020 IEEE. Reprinted, with permission, from "Performance improvement via iterative feedback connection of passive systems, *IEEE Transactions on Automatic Control*, 2019(online), DOI:10.1109/TAC.2019.2930806. ”

i.e., the topology of the network in the baseline power system is described by the strongly connected graph [48]. Let $\mathcal{V} := \{1, 2, \ldots, N_{\mathrm{B}}\}$ be the label set of the buses. Then, the buses in the power system are classified as buses with generators, those with loads, those with RE farms, and those to which nothing is connected. In particular, the label sets of RE resource and generator nodes are denoted by $\mathcal{V}_{\mathrm{R}} := \{1, 2, \ldots, N_{\mathrm{R}}\}$ and $\mathcal{V}_{\mathrm{G}} \subseteq \mathcal{V} \setminus \mathcal{V}_{\mathrm{R}}$, respectively. The power system model is represented by the dynamic component describing generator dynamics in the node $\mathcal{V}_{\mathrm{G}}$ and the static part describing the power flow equations between nodes.

(Generator dynamics) The dynamics of each generator are described as follows:

$$\dot{\delta}_i = \omega_i, \quad m_i \dot{\omega}_i + d_i \omega_i = P_{\mathrm{m}i} - P_{\mathrm{g}i}, \ i \in \mathcal{V}_{\mathrm{G}}, \tag{3.1}$$

where $m_i > 0$ and $d_i > 0$ denote the inertia constant and the damping coefficient, respectively, and δ_i and ω_i are the rotor angle and the frequency deviation of the rotor, respectively. The mechanical power input $P_{\mathrm{m}i}$ is generated by a first-order turbine-governor dynamics [49] that is given by

$$\tau_i \dot{P}_{\mathrm{m}i} = -P_{\mathrm{m}i} + P_{\mathrm{m}i}^* - k_{\omega_i} \omega_i, \tag{3.2}$$

where $\tau_i > 0$, $k_{\omega_i} > 0$, and $P_{\mathrm{m}i}^*$ are the time constant, the governor gain, and a desired reference input. In addition, $P_{\mathrm{g}i}$ is the electrical output given by

$$P_{\mathrm{g}i} = \frac{E_i V_i}{x_{di}} \sin(\delta_i - \theta_i),$$

where x_{di}, E_i, and V_i are the direct axis transient reactance, the voltage magnitude behind the direct axis transient reactance of ith generator, and the voltage magnitude at a terminal bus of the ith generator, respectively. The symbol θ_i denotes the phase angle of the ith terminal bus.

(Power flow equation) Suppose that the baseline power system is a lossless network. Then, the power flow between some connected buses can be represented as

$$P_{\mathrm{e}i} = \sum_{j \in \mathcal{N}_i}^{N_{\mathrm{B}}} B_{ij} V_i V_j \sin(\theta_i - \theta_j), \tag{3.3}$$

$$Q_{\mathrm{e}i} = -B_{ii} V_i^2 - \sum_{j \in \mathcal{N}_i}^{N_{\mathrm{B}}} B_{ij} V_i V_j \cos(\theta_i - \theta_j), \tag{3.4}$$

where $\mathcal{N}_i$ and $B_{ij} > 0$ is the index set associated with the neighborhood of the ith bus and the susceptance between the ith and jth buses, respectively. The symbol $P_{\mathrm{L}i}$ and $P_{\mathrm{R}i}$

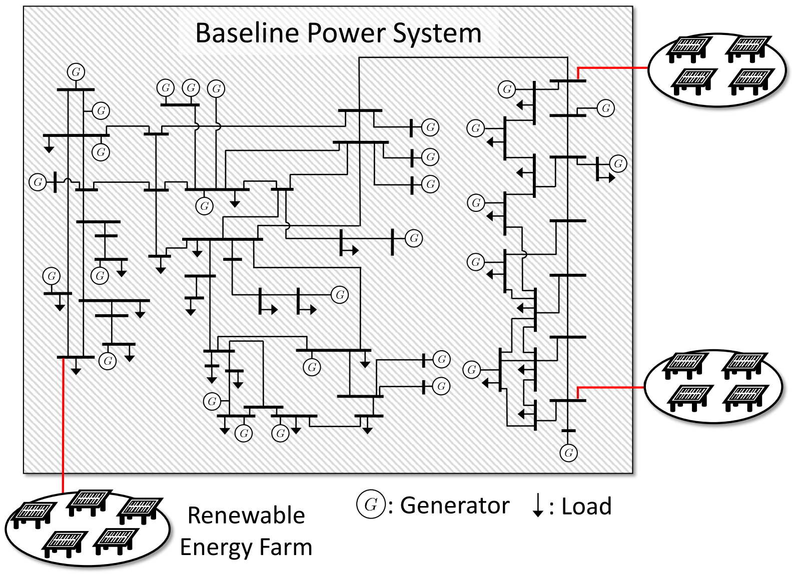

Figure 3.2: A power network system involving some renewable energy farms, which comprise a large number of RE resources. In the power system, a baseline power system is composed of multiple generators and loads.

denote the active power of the load and the RE resource, while $Q_{\mathrm{L}i}$ be the reactive power of the load. In addition, the reactive power of each generator is given by

$$Q_{\mathrm{g}i} = \frac{E_i V_i}{x_{di}} \cos(\delta_i - \theta_i) - \frac{V_i^2}{x_{di}}.$$

For each node $i \in \mathcal{V}$, the power flow equation is described by the following algebraic equation

$$\begin{cases} -P_{\mathrm{e}i} + P_{\mathrm{g}i} - P_{\mathrm{L}i} + P_{\mathrm{R}i} = 0, \\ -Q_{\mathrm{e}i} + Q_{\mathrm{g}i} - Q_{\mathrm{L}i} = 0. \end{cases} \tag{3.5}$$

The generator dynamics (3.1) and (3.2) and the power flow equation (3.5) represent the power system that includes the RE farms.

3.2.2 Decentralized Control for Power System

RE farms may not provide desirable power outputs due to their uncertain power output. From this fact, it follows that the fluctuations from the desirable power output behave as the disturbance. Furthermore, we consider the case where the power outputs of the RE farms are compensated with those of battery storages. Then, $P_{\mathrm{R}i}$ is replaced by

$$P_{\mathrm{R}i} = -v_i + w_i + P_{\mathrm{R}i}^*, \tag{3.6}$$

where $v_i \in \mathbb{R}$, $w_i \in \mathbb{R}$, and $P_{\mathrm{R}i}^* \in \mathbb{R}$ are the control input, disturbance, and desired power output. The input and disturbance are related to the battery output and the fluctuating output of the RE resource, respectively. Each local controller K_i is given as a proportional and integral (PI) controller:

$$K_i : v_i = \left(k_{P_i} + \frac{k_{I_i}}{s}\right) y_i, \quad i \in \mathcal{V}_{\mathrm{R}}, \tag{3.7}$$

where k_{P_i} and k_{I_i} are the proportional gain and integral gain, respectively. In addition, $y_i \in \mathbb{R}$ is defined as

$$y_i := \sum_{j \in \mathcal{V}_{\mathrm{G}}} \pi_{ij} \omega_j, \tag{3.8}$$

where $\pi_{ij} \in \mathbb{R}$ is a weighting factor of the frequency deviation. The weighting factor is formally determined in Subsection 3.2.3. Each controller K_i is connected to the power system in a step-by-step manner. Then, we construct the power system in which the input and output are $w := \mathrm{col}(w_i)_{i\in\mathcal{V}_{\mathrm{R}}}$ and $y := \mathrm{col}(y_i)_{i\in\mathcal{V}_{\mathrm{R}}}$, respectively.

3.2.3 Motivating Example: Disturbance Response of Power System

The baseline power system employed the IEEJ EAST 30-machine power model representing the power system in the eastern half of Japan [45], where $N_{\mathrm{G}} = 30$, $N_{\mathrm{L}} = 31$, and $N_{\mathrm{B}} = 107$. In addition, we set $N_{\mathrm{R}} = 6$. For the generator dynamics, the values of E_i and m_i were given by [45], and d_i was randomly selected from [0.1 1]. For the governor-free dynamics (3.2), we set $\tau_i = 1$ and $k_{\omega_i} = 0.1$ for all $i \in \mathcal{V}_{\mathrm{G}}$. The topology parameters B_{ij} were given by [45]. For the controller (3.7), k_{I_i} was randomly selected from [1 4] and the choice of k_{P_i} is formally given in in Section 3.5. The weighting factor is also formally defined in Section 3.5.

Figure 3.3 illustrates the disturbance responses of the power system. From the figure, we see that the disturbance effect is suppressed with the increase of the number of additional controllers. The key to realizing the performance improvement is the *passivity* property, which is formally defined in Subsection 3.3.2. Although the detailed analysis of the power system model is presented in Section 3.5, it should be noted that the linearized power system with the input $v := \mathrm{col}(v_i)_{i\in\mathcal{V}_{\mathrm{R}}}$ and output y has a *passivity* property. In addition, K_i has another *passivity* property. The aim of this paper is to theoretically prove

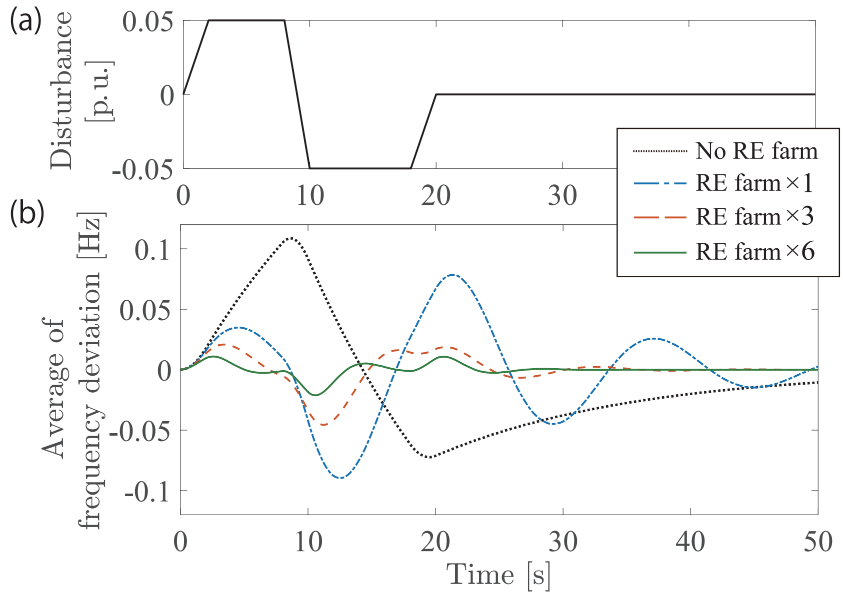

Figure 3.3: Disturbance responses of the power system that is composed of the baseline power system given (3.1), (3.2), and (3.5) and local PI controllers (3.7). The power system evolves with the increase of the number of the RE farms. Figure (a) shows the disturbance input that is injected into all RE buses, while Fig. (b) show the average of all frequency deviations in all generators. The increase of the number of RE farms contributes to increasingly suppress the average. This figure cites from [50].

the performance improvement. Even if the previous works [36, 37, 51] are applied to this example, the performance improvement as illustrated in this example can be neither shown nor explained. On the basis of this motivation, we aim at finding a special passivity class of each subsystem such that the performance improvement is achieved.

3.3 Problem Setting of Model-set-based Performance Analysis

3.3.1 Model-set-based Performance Improvement Problem

We consider a feedback system $\Sigma_{\mathrm{FB}}(\Sigma_1, \Sigma_2)$ composed of two subsystems:

$$\Sigma_i : y_i = \mathcal{S}_i u_i, \; i \in \{1, 2\}, \tag{3.9}$$

where $\mathcal{S}_i : \mathbb{L}_{2e} \to \mathbb{L}_{2e}$ is a causal operator, and u_i and y_i is the input and output of Σ_i, respectively. In particular, if Σ_i is a linear time-invariant (LTI) dynamical system, $\mathcal{S}_i$ represents its transfer function denoted by $\mathcal{S}_i(s)$, where $u_i(s)$ and $y_i(s)$ are the Laplace transforms of u_i and y_i, respectively. To construct the feedback system, Σ_1 and Σ_2 are interconnected via a negative feedback manner. Letting $w \in \mathbb{R}^m$ and $z \in \mathbb{R}^m$ be the external input and evaluation output of $\Sigma_{\mathrm{FB}}(\Sigma_1, \Sigma_2)$, we describe the negative feedback connection as

$$u_1 = w - y_2, \tag{3.10}$$

$$u_2 = y_1 = z. \tag{3.11}$$

In this chapter, $\Sigma_{\mathrm{FB}}(\Sigma_1, \Sigma_2)$ is assumed to be well-posed, i.e., there uniquely exist y_1 and y_2 of $\Sigma_{\mathrm{FB}}(\Sigma_1, \Sigma_2)$ that belong to $\mathbb{L}_{2e}$ for all $w \in \mathbb{L}_{2e}$.

In order to formulate the performance improvement problem for the feedback system, we define a notion of model sets and its performance measure. The formulation and a solution for the problem setting are one of the main contribution of this chapter. Let $\mathcal{P}_i, i \in \{1, 2\}$ be model set describing each subsystem $\Sigma_i, i \in \{1, 2\}$, i.e., some specific property is imposed on all Σ_i belonging to $\mathcal{P}_i$. Then, we define the model set describing the feedback system Σ_{FB} as

$$\mathcal{P}_{\mathrm{FB}}(\mathcal{P}_1, \mathcal{P}_2) := \{\Sigma_{\mathrm{FB}}(\Sigma_1, \Sigma_2) | \Sigma_i \in \mathcal{P}_i, i \in \{1, 2\}\}.$$

For example, let us consider Σ_1 and Σ_2 are single-input-single-output (SISO) systems. In such a situation, each model set $\mathcal{P}_i, i \in \{1, 2\}$ describing Σ_i is represented by the set of all Nyquist plots of $\Sigma_i \in \mathcal{P}_i$, as illustrated in Fig. 3.4a. Then, the set of Nyquist plots of Σ_{FB}, which represents the model set $\mathcal{P}_{\mathrm{FB}}(\mathcal{P}_1, \mathcal{P}_2)$, is shown in Fig. 3.4b. This chapter addresses the model-set-based performance analysis of the feedback system, such as the L_2-gain evaluation. To this end, the L_2-gain of the *model set* $\mathcal{P}_i$ is defined as follows.

Definition 2. *Suppose that all Σ_i that belong to $\mathcal{P}_i$ are L_2-stable. Then,*

$$\gamma(\mathcal{P}_i) := \sup_{\Sigma_i \in \mathcal{P}_i} \|\Sigma_i\|_{L_2}$$

is said to be the L_2-gain of $\mathcal{P}_i$.

The L_2-gain of the *model set* $\mathcal{P}_i$ is defined as the worst-case system in $\mathcal{P}_i$. The following problem of performance improvement is addressed in this chapter.

Problem 1: Find $\mathcal{P}_i, i \in \{1, 2\}$ such that the performance improvement is achieved, i.e.,

$$\gamma(\mathcal{P}_{\mathrm{FB}}(\mathcal{P}_1, \mathcal{P}_2)) < \gamma(\mathcal{P}_1) \tag{3.12}$$

holds.

In this chapter, Problem 1 can be referred to as *model-set-based* performance improvement problem of Σ_{FB}. In this problem setting, the description of $\Sigma_i, i \in \{1, 2\}$ and Σ_{FB} are given by model sets $\mathcal{P}_i$ and $\mathcal{P}_{\mathrm{FB}}$, rather than detailed models such as a transfer function and a state-space representation. In the model-set-based analysis, only the model set describing Σ_i is utilized for the performance analysis of Σ_{FB}, while the detailed model of Σ_i is not utilized. The aim of this chapter is to find each model set $\mathcal{P}_i$ such that the L_2-gain of $\mathcal{P}_{\mathrm{FB}}(\mathcal{P}_1, \mathcal{P}_2)$ decreases as compared to that of $\mathcal{P}_1$, i.e., the performance improvement (3.12) is achieved.

3.3.2 Definition of Dissipativity and Passivity

To describe the model set for input-output systems, we focus on the notion of dissipativity, in particular (Q, S, R)-dissipativity [21, 22], which is defined as follows.

Definition 3. *Let $Q = Q^\top \in \mathbb{R}^{m \times m}$, $S \in \mathbb{R}^{m \times m}$, and $R = R^\top \in \mathbb{R}^{m \times m}$. Then, the system Σ_i is said to be (Q, S, R)-dissipative if there exists $\rho_i \in \mathbb{R}$ such that for any $u_i \in \mathbb{L}_{2e}$ and its corresponding output y_i,*

$$\int_0^T \left\{ u_i^\top(\tau) S y_i(\tau) - \frac{1}{2} y_i^\top(\tau) Q y_i(\tau) - \frac{1}{2} u_i^\top(\tau) R u_i(\tau) \right\} d\tau \geq \rho_i \tag{3.13}$$

holds for all $T \in \mathbb{R}_+$.

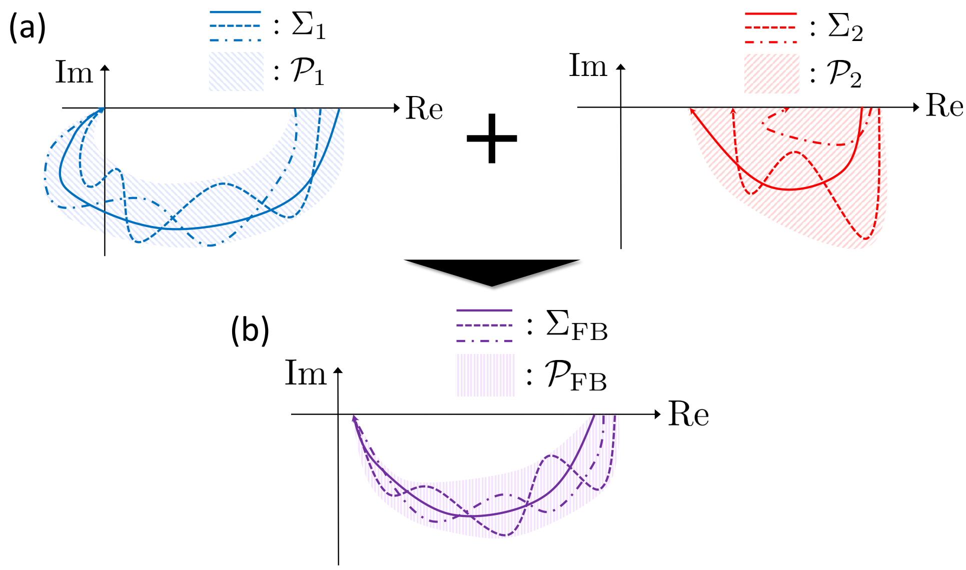

Figure 3.4: An explanation of model set for SISO systems: (a) All Nyquist plots of Σ_i that belong $\mathcal{P}_i, i \in \{1, 2\}$. (b) All Nyquist plots of Σ_{FB} that belong to $\mathcal{P}_{\text{FB}}$, which are generated from $\Sigma_i \in \mathcal{P}_i, i \in \{1, 2\}$ in subfigure a.

In the notion of the (Q, S, R)-dissipativity, the parameters Q, S, and R characterize the set of dynamical systems. They have been utilized for the *qualitative* analysis of large-scale systems [24, 26–28, 52], such as the stability, consensus, and synchronization. In this chapter, each subsystem is assumed to be (Q, S, R)-dissipavity. Then, we aim at finding conditions on the parameters in the subsystems such that the performance improvement is achieved. Even though the L_2-gain of (Q, S, R)-dissipative systems is evaluated based on the the parameters Q, S, and R, the performance improvement (3.12) cannot be shown for the general parameters. In order to solve Problem 1, the (Q, S, R)-dissipativity is restricted to the passivity [22, 53].

Definition 4. *Let $Q \geq 0, S = I_m$, and $R \geq 0$. Then, the system Σ_i is said to be (Q, R)-passive if it is (Q, S, R)-dissipative. In addition, the symbol $\mathcal{P}(Q, R)$ denotes the set of all (Q, R)-passive systems.*

In the definition, it is necessary to hold $Q^{-1} \geq R$ because the model-set $\mathcal{P}(Q, R)$ should be non-empty set. The model set $\mathcal{P}(Q, R)$ is characterized by the matrix parameters Q and R expressing the passivity level of dynamical systems. In the following discussion, the model set $\mathcal{P}_i$ in Problem 1 is confined to $\mathcal{P}(Q_i, R_i)$, i.e., $\mathcal{P}_i = \mathcal{P}(Q_i, R_i), i \in \{1, 2\}$ holds. In other words, the (Q, R)-passivity property is imposed on Σ_i.

3.4 Performance Improvement of Passive Systems

In this section, we provide a solution to Problem 1. First, the performance evaluation of L_2-gain of $\mathcal{P}(Q_1, R_1)$ and $\mathcal{P}_{\mathrm{FB}}(\mathcal{P}_1, \mathcal{P}_2)$ are provided. In order to achieve the performance improvement the feedback system, a model set describing subsystems $\Sigma_i, i \in \{1, 2\}$ is derived by using on the performance evaluation. In other words, conditions on Q_i and $R_i, i \in \{1, 2\}$ is derived such that (3.12) holds. Subsequently, we extend the performance improvement of the feedback system to that of an *iterative* feedback system, which is a class of an evolving network system as stated in Chapter 1. The iterative feedback system is formally defined in Subsection 3.4.2.

3.4.1 Performance Evaluation and Improvement of Feedback Systems

In order to evaluate the L_2-gain of the model set $\mathcal{P}(Q, R)$, we introduce a performance index given by

$$\varepsilon(Q, R) := \frac{1 + \sqrt{\underline{\lambda}(Q)\bar{\lambda}(Q^{-1} - R)}}{\underline{\lambda}(Q)} \tag{3.14}$$

Using the index $\varepsilon(Q, R)$, we provide the performance evaluation of the L_2-gains of $\mathcal{P}(Q_1, R_1)$ and $\mathcal{P}_{\mathrm{FB}}$ in the following lemmas.

Lemma 1. *Suppose that $Q_1 > 0$ holds. Then, the L_2-gain of $\mathcal{P}(Q_1, R_1)$ satisfies*

$$\gamma(\mathcal{P}_1) = \varepsilon(Q_1, R_1), \tag{3.15}$$

where $\varepsilon(Q_1, R_1)$ is given by (3.14).

Lemma 2. *Suppose that $\mathcal{P}_i = \mathcal{P}(Q_i, R_i), i \in \{1, 2\}$ holds. Then, letting $Q_{\mathrm{FB}} \geq 0$ and $R_{\mathrm{FB}} \geq 0$ be given by*

$$Q_{\mathrm{FB}} = Q_1 + R_2, \tag{3.16}$$

$$R_{\mathrm{FB}} = R_1(Q_2 + R_1)^{\dagger} Q_2, \tag{3.17}$$

it holds that $\mathcal{P}_{\mathrm{FB}}(\mathcal{P}_1, \mathcal{P}_2) \subseteq \mathcal{P}(Q_{\mathrm{FB}}, R_{\mathrm{FB}})$. Furthermore, if $Q_{\mathrm{FB}} > 0$ holds, the L_2-gain of $\mathcal{P}_{\mathrm{FB}}(\mathcal{P}_1, \mathcal{P}_2)$ satisfies

$$\gamma(\mathcal{P}_{\mathrm{FB}}) \leq \varepsilon(Q_{\mathrm{FB}}, R_{\mathrm{FB}}), \tag{3.18}$$

where $\varepsilon(\cdot, \cdot)$ is given by (3.14).

Proof of Lemma 1. Let $S_1 = 0$ and $\tilde{y}_1 := y_1 - Q_1^{-1}u_1$. Then, it follows from (3.13) that for any $u_1 \in \mathbb{L}_{2e}$,

$$\int_0^T \tilde{y}_1^\top(\tau)Q_1\tilde{y}_1(\tau)d\tau \leq \int_0^T u_1^\top(\tau)(Q_1^{-1} - R_1)u_1(\tau)d\tau - \rho_1.$$

holds. Because $u_1^\top(Q_1^{-1} - R_1)u_1 \leq \bar{\lambda}(Q_1^{-1} - R)u_1^\top u_1$ and $\underline{\lambda}(Q_1)\tilde{y}_1^\top\tilde{y}_1 \leq \tilde{y}_1^\top Q_1\tilde{y}_1$ hold, we have that

$$\underline{\lambda}(Q_1)\int_0^T \tilde{y}_1{}^\top(\tau)\tilde{y}_1(\tau)d\tau \leq \bar{\lambda}(Q_1^{-1} - R_1)\int_0^T u_1^\top(\tau)u_1(\tau)d\tau - \rho_1$$

holds for all $T \in \mathbb{R}_+$. It follows that

$$\|\tilde{y}_1\|_{L_2,T} \leq \frac{\sqrt{\underline{\lambda}(Q_1)\bar{\lambda}(Q_1^{-1} - R_1)}}{\underline{\lambda}(Q_1)}\|u_1\|_{L_2,T} - \frac{1}{\underline{\lambda}(Q_1)}\rho_1$$

for all $u_1 \in \mathbb{L}_{2e}$ and $T \in [0, \infty)$. Recalling that $y_1 = \tilde{y}_1 + Q_1^{-1}u_1$, we have

$$\|y_1\|_{L_2,T} \leq \|\tilde{y}_1\|_{L_2,T} + \frac{1}{\underline{\lambda}(Q_1)}\|u_1\|_{L_2,T} \leq \varepsilon(Q_1, R_1)\|u_1\|_{L_2,T} - \frac{1}{\underline{\lambda}(Q_1)}\rho_1.$$

Because $\|u_1\|_{L_2,T} \leq \|u_1\|_{L_2}$ holds for any $u_1 \in \mathbb{L}_2$, we show that

$$\|y_1\|_{L_2,T} \leq \varepsilon(Q_1, R_1)\|u_1\|_{L_2} - \frac{1}{\underline{\lambda}(Q_1)}\rho_1. \tag{3.19}$$

This implies that (3.19) holds as $T \to \infty$. It follows that $\Sigma_1 \in \mathcal{P}(Q_1, R_1)$ with $Q_1 > 0$ is L_2-stable, and (3.19) is reduced to

$$\|\Sigma_1\|_{L_2} \leq \varepsilon(Q_1, R_1) \tag{3.20}$$

with $\varepsilon(Q_1, R_1)$ of (3.14).

Finally, to show (3.15), we aim to find an example of the "worst" Σ_1 in $\mathcal{P}(Q_1, R_1)$ such that (3.20) is satisfied with the equality. Let us consider the state space representation of Σ_1 given by

$$y_1(s) = \left(\frac{2\sqrt{\underline{\lambda}(Q_1)\bar{\lambda}(Q_1^{-1} - R_1)}}{\underline{\lambda}(Q_1)}\frac{1}{Ts + 1} + \frac{1 - \sqrt{\underline{\lambda}(Q_1)\bar{\lambda}(Q_1^{-1} - R_1)}}{\underline{\lambda}(Q_1)}\right)u_1(s),$$

where $Q_1 > 0$ and $R_1 \geq 0$ with $Q_1^{-1} \geq R_1$. Then, we see that $\Sigma_1 \in \mathcal{P}(Q_1, R_1)$ holds. Note that the value of $\varepsilon(Q, R)$ in (3.14), which corresponds to performance criterion of $\mathcal{P}(Q_1, R_1)$, is equivalent to the actual L_2-gain $\|\Sigma_1\|_{L_2}$. This completes that (3.15) holds. □

Proof of Lemma 2. From Definition 4, we have that there exists $\rho_{\rm FB} \in \mathbb{R}$ such that the following inequality

$$
\begin{aligned}
&\sum_{i=1}^{2}\int_0^T (2u_i^\top(\tau)y_i(\tau) - y_i^\top(\tau)Q_i y_i(\tau) - u_i^\top(\tau)R_i u_i(\tau))d\tau \\
&= \int_0^T \sum_{i=1}^{2} \begin{bmatrix} u_i(\tau) \\ y_i(\tau) \end{bmatrix}^\top \begin{bmatrix} -R_i & I_m \\ I_m & -Q_i \end{bmatrix} \begin{bmatrix} u_i(\tau) \\ y_i(\tau) \end{bmatrix} d\tau \geq \rho_{\rm FB}
\end{aligned}
$$

holds for all $T \in \mathbb{R}_+$. Using (3.10) and (3.11), we show

$$
\begin{aligned}
&\sum_{i=1}^{2} \begin{bmatrix} u_i(\tau) \\ y_i(\tau) \end{bmatrix}^\top \begin{bmatrix} -R_i & I_m \\ I_m & -Q_i \end{bmatrix} \begin{bmatrix} u_i(\tau) \\ y_i(\tau) \end{bmatrix} \\
&= \begin{bmatrix} w(\tau) - y_2(\tau) \\ y_1(\tau) \end{bmatrix}^\top \begin{bmatrix} R_1 & I_m \\ I_m & -Q_1 \end{bmatrix} \begin{bmatrix} w(\tau) - y_2(\tau) \\ y_1(\tau) \end{bmatrix} + \begin{bmatrix} y_1(\tau) \\ y_2(\tau) \end{bmatrix}^\top \begin{bmatrix} -R_2 & I_m \\ I_m & -Q_2 \end{bmatrix} \begin{bmatrix} y_1(\tau) \\ y_2(\tau) \end{bmatrix} \\
&= \begin{bmatrix} w(\tau) \\ z(\tau) \\ y_2(\tau) \end{bmatrix}^\top \begin{bmatrix} -R_1 & I_m & R_1 \\ I_m & -Q_1 - R_2 & 0 \\ R_1 & 0 & -Q_2 - R_1 \end{bmatrix} \begin{bmatrix} w(\tau) \\ z(\tau) \\ y_2(\tau) \end{bmatrix}.
\end{aligned}
\tag{3.21}
$$

Note that $\mathrm{Ker}\,(Q_2 + R_1) \subseteq \mathrm{Ker}\,R_1$ holds. It follows that $Q_2 + R_1 \geq 0$ and

$$
R_1(Q_2 + R_1)^\dagger (Q_2 + R_1) = R_1 \tag{3.22}
$$

hold. This implies that completing the square with respect to y_2 is applied to the right hand side of (3.21). It follows that (3.21) satisfies

$$
\begin{aligned}
&\sum_{i=1}^{2} \begin{bmatrix} u_i(\tau) \\ y_i(\tau) \end{bmatrix}^\top \begin{bmatrix} -R_i & I_m \\ I_m & -Q_i \end{bmatrix} \begin{bmatrix} u_i(\tau) \\ y_i(\tau) \end{bmatrix} \\
&\leq \begin{bmatrix} w(\tau) \\ z(\tau) \end{bmatrix}^\top \begin{bmatrix} -R_1 & I_m \\ I_m & -Q_1 - R_2 \end{bmatrix} \begin{bmatrix} w(\tau) \\ z(\tau) \end{bmatrix} + \begin{bmatrix} w(\tau) \\ z(\tau) \end{bmatrix}^\top \begin{bmatrix} R_1 \\ 0 \end{bmatrix} (Q_2 + R_1)^\dagger \begin{bmatrix} R_1 \\ 0 \end{bmatrix}^\top \begin{bmatrix} w(\tau) \\ z(\tau) \end{bmatrix}.
\end{aligned}
$$

Substituting (3.22) into $-R_1 + R_1(Q_2 + R_1)^\dagger R_1$, we show that

$$\int_0^T \begin{bmatrix} w(\tau) \\ z(\tau) \end{bmatrix}^\top \begin{bmatrix} -R_{\mathrm{FB}} & I_m \\ I_m & -Q_{\mathrm{FB}} \end{bmatrix} \begin{bmatrix} w(\tau) \\ z(\tau) \end{bmatrix} d\tau \geq \rho_{\mathrm{FB}} \tag{3.23}$$

holds for all $T \in \mathbb{R}_+$, where Q_{FB} and R_{FB} are given by (3.16) and (3.17), i.e., $\Sigma_{\mathrm{FB}}(\Sigma_1, \Sigma_2) \in \mathcal{P}(Q_{\mathrm{FB}}, R_{\mathrm{FB}})$ holds. In addition, applying (3.20) to $\Sigma_{\mathrm{FB}}(\Sigma_1, \Sigma_2) \in \mathcal{P}(Q_{\mathrm{FB}}, R_{\mathrm{FB}})$, we show that $\mathcal{P}_{\mathrm{FB}} \subseteq \mathcal{P}(Q_{\mathrm{FB}}, R_{\mathrm{FB}})$ holds. This proves Lemma 2. □

As stated in Lemma 1, the value of $\varepsilon(Q_1, R_1)$ in (3.14) evaluates the L_2-gain of the model set $\mathcal{P}(Q_1, R_1)$. In particular, it should be emphasized that $\gamma(\mathcal{P}(Q_1, R_1))$ provides a *tight* performance evaluation for which only the passivity parameters Q_1 and R_1 is utilized. We see that the detailed models of Σ_1 is not required for the L_2-gain evaluation. On the other hand, Lemma 2 provides the performance evaluation of the L_2-gain of $\mathcal{P}_{\mathrm{FB}}(\mathcal{P}_1, \mathcal{P}_2)$. The evaluation is provided based on an outer-approximation of $\mathcal{P}_{\mathrm{FB}}(\mathcal{P}_1, \mathcal{P}_2)$, which is given by $\mathcal{P}(Q_{\mathrm{FB}}, R_{\mathrm{FB}})$. The outer-approximation is explicitly characterized by the parameter transition in (3.16) and (3.17). Let us consider Σ_{FB} described by a SISO system. Then, the outer-approximation $\mathcal{P}(Q_{\mathrm{FB}}, R_{\mathrm{FB}})$ is expressed by the disk region that contains the model set $\mathcal{P}_{\mathrm{FB}}(\mathcal{P}_1, \mathcal{P}_2)$, as shown in Fig. 3.5. It should be emphasized that only the passivity parameters characterizing each subsystem is utilized for the quantitative analysis of the feedback system, while the detailed model of the subsystem is not utilized. With the parameters in the outer-approximation, the L_2-gain of $\mathcal{P}_{\mathrm{FB}}$ can be evaluated in the sense of the upper bound $\varepsilon(Q_{\mathrm{FB}}, R_{\mathrm{FB}})$. To provide a solution to Problem 1, we introduce the following supplementary lemma.

Lemma 3. *Let $Y \geq 0$ and $Z \geq 0$. Then, (i) $\underline{\mathbb{V}}(Y)$ and* Ker Z *are disjoint if and only if (i i) $\underline{\lambda}(Y + Z) > \underline{\lambda}(Y)$ holds.*

Proof. (i ⇒ ii) We decompose any vector $q \in \underline{\mathbb{V}}(Y + Z)$ as $q = q_1 + q_2$, where $q_1 \in \mathrm{Im}\, Z$ and $q_2 \in \mathrm{Ker}\, Z$. Then, it follows that

$$\begin{aligned} \underline{\lambda}(Y + Z) &= q^\top (Y + Z) q \\ &= (q_1 + q_2)^\top Y (q_1 + q_2) + q_1^\top Z q_1. \end{aligned} \tag{3.24}$$

First, suppose that $q_1 \neq 0$. Note $(q_1 + q_2)^\top Y (q_1 + q_2) \geq \underline{\lambda}(Y)$ and $q_1^\top Z q_1 > 0$ hold. This implies that $\underline{\lambda}(Y + Z) > \underline{\lambda}(Y)$ holds. Next, suppose that $q_1 = 0$ or $q \in \mathrm{Ker}\, Z$ holds. Then, it is shown that the right-hand side of (3.24) is equivalent to $q_2^\top Y q_2$. From the statement

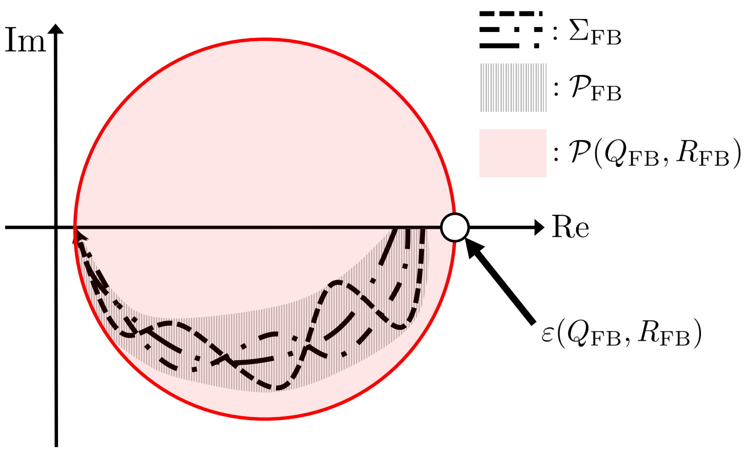

Figure 3.5: The graphical illustration of the outer-approximation of $\mathcal{P}_{\mathrm{FB}}$ given by $\mathcal{P}(Q_{\mathrm{FB}}, R_{\mathrm{FB}})$ in the closed right-half plane of the complex plane. The outer-approximation is expressed by the disk region that is explicitly characterized by two parameters Q_{FB} and R_{FB}. In the figure, the white circle depicts the performance index $\varepsilon(Q_{\mathrm{FB}}, R_{\mathrm{FB}})$.

i), we show that $q_2 \notin \underline{\mathbb{V}}(Y) \setminus \{0\}$ holds, which implies $q_2^\top Y q_2 > \underline{\lambda}(Y)$. This completes that $\underline{\lambda}(Y+Z) > \underline{\lambda}(Y)$.

(ii $\Rightarrow$ i) suppose that $\underline{\mathbb{V}}(Y)$ and $\operatorname{Ker} Z$ are not disjoint to show a contradiction, equivalently, there exists $v \in \underline{\mathbb{V}}(Y)$ satisfying $v \in \operatorname{Ker} Z \setminus \{0\}$. From this supposition, we show that $\underline{\lambda}(Y+Z) \leq v^\top (Y+Z) v = \underline{\lambda}(Y)$ holds. This contradicts the statement ii). □

On the basis of Lemmas 1, 2, and 3, we provide a solution to Problem 1, i.e., conditions on Q_i and R_i to achieve the performance improvement (3.12) in the following theorem.

Theorem 2. *In addition to the condition of Lemma 2, suppose that $Q_1 > 0$ holds. Then, the following two statements hold:*

i) Suppose that $Q_2 = q_2 I_m > 0$, $R_1 = r_1 I_m > 0$, and $q_2 \underline{\lambda}(R_2) \geq \underline{\lambda}(Q_1) r_1$ hold. Then, (3.12) holds.

ii) Suppose that either $Q_2 = 0$ or $R_1 = 0$ holds. Then, $\underline{\mathbb{V}}(Q_1)$ and $\operatorname{Ker} R_2$ are disjoint if and only if (3.12) holds.

Proof. i) Suppose that $R_1 = r_1 I_m > 0$ and $Q_2 = q_2 I_m \geq 0$ hold. From Lemma 2, $\mathcal{P}_{\mathrm{FB}} \subseteq \mathcal{P}(Q_{\mathrm{FB}}, R_{\mathrm{FB}})$ holds, where Q_{FB} and R_{FB} are given in (3.16) and (3.17). In addition, from Lemma 1, $\varepsilon(Q_1, R_1)$ and $\varepsilon(Q_{\mathrm{FB}}, R_{\mathrm{FB}})$ are given by

$$\begin{aligned}\varepsilon(Q_1, R_1) &= \frac{1+\sqrt{1-\underline{\lambda}(Q_1)r_1}}{\underline{\lambda}(Q_1)},\\ \varepsilon(Q_{\mathrm{FB}}, R_{\mathrm{FB}}) &= \frac{1+\sqrt{1-\underline{\lambda}(Q_1+R_2)\dfrac{q_2 r_1}{q_2+r_1}}}{\underline{\lambda}(Q_1+R_2)}.\end{aligned}$$

Note that $\underline{\lambda}(Q_1+R_2) \geq \underline{\lambda}(Q_1)+\underline{\lambda}(R_2)$ and suppose that $q_2\underline{\lambda}(R_2) \geq \underline{\lambda}(Q_1)r_1$ holds. Then, we show that

$$\begin{aligned}\underline{\lambda}(Q_1+R_2)\frac{q_2 r_1}{q_2+r_1} - \underline{\lambda}(Q_1)r_1 &= \frac{q_2 r_1}{q_2+r_1}(\underline{\lambda}(Q_1+R_2)-\underline{\lambda}(Q_1)) - \frac{r_1^2}{q_2+r_1}\underline{\lambda}(Q_1)\\ &\geq \frac{r_1}{q_2+r_1}(q_2\underline{\lambda}(R_2)-\underline{\lambda}(Q_1)r_1) \geq 0 \end{aligned} \tag{3.25}$$

holds. Noting that $q_2/(q_2+r_1) < 1$ holds in (3.25), we have

$$\underline{\lambda}(Q_1+R_2) > \underline{\lambda}(Q_1). \tag{3.26}$$

From (3.25) and (3.26), we show that

$$\varepsilon(Q_{\mathrm{FB}}, R_{\mathrm{FB}}) < \varepsilon(Q_1, R_1) \tag{3.27}$$

holds. This completes that (3.12) holds.

ii) Suppose that either $Q_2 = 0$ or $R_1 = 0$ holds. Then, $\varepsilon(Q_1, R_1)$ and $\varepsilon(Q_{\mathrm{FB}}, R_{\mathrm{FB}})$ are given by

$$\varepsilon(Q_1, R_1) = \frac{2}{\underline{\lambda}(Q_1)}, \quad \varepsilon(Q_{\mathrm{FB}}, R_{\mathrm{FB}}) = \frac{2}{\underline{\lambda}(Q_1+R_2)}.$$

As stated in Lemma 3, we show that $\underline{\mathbb{V}}(Q_1)$ and $\operatorname{Ker} R_2$ are disjoint if and only if (3.26) holds. It follows that (3.27) holds, equivalently, (3.12) holds. This completes the proof of Theorem 2. □

Theorem 2 provides a model set describing subsystems to achieve the performance improvement of the feedback system, which corresponds to a solution to Problem 1. This theorem is one of the main contribution of this chapter.

Remark 1. *Suppose that Σ_i in (3.9) is L_2-stable and the initial state of Σ_i is zero. Then, for any $u_i \in \mathbb{L}_2$ and its corresponding output y_i, the inequality (3.13) holds even if $T \rightarrow$*

∞ and $\rho_i = 0$. By Parseval's theorem, the inequality (3.13) as $T \to \infty$ is equivalently transformed into the inequality to

$$\int_{-\infty}^{\infty} \left\{ \hat{u}_i^\top(j\omega)\hat{y}_i(j\omega) - \frac{1}{2}\hat{y}_i^\top(j\omega)Q(\omega)\hat{y}_i(j\omega) - \frac{1}{2}\hat{u}_i^\top(j\omega)R(\omega)\hat{u}_i(j\omega) \right\} d\omega \geq 0, \tag{3.28}$$

where $Q(\omega)$ and $R(\omega)$ are positive semidefinite and bounded matrix-valued frequency functions, and $\hat{u}_i$ and $\hat{y}_i$ denote the Fourier transforms of u_i and y_i, respectively. On the basis of (3.28), we introduce the following expression. The system Σ_i is said to be the frequency-dependent (Q, R)-passive if, for any $u_i \in \mathbb{L}_2$ and its corresponding output y_i, (3.28) holds. If $Q(\omega) = Q$ and $R(\omega) = R$ hold, i.e., the parameters are independent of ω, the inequality (3.28) is equivalent to (3.13) in Definition 4. For some $Q(\omega)$ and $R(\omega)$, let $\mathcal{P}_\omega(Q(\omega), R(\omega))$ be defined as the set of dynamical systems satisfying (3.28). The definition of the model set $\mathcal{P}_\omega(Q(\omega), R(\omega))$ implies that $\mathcal{P}_\omega(Q(\omega), R(\omega))$ is a more general description than $\mathcal{P}(Q, R)$. The introduction of the frequency-dependent model set enables us to address the performance improvement problem in the sense of the frequency-dependent gain of the model set. Let us assume that Σ_i is given a LTI system and recall that the transfer function is represented by $\mathcal{S}_i(s)$. Then, the frequency-dependent gain of $\mathcal{P}_i = \mathcal{P}_\omega(Q_i(\omega), R_i(\omega))$ is defined as

$$\tilde{\gamma}(\mathcal{P}_i, \omega) := \sup_{\mathcal{S}_i \in \mathcal{P}_i} \bar{\sigma}(\mathcal{S}_i(j\omega)).$$

Suppose that $\mathcal{P}_1 = \mathcal{P}_\omega(Q_1(\omega), R_1(\omega))$ and $Q_1(\omega) > 0$ for all $\omega \in \mathbb{R}$. Then, is is shown that the gains of $\mathcal{P}_1$ and $\mathcal{P}_{\mathrm{FB}}$ satisfies

$$\begin{aligned} \tilde{\gamma}(\mathcal{P}_1, \omega) &= \varepsilon(Q_1(\omega), R_1(\omega)), \quad \forall \omega \in \mathbb{R}, \\ \tilde{\gamma}(\mathcal{P}_{\mathrm{FB}}, \omega) &\leq \varepsilon(Q_{\mathrm{FB}}(\omega), R_{\mathrm{FB}}(\omega)), \quad \forall \omega \in \mathbb{R}, \end{aligned}$$

where $Q_{\mathrm{FB}}(\omega)$ and $R_{\mathrm{FB}}(\omega)$ are given by (3.16) and (3.17), and $\varepsilon(\cdot, \cdot)$ is given by (3.14). In a similar manner to the analysis in Theorem 1, we can find conditions on $Q_i(\omega)$ and $R_i(\omega)$ such that for all frequency points the performance improvement is achieved, i.e., it follows that

$$\tilde{\gamma}(\mathcal{P}_{\mathrm{FB}}, \omega) < \tilde{\gamma}(\mathcal{P}_1, \omega)$$

for all $\omega \in \mathbb{R}$. In addition, letting $\Omega \subset \mathbb{R}_+$ be a finite interval, we consider $Q_i(\omega)$ and $R_i(\omega)$ given by

$$Q_i(\omega) = \begin{cases} Q_i, & \omega \in \Omega \\ 0, & \text{otherwise}, \end{cases} \qquad R_i(\omega) = \begin{cases} R_i, & \omega \in \Omega \\ 0, & \text{otherwise}. \end{cases}$$

The frequency-dependent (Q, R)-passivity with the above parameters is defined on a finite frequency range specified by Ω, rather than infinite integration interval. On the basis of this fact, we can find conditions on Q_i and R_i such that the performance improvement of the feedback system involving non-passive subsystems is achieved in the range Ω.

3.4.2 Performance Analysis and Improvement of Iterative Feedback Systems

In this subsection, the model-set-based performance improvement in Theorem 2 is extended to that of the iterative feedback system, which expresses a simplified class of an evolving network system. The iterative feedback system is constructed by connecting multiple subsystems to a baseline system in a step-by-step manner. In particular, each subsystem in the iterative feedback system is assumed to be locally implemented to the baseline system as shown in Fig. 3.1. In this subsection, we aim at finding a model set describing connected subsystems such that the performance improvement of the iterative feedback system is *gradually* achieved with the implementation progress. For simplicity of analysis, we focus on the one progress of the connection of one subsystem. Then, a port selection of the subsystem connection is provided to achieve the performance improvement, i.e., the L_2-gain of the model set describing the entire iterative feedback system strictly decreases as compared to that describing the connected subsystem.

To construct an iterative feedback system, let us first consider a baseline system Σ_0 given by

$$\Sigma_0 : y = \mathcal{S}_0 u, \tag{3.29}$$

where $u \in \mathbb{R}^m$ and $y \in \mathbb{R}^m$ is the input and output of Σ_0, and $\mathcal{S}_0 : \mathbb{L}_{2e} \to \mathbb{L}_{2e}$ is a causal operator. In order to explicitly describe the port number in the output of Σ_0, let y be partitioned as $y =: [y_1^\top \ y_2^\top \ \cdots \ y_m^\top]^\top$, where the symbol ℓ in $y_\ell \in \mathbb{R}$ denotes the port number of the output. Furthermore, let us consider a subsystem Σ_ℓ, which is connected to the ℓ-th port of Σ_0, described by

$$\Sigma_\ell : v_\ell = \mathcal{S}_\ell y_\ell, \tag{3.30}$$

where $v_\ell \in \mathbb{R}$ is the output of Σ_ℓ and $\mathcal{S}_\ell : \mathbb{L}_{2e} \to \mathbb{L}_{2e}$ is a causal operator. Now, let an operator $\mathcal{F}_\ell$ be defined as

$$\mathcal{F}_\ell = E_\ell \otimes \mathcal{S}_\ell, \tag{3.31}$$

where $E_\ell = e_\ell e_\ell^\top \in \mathbb{R}^{m\times m}$. The symbol e_ℓ denotes the unit vector whose the only ℓ-th element is one. By using the input-output operator of (3.31), each subsystem Σ_ℓ can be rewritten as an another subsystem Π_ℓ, which is described by

$$\Pi_\ell : v = \mathcal{F}_\ell y, \tag{3.32}$$

where $v = [v_1^\top \; v_2^\top \; \cdots \; v_m^\top]^\top$. From (3.31) and (3.32), we see that Π_ℓ is a redundant description of Σ_ℓ, which comes from implementation of the subsystem Σ_ℓ in a decentralized manner. The feedback connection of Π_ℓ to Σ_0 is described by

$$u = w - v, \tag{3.33}$$

$$z = y. \tag{3.34}$$

We interconnect Σ and Π_ℓ via the the negative feedback connection in (3.33) and (3.34). Then, the entire control system with the input w and output z is constructed and denoted by $\Sigma_{\text{ent}}(\Sigma_0, \Sigma_\ell)$. Let $\mathcal{P}_0$ and $\mathcal{P}_\ell$ be the model sets describing Σ_0 and Σ_ℓ, respectively. Then, the model set describing $\Sigma_{\text{ent}}(\Sigma_0, \Sigma_\ell)$ is described as

$$\mathcal{P}_{\text{ent},\ell} := \mathcal{P}_{\text{FB}}(\mathcal{P}_0, \mathcal{P}_\ell).$$

In the following discussion, Σ_0 is assumed to be passive and strictly proper. In addition, $\mathcal{P}_0 = \mathcal{P}(Q, 0)$ holds for some $Q \geq 0$. Under these preliminary, we show the performance improvement of $\Sigma_{\text{ent}}(\Sigma, \Sigma_\ell)$ in the following theorem.

Theorem 3. *Suppose that for some $q_\ell \geq 0$ and $r_\ell \geq 0$, $\mathcal{P}_0 = \mathcal{P}(Q, 0)$ and $\mathcal{P}_\ell = \mathcal{P}(q_\ell E_\ell, r_\ell E_\ell)$ hold. Then, for $Q_{\text{ent},\ell} \geq 0$ given by*

$$Q_{\text{ent},\ell} = Q + r_\ell E_\ell, \tag{3.35}$$

it holds that $\mathcal{P}_{\text{ent},\ell} \subseteq \mathcal{P}(Q_{\text{ent},\ell}, 0)$. In addition, suppose that $Q > 0$ and $r_\ell > 0$ hold. Then, the ℓ-th entry of any $v \in \underline{\mathbb{V}}(Q)$ is nonzero if and only if

$$\gamma(\mathcal{P}_{\text{ent},\ell}) < \gamma(\mathcal{P}_0). \tag{3.36}$$

Proof. As stated in Lemma 2, it is shown that $\mathcal{P}_{\text{ent},\ell} \subseteq \mathcal{P}(Q_{\text{ent},\ell}, 0)$ holds. Next, we show that the ℓ-th entry of any vector $v \in \underline{\mathbb{V}}(Q)$ is nonzero if and only if (3.36) holds.

(Necessary condition for (3.36)) Suppose that $Q > 0$, $r_\ell > 0$, and (3.36) hold, and equivalently

$$\underline{\lambda}(Q_{\text{ent},\ell}) > \underline{\lambda}(Q). \tag{3.37}$$

As stated in Lemma 3, we see that $\underline{\mathbb{V}}(Q)$ and $\operatorname{Ker} E_\ell$ are disjoint, and equivalently for any $v \in \underline{\mathbb{V}}(Q)$, $v \notin \operatorname{Ker} E_\ell \setminus \{0\}$ holds. This implies that the ℓ-th entry of any $v \in \underline{\mathbb{V}}(Q)$ is nonzero because $\operatorname{Ker} E_\ell = \operatorname{span}\{e_1, \ldots, e_{\ell-1}, e_{\ell+1}, \ldots, e_m\}$ holds.

(Sufficient condition for (3.36)) Suppose that the ℓ-th element of any vector $v \in \underline{\mathbb{V}}(Q)$ is nonzero. Then, $v \notin \operatorname{Ker} E_\ell \setminus \{0\}$ holds, equivalently $\underline{\mathbb{V}}(Q)$ and $\operatorname{Ker} E_\ell$ are disjoint. As stated in Lemma 3, it is shown that $\underline{\lambda}(Q_{\mathrm{ent},\ell}) > \underline{\lambda}(Q)$ holds. This completes that (3.36) holds. □

Theorem 3 states that $\mathcal{P}_{\mathrm{ent},\ell}$ has the passivity property independently of the port selection of connected subsystems. In a similar manner to Lemma 2, Theorem 3 provides the performance evaluation of $\mathcal{P}_{\mathrm{ent},\ell}$. The L_2-gain evaluation is provided based on an outer-approximation of $\mathcal{P}_{\mathrm{ent},\ell}$ given by $\mathcal{P}(Q_{\mathrm{ent},\ell}, 0)$, which is explicitly characterized by the parameter transition in (3.35). In addition, as stated in Theorem 3, we find a condition of port selection to achieve the performance improvement, i.e., the L_2-gain of $\mathcal{P}_{\mathrm{ent},\ell}$ is strictly less than that of $\mathcal{P}(Q, 0)$. In both of Theorems 2 and 3, a condition of the passivity parameters to achieve the performance improvement is provided. Theorem 2 addresses the feedback system composed of general subsystems and provides a general condition for the improvement. On the other hand, Theorem 3 is a special result of Theorem 2 by focusing on the specified structure in subsystems due to the implementation in the decentralized manner.

On the basis of Theorem 3, it is easy to find conditions on the passivity parameters to achieve performance improvement of the iterative feedback system. It should be emphasized here that the condition for performance improvement in Theorem 3 is imposed on the connection port of the subsystem Σ_ℓ (equivalently subsystem Π_ℓ with the specified structure). This implies that we need to check the condition for the performance improvement at every connection step. By restricting the class of Q, the performance improvement can be shown under a requirement only on the baseline system Σ_0 independently of the port selection.

Proposition 2. *Suppose that $\mathcal{P}_0 = \mathcal{P}(Q, 0)$ and $\mathcal{P}_\ell = \mathcal{P}(q_\ell E_\ell, r_\ell E_\ell)$ hold for $Q \in \mathbb{M}$, $q_\ell \geq 0$, and $r_\ell > 0$, where $\mathbb{M}$ denotes the set of M-matrices [54]. Then, for any ℓ, $Q_{\mathrm{ent},\ell} \in \mathbb{M}$ and $\mathcal{P}_{\mathrm{ent},\ell} \subseteq \mathcal{P}(Q_{\mathrm{ent},\ell}, 0)$ hold. Furthermore, Q is irreducible if and only if for any ℓ, (3.36) holds.*

Proof. Because of the parameter transition (3.35), we straightforwardly show that, for any ℓ, all off-diagonal entries of $Q_{\mathrm{ent},\ell}$ do not vary from those of Q. It follows that, for any ℓ, $Q_{\mathrm{ent},\ell} \in \mathbb{M}$ and $\mathcal{P}_{\mathrm{ent},\ell} \subseteq \mathcal{P}(Q_{\mathrm{ent},\ell}, 0)$ hold.

Next, we show that Q is irreducible if and only if for any ℓ, (3.36) holds.

(Necessary condition for (3.36)) Suppose that $Q > 0$, $r_\ell > 0$, and (3.36) hold, and equivalently (3.37) holds. As stated in Lemma 3, we have that $\underline{\mathbb{V}}(Q)$ and $\mathrm{Ker}\, E_\ell$ are disjoint. To derive a contradiction, we suppose that Q is reducible. Then, it is shown that there exists a permutation matrix U such that $UQU^\top$ is a block diagonal because the symmetric and reducible property of Q. This implies that at least one element of $v \in \underline{\mathbb{V}}(Q)$ is zero. This contradicts that, for any ℓ, (3.36) holds.

(Sufficient condition for (3.36)) Suppose that $Q \in \mathbb{M}$ is irreducible. Let δ be the maximum value of the diagonal element of Q. Then, Q can be described by

$$Q = \delta I_m - \Xi, \tag{3.38}$$

where $\Xi \in \mathbb{R}^{m\times m}$ is an irreducible non-negative matrix. By the Perron–Frobenius theorem [55], all entries of the eigenvector corresponding to $\bar{\lambda}(\Xi)$ take positive values. It follows that, from (3.38), all entries of $v \in \underline{\mathbb{V}}(Q) \setminus \{0\}$ are positive, equivalently, for any ℓ, $v \notin \mathrm{Ker}\, E_\ell$ holds. As stated in Lemma 3, it is shown that (3.37) holds. Therefore, it follows that for any ℓ, (3.36) holds. $\square$

As stated in Proposition 2, we provide conditions on a passivity parameter Q in $\mathcal{P}(Q, 0)$ describing Σ_0 to achieve the *gradual* performance improvement. In Proposition 2, it is shown that the parameter $Q_{\mathrm{ent},\ell}$ preserves being the M-matrix independently of the port selection of the connected system. Furthermore, as long as Q is *irreducible*, the performance improvement is achieved for *any* port selection. These facts implies that as long as the passivity parameter in the model set describing Σ_0 is characterized by the irreducible M-matrix and the connected system is input strictly passive, the performance improvement is always achieved for the connection to any *any port* of the baseline system at *any step*. In this sense, Proposition 2 provides a condition for Q to achieve a *gradual* improvement.

On the basis of the fact stated in Remark 1, the analysis in this section can also be extendable to a more general analysis in which the model set is characterized by the frequency dependent parameters.

Remark 2. *As stated in Proposition 2, the model set describing Σ_0 requires a severe condition to mathematically show the performance improvement. The condition that Q is an M-matrix is technical. In most cases, even though Q is not an M-matrix, $v \in \underline{\mathbb{V}}(Q)$ can have no zero entries. Essentially, the irreducibility of Q plays an important role to achieve the gradual improvement of iterative feedback system.*

3.5 Performance Improvement Analysis of Frequency Control in Power Systems

In this section, we illustrate the performance improvement of the iterative feedback system, which is studied in Subsection 3.4.2, through the frequency control of power systems.

3.5.1 Linearized Power System Model

At an equilibrium point $(\delta_i^*, \omega_i^*, P_{\mathrm{m}i}^*, \theta_i^*, V_i^*)$of the nonlinear power system given by (3.1), (3.2) and (3.5), we assume that the differences between the phase angles at the terminal and between the rotor angle of the generator and the phase angle at the terminal bus are sufficiently small; i.e., $\theta_i^* - \theta_j^* \approx 0$ and $\delta_i^* - \theta_i^* \approx 0$ hold [56,57]. In all variables of generator dynamics and the power flow equation, we define $\tilde{\cdot}$ as the deviation variables from the equilibrium point. Let

$$\begin{aligned}
&\delta := \mathrm{col}(\tilde{\delta}_i)_{i\in\mathcal{V}_{\mathrm{G}}},\ \omega := \mathrm{col}(\omega_i)_{i\in\mathcal{V}_{\mathrm{G}}},\ P_{\mathrm{m}} := \mathrm{col}(\tilde{P}_{\mathrm{m}i})_{i\in\mathcal{V}_{\mathrm{G}}},\\
&\theta := \begin{bmatrix}\mathrm{col}(\tilde{\theta}_i)_{i\in\mathcal{V}_{\mathrm{G}}}^\top & \mathrm{col}(\tilde{\theta}_i)_{i\in\mathcal{V}\setminus\mathcal{V}_{\mathrm{G}}}^\top\end{bmatrix}^\top,\ x := \begin{bmatrix}\delta^\top & \omega^\top & P_{\mathrm{m}}^\top\end{bmatrix}^\top,\\
&u := \mathrm{col}(\tilde{P}_{\mathrm{R}i})_{i\in\mathcal{V}_{\mathrm{R}}}.
\end{aligned} \tag{3.39}$$

Linearizing (3.1) and (3.2) around $(\delta_i^*, \omega_i^*, P_{\mathrm{m}i}^*, \theta_i^*, V_i^*)$ and assuming that $\theta_i^* - \theta_j^* \approx 0$ and $\delta^* - \theta^* \approx 0$ hold, we have

$$\dot{x} = A_{11}x + A_{12}\theta, \tag{3.40}$$

where the coefficient matrices are described by

$$A_{11} := \begin{bmatrix} 0 & I & 0 \\ -M^{-1}X_d & -M^{-1}D & M^{-1} \\ 0 & -T^{-1}K_\omega & -T^{-1}\end{bmatrix},\ A_{12} := \begin{bmatrix} 0 & 0 \\ M^{-1}X_d & 0 \\ 0 & 0\end{bmatrix}.$$

The symbols M, D, T, K_ω, and X_d represent diagonal matrices in which diagonal entries are $m_i, d_i, \tau_i, k_{\omega_i}$, and $E_iV_i^*/x_{di}, i \in \mathcal{V}_{\mathrm{G}}$, respectively. From the linearized generator dynamics in (3.40), we see that the term pertaining to the voltage amplitude at buses does not appear. In addition, linearizing (3.5) around $(\delta_i^*, \omega_i^*, P_{\mathrm{m}i}^*, \theta_i^*, V_i^*)$, we have

$$A_{21}x + A_{22}\theta + B_{\mathrm{R}}u = 0,\ L_V V = 0, \tag{3.41}$$

where $V := \mathrm{col}(\tilde{V}_i)_{i\in\mathcal{V}}$ and $L_V \in \mathbb{R}^{N_\mathrm{B}\times N_\mathrm{B}}$ is a positive definite matrix and the coefficient matrices are described by

$$A_{21} := \begin{bmatrix} X_d & 0 & 0 \\ 0 & 0 & 0 \end{bmatrix},\ A_{22} := -L - \mathrm{diag}(X_d, O_{N_\mathrm{B}-N_\mathrm{G}}),$$
$$B_\mathrm{R} := \begin{bmatrix} 0 \\ F \end{bmatrix} \in \mathbb{R}^{N_\mathrm{B}\times N_\mathrm{R}},\ F := \begin{bmatrix} I_{N_\mathrm{R}} \\ 0 \end{bmatrix} \in \mathbb{R}^{(N_\mathrm{B}-N_\mathrm{G})\times N_\mathrm{R}}.$$

The symbol $L \in \mathbb{R}^{N_\mathrm{B}\times N_\mathrm{B}}$ is a Laplacian matrix that is described by

$$\{L\}_{ij} := \begin{cases} \displaystyle\sum_{j\in\mathcal{N}_i}^{N_\mathrm{B}} B_{ij}V_i^* V_j^*, & i = j, \\ -B_{ij}V_i^* V_j^*, & i \neq j, \end{cases}$$

which represents the interconnection between buses. From (3.40) and (3.41), the dynamics with respect to θ and V is completely decoupled in the linearized model; therefore V does not affect the dynamics of the linearized model. Thus, the linearized power system model is given by

$$\begin{bmatrix} \dot{x} \\ 0 \end{bmatrix} = \begin{bmatrix} A_{11} & A_{12} \\ A_{21} & A_{22} \end{bmatrix} \begin{bmatrix} x \\ \theta \end{bmatrix} + \begin{bmatrix} 0 \\ B_\mathrm{R} \end{bmatrix} u. \tag{3.42}$$

In (3.42), we show that A_{22} is non-singular because the topology of the baseline power system is described by the strongly connected graph. It follows that $\theta = -A_{22}^{-1}(A_{21}x + B_\mathrm{R}\tilde{P}_\mathrm{R})$ holds. Let L be partitioned as

$$L = \begin{bmatrix} L_{11} & L_{12} \\ L_{12}^\top & L_{22} \end{bmatrix},$$

where $L_{11} \in \mathbb{R}^{N_\mathrm{G}\times N_\mathrm{G}}$, $L_{12} \in \mathbb{R}^{N_\mathrm{G}\times(N_\mathrm{B}-N_\mathrm{G})}$, and $L_{22} \in \mathbb{R}^{(N_\mathrm{B}-N_\mathrm{G})\times(N_\mathrm{B}-N_\mathrm{G})}$. Then, the power system (3.42) is reduced to the following state-space equation:

$$\dot{x} = Ax + Bu, \tag{3.43}$$

where the coefficient matrices are described by

$$A = \begin{bmatrix} 0 & I & 0 \\ -M^{-1}\Gamma & -M^{-1}D & M^{-1} \\ 0 & -T^{-1}K_\omega & -T^{-1} \end{bmatrix}, \, B = \begin{bmatrix} 0 \\ -M^{-1}X_d(L_{\mathrm{red}} + X_d)^{-1}L_{12}L_{22}^{-1}F \\ 0 \end{bmatrix}$$

and

$$\begin{aligned} \Gamma &= X_d - X_d(L_{\mathrm{red}} + X_d)^{-1}X_d, \\ L_{\mathrm{red}} &= L_{11} - L_{12}L_{22}^{-1}L_{12}^\top. \end{aligned} \tag{3.44}$$

Furthermore, the output equation of the power system is described as

$$y = Cx, \tag{3.45}$$

where the coefficient matrix $C \in \mathbb{R}^{N_{\mathrm{R}} \times 3N_{\mathrm{G}}}$ is given by

$$C = \begin{bmatrix} 0 & \Pi & 0 \end{bmatrix}$$

and $\Pi \in \mathbb{R}^{N_{\mathrm{R}} \times N_{\mathrm{G}}}$ is given by

$$\Pi := -(X_d(L_{\mathrm{red}} + X_d)^{-1}L_{12}L_{22}^{-1}F)^\top. \tag{3.46}$$

The output y means the weighted sum of the frequency deviations ω. In addition, each element of Π corresponds to the weighting factor π_{ij} in (3.8) as stated in Section 3.2. The baseline power system, denoted by Σ, is described as

$$\Sigma : \begin{cases} \dot{x} = Ax + Bu, \\ y = Cx. \end{cases} \tag{3.47}$$

3.5.2 Analysis of Model Set of Power System Based on Port-Hamiltonian Systems

In this subsection, we provide analysis of the model set of the baseline power system in (3.47). To this end, we first introduce a port-Hamiltonian system as follow.

The port-Hamiltonian system [58] is well known as a standard description of passive systems. It focuses on the stored energy and the energy dissipation of the system. For simplicity, consider that $\Sigma \in \mathcal{P}(Q, 0)$ holds. Then, the aim of this subsection is to provide a physical interpretation of the passivity parameter Q. To this end, we extract the passivity parameter from the port-Hamiltonian system. A linear port-Hamiltonian system is described by

$$\Sigma : \begin{cases} \dot{x} = (J - S)Px + Bu, \\ y = B^\top Px, \end{cases} \tag{3.48}$$

where $x \in \mathbb{R}^n$, $u \in \mathbb{R}^m$, and $y \in \mathbb{R}^m$ denote the state, input, and output of Σ, respectively, and $B \in \mathbb{R}^{n\times m}$ is a coefficient matrix. In addition, $J \in \mathbb{R}^{n\times n}$ and $S \in \mathbb{R}^{n\times n}$ with $J = -J^\top$ and $S \geq 0$ represent the interconnection of the internal state and the energy dissipation of Σ, respectively. The positive semi-definite matrix $P \in \mathbb{R}^{n\times n}$ is related to the energy function of $\mathcal{H}(x) = \frac{1}{2}x^\top Px$. For the given port-Hamiltonian system (3.48), we find Q that describes Σ with $\mathcal{P}(Q, 0)$ in the following proposition.

Proposition 3. *Given Σ in (3.48), there exists $Q \geq 0$ satisfying $2S \geq BQB^\top$ such that $\Sigma \in \mathcal{P}(Q, 0)$ holds. In addition, the following statements hold:*

i) If $\operatorname{Im} S \subseteq \operatorname{Im} B$ holds, there exists $Q \geq 0$ satisfying $2S = BQB^\top$ such that $\Sigma \in \mathcal{P}(Q, 0)$ holds.

ii) If $\operatorname{Im} B \subseteq \operatorname{Im} S$ holds, there exists $Q > 0$ satisfying $2S \geq BQB^\top$ such that $\Sigma \in \mathcal{P}(Q, 0)$ holds.

iii) If $\operatorname{Im} B = \operatorname{Im} S$ holds, there exists $Q > 0$ satisfying $2S = BQB^\top$ such that $\Sigma \in \mathcal{P}(Q, 0)$ holds.

Proof. The derivative of the energy function $\mathcal{H}(x)$ along a trajectory of (3.48) is given by

$$\frac{d}{dt}\mathcal{H} = u^\top y - x^\top PSPx.$$

Noting that we can always obtain $Q \geq 0$ satisfying $2S \geq BQB^\top$, we have

$$\frac{d}{dt}\mathcal{H} \leq u^\top y - \frac{1}{2}y^\top Qy. \tag{3.49}$$

Integrating (3.49) from $t = 0$ to $t = T$, and letting $\mathcal{H}(x(0)) := -\rho$, we show

$$\begin{aligned} \int_0^T \left\{ u^\top(\tau)y(\tau) - \frac{1}{2}y^\top(\tau)Qy(\tau) \right\} d\tau &\geq \mathcal{H}(x(T)) + \rho \\ &\geq \rho \end{aligned}$$

holds. This means that $\Sigma \in \mathcal{P}(Q,0)$ holds for $Q \geq 0$ satisfying $2S \geq BQB^\top$.

Next, we prove the three statements i), ii), and iii).

i) This statement is trivial. The proof is omitted.

ii) Some $Q = qI_m > 0$ satisfies this statement.

iii) The statements i) and ii) imply iii). □

Proposition 3 provides some examples of Q that describe passive systems. To further understand the proposition, for simplicity, we assume that $B = I_m$ and $\mathrm{Im}\, B = \mathrm{Im}\, S$ hold. From statement iii), we see that $Q = 2S$ holds. This implies that Q represents the energy dissipation given by S. On the basis of Proposition 3, we provide the model set analysis of the baseline power system (3.47) as follows.

Lemma 4. *Consider Σ given by (3.47). Then, there exists $Q > 0$ satisfying $2S \geq BQB^\top$ such that $\Sigma \in \mathcal{P}(Q,0)$ holds for $S = \mathrm{diag}(O_{N_\mathrm{G}}, M^{-2}D, T^{-2}K_\omega)$.*

Proof. Applying the Schur complement to L, we show that L_red of (3.44) is positive semi-definite. From this fact, $L_\mathrm{red} + X_d \geq X_d$ holds. It follows that

$$\begin{aligned} \mathit{\Gamma} &= X_d - X_d(L_\mathrm{red} + X_d)^{-1}X_d \\ &\geq X_d - X_d X_d^{-1} X_d = 0. \end{aligned}$$

This implies that $\mathit{\Gamma}$ is positive semi-definite. We define a positive semi-definite $P \in \mathbb{R}^{2N_\mathrm{G} \times 2N_\mathrm{G}}$ as

$$P = \begin{bmatrix} \mathit{\Gamma} & 0 & 0 \\ 0 & M & 0 \\ 0 & 0 & TK_\omega^{-1} \end{bmatrix}.$$

Then, Σ has the port-Hamiltonian form, where $J \in \mathbb{R}^{3N_\mathrm{G} \times 3N_\mathrm{G}}$ and $S \in \mathbb{R}^{3N_\mathrm{G} \times 3N_\mathrm{G}}$ are given by

$$J = \begin{bmatrix} 0 & M^{-1} & 0 \\ -M^{-1} & 0 & M^{-1}T^{-1}K_\omega \\ 0 & -M^{-1}T^{-1}K_\omega & 0 \end{bmatrix},$$

and $S = \mathrm{diag}(O_{N_\mathrm{G}}, M^{-2}D, T^{-2}K_\omega)$. Because $J = -J^\top$ and $S \geq 0$ hold, we see that the port-Hamiltonian system Σ is passive. Note that $\mathrm{Im}\, B \subseteq \mathrm{Im}\, S$ holds. From Proposition 3, it follows that there exists $Q > 0$ satisfying $2S \geq BQB^\top$ such that $\Sigma \in \mathcal{P}(Q,0)$. □

In Lemma 4, it should be emphasized that $\operatorname{Im} B \subseteq \operatorname{Im} S$ holds independently of the choice of B_{R} that assigns the installation bus for the RE farms. This implies that the (Q, R)-passivity of Σ is independent of the choice of the the installation bus for the RE farms. The passive power system is realized by the weighted sum of the frequency deviations given by (3.45).

As stated in Section 3.2, from (3.6), the RE farm output $P_{\mathrm{R}i}$ is decomposed into the disturbance effect w_i and the control input v_i, which is related to the fluctuating output and the battery output, respectively. From the definition of u in (3.39) and (3.6), we see that $u = -v + w$ holds in (3.47). Each controller $K_i, i \in \mathcal{V}_{\mathrm{R}}$, which satisfies the model set $\mathcal{P}(0, r_i)$ with $r_i > 0$, is connected to Σ in a step-by-step manner. A typical example of such a controller satisfying $K_i \in \mathcal{P}(0, r_i)$ is the PI controller given by (3.7). We construct a control system in which the input and output are w and y. The control system is represented by an iterative feedback system, and denoted by $\Sigma_{\mathrm{IFB}}(n), n \in \mathcal{I}$. In addition, the model set describing $\Sigma_{\mathrm{IFB}}(n)$ is denoted by $\mathcal{P}_{\mathrm{IFB}}(n)$. In $\Sigma_{\mathrm{IFB}}(n)$ and $\Sigma_{\mathrm{IFB}}(n)$, the symbol n denotes the number of the connected controllers. On the basis of the proposed analysis in Subsection 3.4.2, the performance improvement in the control system is theoretically guaranteed.

Remark 3. *In the actual operation of the power system, it is more desirable to improve the L_2-gain performance from w to the average of ω, rather than the weighted average of ω, denoted by y. For some cases, the average performance is gradually improved in addition to the improvement in Σ. Consider that $\Sigma \in \mathcal{P}(Q, 0)$ holds for some $Q > 0$. In addition, let $\mathcal{Y}_\Pi$ and $\bar{y}$ be the space spanned by the column vector of $\Pi^\top$ and the average frequency deviation, i.e., $\bar{y} := \mathbf{1}_{N_{\mathrm{G}}}\omega$, respectively. Suppose that $\mathbf{1}_{N_{\mathrm{G}}}$ is in $\mathcal{Y}_\Pi$. Then, $\bar{y}$ is described as*

$$\bar{y} = \alpha^\top \Pi \omega = \alpha^\top y, \tag{3.50}$$

where $\alpha := \operatorname{col}(\alpha_i)_{i \in \mathcal{V}_{\mathrm{R}}}$ for positive constants $\alpha_i, i \in \mathcal{V}_{\mathrm{R}}$. Using Lemma 1, we have

$$\sup_{w \in \mathbb{L}_2 \setminus \{0\}, \Sigma \in \mathcal{P}(Q,0)} \frac{\|\bar{y}\|_{L_2}}{\|w\|_{L_2}} \leq \|\alpha\|_{L_2} \sup_{\Sigma \in \mathcal{P}(Q,0)} \|\Sigma\|_{L_2} = \|\alpha\|_{L_2} \varepsilon(Q, 0) =: \bar{\varepsilon}.$$

From this inequality, $\bar{\varepsilon}$ evaluates the L_2-gain of the model set of the system with the input w and output $\bar{y}$. Note that $\varepsilon(Q, 0)$ decreases with the number of connected controllers in a step-by-step manner. Then, $\bar{\varepsilon}$ also gradually decreases. In this sense, the average frequency deviation is gradually suppressed.

3.5.3 Performance Improvement Analysis of Power System

Let us consider the power system Σ employing the IEEJ EAST 30-machine power model as stated in Subsection 3.2.1. From Lemma 4, $\Sigma \in \mathcal{P}(Q, 0)$ holds for $Q > 0$ satisfying $2S \geq BQB^\top$. Solving the linear matrix inequality $2S \geq BQB^\top$, we obtain an irreducible Q whose minimum eigenvector has no zero entries. Let us define $Q_{\mathrm{IFB}}(n)$ as

$$Q_{\mathrm{IFB}}(n) = Q + \sum_{i=1}^{n} r_i E_i.$$

Then, applying Theorem 3 and Proposition 2 into $\Sigma_{\mathrm{IFB}}(n)$, we show that $\mathcal{P}_{\mathrm{IFB}}(n) \subseteq \mathcal{P}(Q_{\mathrm{IFB}}(n), 0)$ holds. Accordingly, it is shown that for any n, $\gamma(\mathcal{P}_{\mathrm{IFB}}(n)) < \gamma(\mathcal{P}(Q, 0))$ holds. In this subsection, two experiments are performed to achieve the following two aims:

i) a gradual improvement of the actual L_2-gain performance of $\Sigma_{\mathrm{IFB}}(n)$ as well as the L_2-gain of the model set of $\Sigma_{\mathrm{IFB}}(n)$ at any step of the controller connection.

ii) less conservativeness in the L_2 gain evaluation of the model set of $\Sigma_{\mathrm{IFB}}(n)$ than in the previous works [36, 37, 51].

In the two experiments, the parameter r_i in the model set of each controller is randomly selected from [2 8]. Accordingly, the proportional gain k_{P_i} is given by $k_{\mathrm{P}_i} = r_i/2$. In addition, the integral gain k_{I_i} is selected as the same parameter as utilized in Section 3.2.

i) Let $\mathcal{S}(j\omega)$ and $\mathcal{S}_{\mathrm{IFB}}(n, j\omega)$ be the frequency transfer functions of Σ and $\Sigma_{\mathrm{IFB}}(n)$, respectively. Their maximum singular values are illustrated in Fig. 3.6. The performance indices to evaluate the L_2-gains of $\mathcal{P}(Q, 0)$ and $\mathcal{P}(Q_{\mathrm{IFB}}(n), 0)$ with $n = 1, 3, 6$, which are equivalent to $\varepsilon(Q, 0)$ and $\varepsilon(Q_{\mathrm{IFB}}(n), 0)$, are also illustrated in the figure. From the figure, we see that the value of $\varepsilon(Q_{\mathrm{IFB}}(n), 0)$ gradually decreases with the increase in the number of controllers. Correspondingly, the actual L_2-gain also gradually decreases. It should be emphasized here that the gradual improvement of the L_2-gain of the model set cannot be shown by the previous works such as those employing the passivity index [36, 37, 51] because $K_i \notin \mathcal{P}(0, r_i)$ holds and the index for K_i is zero.

ii) We further demonstrate the merit of the choice of irreducible Q. Let us focus on the final step of the controller connection, i.e., $n = N_{\mathrm{R}} = 6$. Then, the control system $\Sigma_{\mathrm{IFB}}(N_{\mathrm{R}})$ is represented by the feedback system composed of Σ and a decentralized controller K, which is described as

$$K : v = \left\{ \sum_{i \in \mathcal{V}_{\mathrm{R}}} E_i \otimes (k_{\mathrm{P}_i} + \frac{k_{\mathrm{I}_i}}{s}) \right\} y.$$

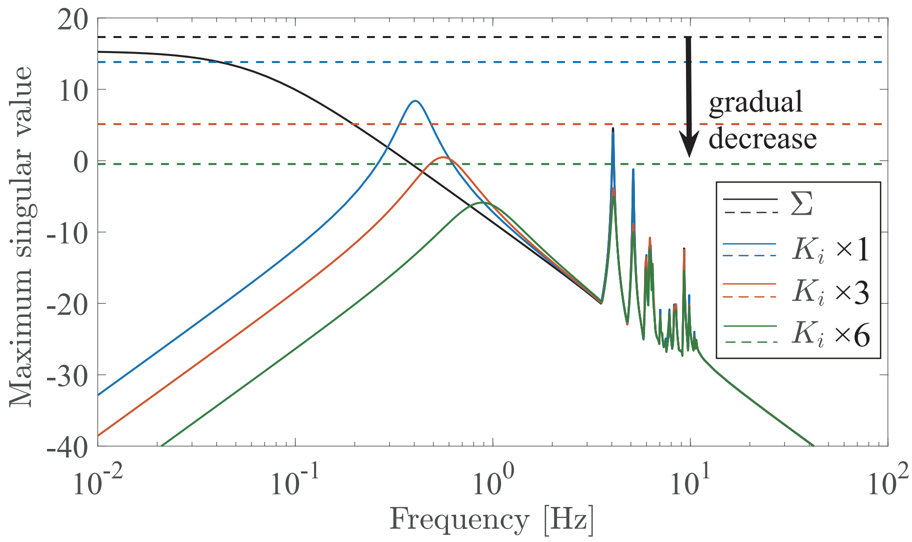

Figure 3.6: Maximum singular values of $\mathcal{S}(j\omega)$ and $\mathcal{S}_{\mathrm{IFB}}(n, j\omega)$ with $n = 1, 3, , 6$, which are represented by the solid lines. In addition, the dashed lines represent the performance indices to evaluate the L_2-gains of $\mathcal{P}(Q, 0)$ and $\mathcal{P}(Q_{\mathrm{IFB}}(n), 0)$ with $n = 1, 3, 6$.

This fact enables the previous works [36,37,51], in which passivity is characterized by scalar parameters, to also derive the performance index to evaluate the L_2-gain of $\mathcal{P}(Q_{\mathrm{IFB}}(N_{\mathrm{R}}), 0)$. This is because $K \in \mathcal{P}(0, r)$ holds for $r = \min\{r_1, r_2, \ldots r_{N_{\mathrm{R}}}\}$. In this experiment, we show that the proposed analysis provides a more accurate evaluation than the previous works. To this end, we compare the performance index to evaluate the L_2-gain of $\mathcal{P}(Q_{\mathrm{IFB}}(N_{\mathrm{R}}), 0)$ in the following two types of system description: Type 1) $\Sigma \in \mathcal{P}(Q, 0)$ for the irreducible Q and $K \in \mathcal{P}(0, \sum_i 2k_{P_i} E_i)$, and Type 2) $\Sigma \in \mathcal{P}(qI_{N_{\mathrm{R}}}, 0)$ for $q = \underline{\lambda}(Q)$ and $K \in \mathcal{P}(0, r)$ for $r = 2\min\{k_{P_1}, k_{P_2}, \ldots k_{P_{N_{\mathrm{R}}}}\}$. Figure 3.7 shows the maximum singular values of $\mathcal{S}_{\mathrm{IFB}}(N_{\mathrm{R}}, j\omega)$ and the performance index to evaluate the L_2-gain of the model set in the two types. From the figure, we see that the the performance index to evaluate L_2-gain in Type 1 provides a more accurate evaluation than that in Type 2. We conclude that the model-set description of Σ with the irreducible Q contributes to the accurate evaluation.

3.6 Summary of Chapter

In this chapter, the problem of the *performance improvement* was addressed for the feedback connection composed of two passive subsystems. In the problem, each subsystem was described by the model set that is characterized by two matrix parameters, as referred to as (Q, R)-passivity. We derived conditions on the parameters in the model sets

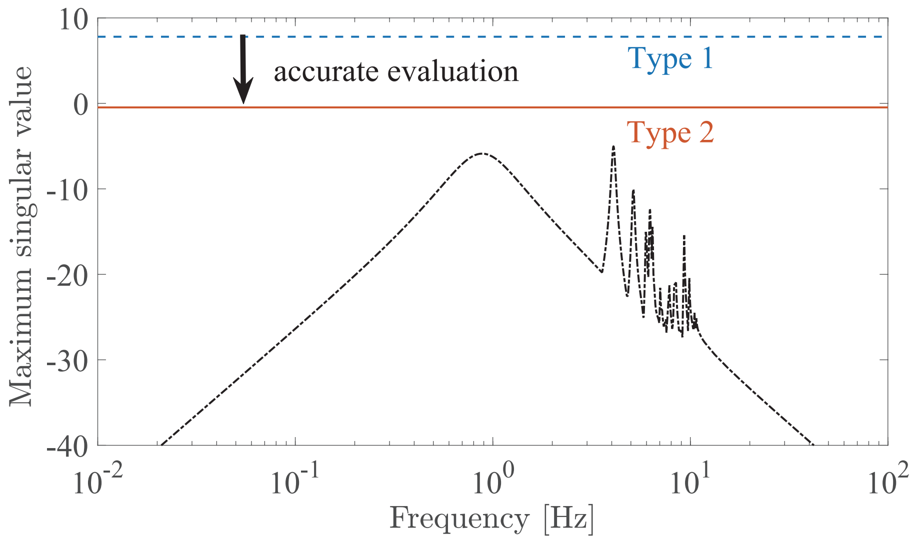

Figure 3.7: Comparison of the performance evaluation of the control system at final step of controller connection in two types. The actual maximum singular value of the control system is represented by the black chain line. In addition, the performance index to evaluate the L_2-gains of $\mathcal{P}(Q_{\mathrm{IFB}}(N_{\mathrm{R}}), 0)$ in Type 1 and 2 are represented by the blue dotted and red dotted lines, respectively. From the figure, we see that the performance index to evaluate the L_2-gain in Type 1 provides a more accurate evaluation than that in Type 2.

describing subsystems to achieve the performance improvement; the L_2-gain of the model set describing the feedback system is strictly reduced as compared to that describing the disconnected subsystem. The main contribution of this chapter is to formulate the performance improvement problem and provide a solution to the problem, which is stated in Theorem 1. Furthermore, the performance improvement analysis of the feedback system was extended to those of an iterative feedback system, which expresses a simplified class of an evolving system. Then, a condition or port selection for the baseline system to achieve the gradual performance improvement was derived. Using the model-set-based analysis, we demonstrated the frequency control performance analysis of the power system.

Chapter 4

Disturbance Sensitivity Analysis of Evolving Network Systems from Viewpoint of Network Structure

4.1 Introduction

In this chapter, we address the performance improvement problem of the homogeneous network system composed of identical clusters, each of which involves multiple nodes. The dynamics of each node is described by a dynamical system with a single integrater, which can express a general system including, e.g., a single integrator and a second-order oscillator employed in [5–12], as special cases. In particular, we give attention to *external* and *internal* network structure: the network structure among clusters and the network structure among nodes inside each cluster. The sensitivity of the network system to disturbances is analyzed from the viewpoints of the sparsity of external and internal networks as well as the increase of the number of nodes that represents the evolution of the network system. In this chapter, the disturbance sensitivity is evaluated by the $\mathcal{H}_\infty$-norm of the overall network system in which input and output ports are assigned at the interconnection links among clusters. The main contributions in this chapter are twofold. First, we numerically find that, as the number of nodes increases, the disturbance sensitivity of the network system tends to be reduced if the external network structure is sparse and the internal network structure is dense. Second, to support the finding observed from the numerical experiment, we further confine our attention to a network involving clusters each of which has identical nodes. Then, we theoretically prove that, in the limit of sufficiently large number of nodes, the minimum disturbance sensitivity level, evaluated by the maximum eigenvalue associated with the external network, is achieved if the internal network is the complete graph.

The remainder of this chapter is organized as follows. Section 4.2 presents the system description of homogeneous network systems. In Section 4.3, we conduct a numerical experiment to analyze the disturbance sensitivity of the homogeneous network system. To support the numerical analysis in Section 4.3, Section 4.4 provides a theoretical contribution. Finally, Section 3.6 concludes this chapter.

4.2 System Description

As illustrated in Fig. 4.1(a), we consider a homogeneous network system composed of N clusters. Each cluster $G_i, i \in \{1, 2, \ldots, N\}$ is described as a sub-network system involving n nodes, the jth node of which is described as a cascade system composed of an SISO dynamical system g_j and a single integrator. Let $g_j(s), j \in \{1, 2, \ldots, n\}$ be the transfer function of g_j and its state-space representation is given by

$$g_j(s) = \left[\begin{array}{c|c} A_j & B_j \\ \hline C_j & D_j \end{array}\right], \tag{4.1}$$

where $A_j \in \mathbb{R}^{m\times m}$, $B_j \in \mathbb{R}^{m\times 1}$, $C_j \in \mathbb{R}^{1\times m}$, $D_j \in \mathbb{R}$ are the coefficient matrices and m is the model order of g_j. In this chapter, $g_j(s)$ is assumed to be stable and the steady-state gain of $g_j(s)$ is assumed to be nonzero, i.e., $-C_jA_j^{-1}B_j + D_j \neq 0$ holds. In addition, the pairs of (A_j, B_j) and (A_j, C_j) are assumed to be controllable and observable, respectively. We define the input and output of the jth node as $\gamma_j \in \mathbb{R}$ and $\eta_j \in \mathbb{R}$, respectively; see Fig. 4.1(a). Then, the dynamics of the jth node is described by

$$\eta_j = \frac{g_j(s)}{s}\gamma_j. \tag{4.2}$$

In the following, we explain the reason why the dynamics of the jth node is described by (4.1). This is motivated by the fact that, in both cases of first- and second-order consensus network systems, the interconnection signal among nodes (agents) is given as the *integrated signal of the output* from each node. In fact, when we choose g_j as a static system or a first-order system, each node indeed describes a single integrator or a second-order oscillator, respectively. From this viewpoint, (4.2) can be regarded as a general description that involves the first- and second-order consensus network systems as special cases.

A part of contents and figures in this chapter cite from the following reference: ©2020 IEEE. Reprinted, with permission, from "Disturbance sensitivity analysis of evolving network systems from viewpoint of network structure, in Proceedings of *IEEE 58th Conference on Decision on Control*, 2019, accepted"

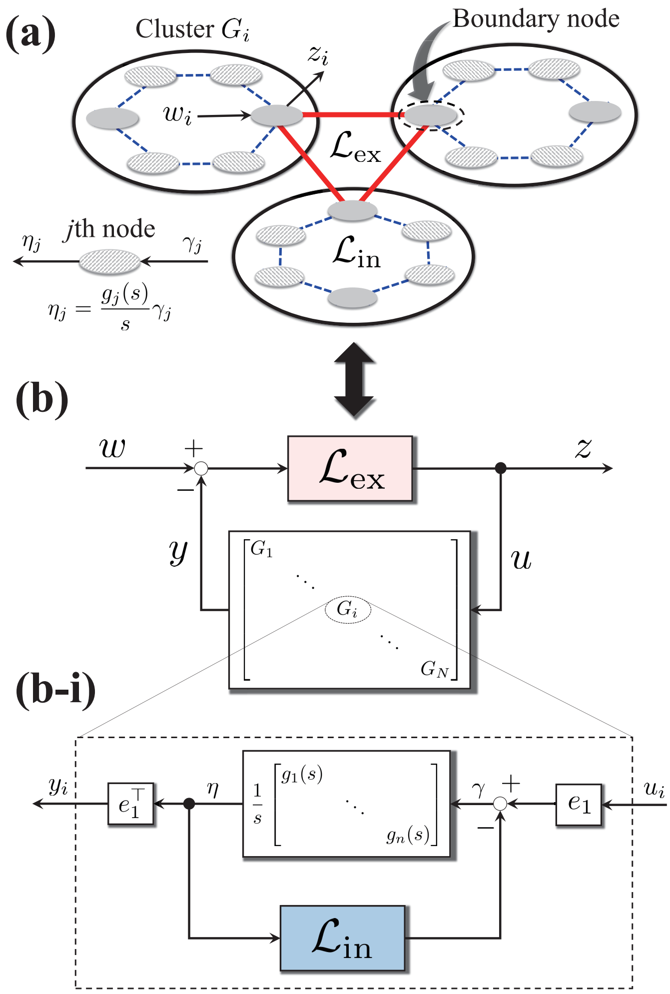

Figure 4.1: (a) An example of homogeneous network system. In the homogeneous network system, identical clusters are interconnected via the external network, the graph Laplacian matrix of which is given by $\mathcal{L}_{\text{ex}}$. In each cluster, nodes being not necessarily identical are interconnected via the internal network, the graph Laplacian matrix of which is given by $\mathcal{L}_{\text{in}}$. Then, each node is described by a dynamical system with a single integrator. In the homogeneous network system, input and output ports are assigned at interconnection links among boundary nodes, i.e., nodes connected to nodes in the other clusters. (b) Block diagram of the overall network system as illustrated in subfigure (a). (b-i) Block diagram of the ith cluster G_i.

For simplicity of analysis, we assume that only the one node inside the ith cluster is interconnected with the other clusters. The interconnection node is referred to as a boundary node. Without loss of generality, we can assign the boundary node at the first node. Let $u_i \in \mathbb{R}$ and $y_i \in \mathbb{R}$ be the input and output of the ith cluster. Then, the interconnection among nodes in (4.2) is given by

$$\gamma = e_1 u_i - \mathcal{L}_{\rm in}\eta, \quad y_i = e_1^\top \eta, \tag{4.3}$$

where $\mathcal{L}_{\rm in} \in \mathbb{R}^{n\times n}$ is the graph Laplacian matrix representing the internal network structure of G_i and $e_1 \in \mathbb{R}^n$ is the unit vector whose the only first entry is one, while the others are zero. In addition, $\gamma \in \mathbb{R}^n$ and $\eta \in \mathbb{R}^n$ are described as

$$\gamma := \mathrm{col}(\gamma_1, \gamma_2, \ldots, \gamma_n), \ \eta := \mathrm{col}(\eta_1, \eta_2, \ldots, \eta_n);$$

see Fig. 4.1(b-i). Note that

$$\frac{\mathrm{diag}(g_j(s))}{s} = \left[\begin{array}{cc|c} A & B & 0 \\ 0 & 0 & I_n \\ \hline C & D & 0 \end{array}\right], \tag{4.4}$$

where $A = \mathrm{diag}(A_j)$, $B = \mathrm{diag}(B_j)$, $C = \mathrm{diag}(C_j)$, and $D = \mathrm{diag}(D_j)$. Then, from (4.3) and (4.4), the dynamics of G_i in Fig. 4.1(b-i) is described by

$$G_i : \begin{cases} \dot{x}_i = E x_i + F u_i, \\ y_i = H x_i, \end{cases} \tag{4.5}$$

where $x_i \in \mathbb{R}^{n(m+1)}$ denotes the state of the ith cluster and the coefficient matrices E, F, and H are given by

$$E = \begin{bmatrix} A & B \\ -\mathcal{L}_{\rm in}C & -\mathcal{L}_{\rm in}D \end{bmatrix}, \ F = \begin{bmatrix} 0 \\ e_1 \end{bmatrix}, \ H = e_1^\top \begin{bmatrix} C & D \end{bmatrix}.$$

Letting $w \in \mathbb{R}^N$ and $z \in \mathbb{R}^N$ be the disturbance input and evaluation output of an ovarall network system. Then, the interconnection among clusters is described by

$$u = \mathcal{L}_{\rm ex}(w - y), \ z = u, \tag{4.6}$$

where $\mathcal{L}_{\rm ex} \in \mathbb{R}^{N\times N}$ is the graph Laplacian matrix representing the external network structure and $u \in \mathbb{R}^N$ and $y \in \mathbb{R}^N$ are given by

$$u := \mathrm{col}(u_1, u_2, \ldots, u_N), \quad y := \mathrm{col}(y_1, y_2, \ldots, y_N).$$

In this chapter, the disturbance input w is assumed to be additively injected at the output of boundary nodes in all clusters. In addition, the evaluation output z is assigned to the input of boundary nodes inside all clusters. A practical meaning of this choice of disturbance input and evaluation output ports is explained by an example of a power system composed of multiple generators. The power system can be basically described by the second-order consensus network system [56]. Then, w corresponds to the fault on the transmission lines among generators. In addition, z corresponds to the assessment of an effect on the propagation to the dynamics of all generators. Furthremore, the disturbance analysis of disturbance input and evaluation output ports given by (4.6) also plays an important role to the network control based on the retrofit control, see e.g., [39, 40].

We construct an overall network system by interconnecting N clusters G_i in (4.5) via the external network (4.6). Then, the overall network system is denoted by $G_{\rm NW}(n)$ and its input and output is w and z, respectively. In the network system, the number of nodes inside each cluster G_i is explicitly signed. The dynamics of $G_{\rm NW}(n)$ is described by

$$G_{\rm NW}(n):\begin{cases}\dot{x}=\mathcal{A}x+\mathcal{B}w,\\ z=\mathcal{C}x+\mathcal{D}w,\end{cases}\tag{4.7}$$

where $x := \mathrm{col}(x_1, x_2, \ldots, x_N)$ and

$$\begin{aligned}&\mathcal{A}=\{I_N\otimes E-(\mathcal{L}_{\rm ex}\otimes FH)\},\ \mathcal{B}=(\mathcal{L}_{\rm ex}\otimes F),\\ &\mathcal{C}=-(\mathcal{L}_{\rm ex}\otimes H),\ \mathcal{D}=\mathcal{L}_{\rm ex}.\end{aligned}$$

For simplicity of discussion, throughout this chapter, we give the following assumption.

Assumption 1. *The network system $G_{\rm NW}(n)$ is L_2-stable for all $n \in \{1, 2, \ldots\}$.*

It should be noted that if g_j in (4.1) is output-strictly passive [22, 23, 53], Assumption 1 holds.

Proposition 4. *Suppose that g_j in (4.1) is output-strictly passive, i.e., there exists $\delta > 0$ such that*

$$g_j(j\omega)+g_j^*(j\omega)\geq\delta|g_j(j\omega)|^2\tag{4.8}$$

for all $\omega \in \mathbb{R}$. Then, $G_{\rm NW}(n)$ is L_2-stable for all $n \in \{1, 2, \ldots\}$.

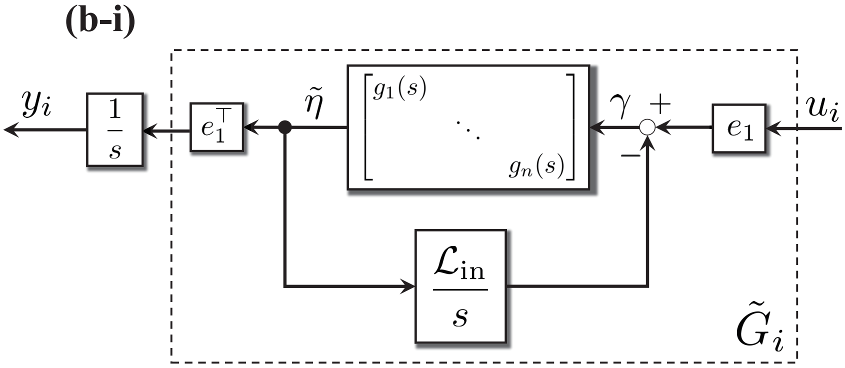

Figure 4.2: Equivalent block diagram of Fig. 4.1(b-i).

Proof. We first transform the block diagram of the overall network system $G_{\rm NW}(n)$ in Fig. 4.1(b). The block diagram of each cluster G_i in Fig. 4.1(b-i) is transformed into that in Fig. 4.2. In Fig. 4.2, let $\tilde{G}_i$ be defined as a feedback system composed of $\mathrm{diag}(g_j(s))$ and $\mathcal{L}_{\rm in}/s$. Then, the block diagram of $G_{\rm NW}(n)$ in Fig. 4.1(b) can be transformed into the upper block diagram in Fig. 4.3. Using the matrix inversion lemma [59], we have

$$\begin{aligned}
&G_{\rm NW}(n,s) = \mathcal{L}_{\rm ex}\left(I + \frac{\mathrm{diag}(\tilde{G}_i(s))}{s}\mathcal{L}_{\rm ex}\right)^{-1} \\
&= \mathcal{L}_{\rm ex} - \mathcal{L}_{\rm ex}\mathrm{diag}(\tilde{G}_i(s))\frac{\mathcal{L}_{\rm ex}}{s}\left(I + \mathrm{diag}(\tilde{G}_i(s))\frac{\mathcal{L}_{\rm ex}}{s}\right)^{-1} \\
&= \mathcal{L}_{\rm ex} - \mathcal{L}_{\rm ex}\left(I + \mathrm{diag}(\tilde{G}_i(s))\frac{\mathcal{L}_{\rm ex}}{s}\right)^{-1}\mathrm{diag}(\tilde{G}_i(s))\frac{\mathcal{L}_{\rm ex}}{s} \\
&:= \mathcal{L}_{\rm ex} - \mathcal{L}_{\rm ex}G_{\rm FB1}(s)\frac{\mathcal{L}_{\rm ex}}{s}.
\end{aligned}$$

This implies that the block diagram of $G_{\rm NW}(n)$ in Fig. 4.1(b) can be further transformed into the lower block diagram in Fig. 4.3. Let $G_{\rm FB2}$ be defined as the system with the input w and output $\hat{z}$ in the lower block diagram in Fig. 4.3. In the following, we show that $G_{\rm FB2}$ is L_2-stable for all n.

Suppose that $g_j, j \in \{1, 2, \ldots, n\}$ is output-strictly passive. Since $\mathcal{L}_{\rm ex}/s$ is passive, from the passivity theorem [22,23], $\tilde{G}_i$ is L_2-stable and output-strictly passive. Accordingly, we show that $G_{\rm FB1}$ is L_2-stable for all n. Let us consider a minimal realization of $\mathrm{diag}(\tilde{G}_i(s))$

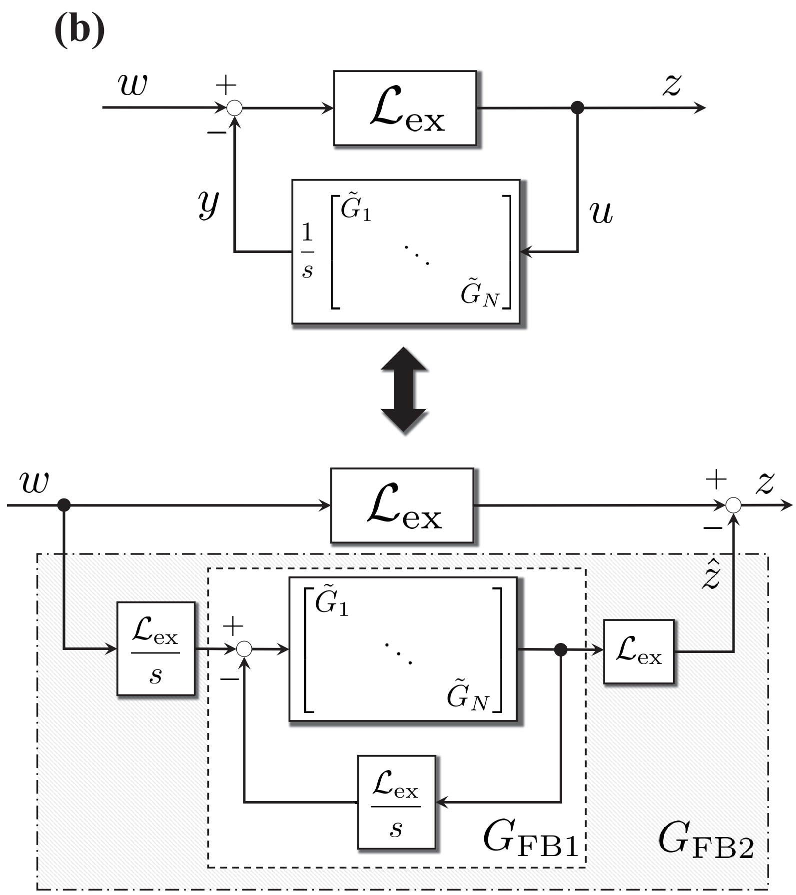

Figure 4.3: Equivalent block diagram of Fig. 4.1(b).

given by

$$\mathrm{diag}(\tilde{G}_i(s)) = \left[\begin{array}{c|c} \tilde{E} & \tilde{F} \\ \hline \tilde{H} & \tilde{D} \end{array}\right],$$

where $\tilde{E}$, $\tilde{F}$, $\tilde{H}$, and $\tilde{D}$ are coefficient matrices with appropriate dimensions. Then, $G_{\mathrm{FB1}}(s)$ can be described by

$$G_{\mathrm{FB1}}(s) = \left[\begin{array}{cc|c} \tilde{E} & -\tilde{F}\mathcal{L}_{\mathrm{ex}} & \tilde{F} \\ \tilde{H} & -\tilde{D}\mathcal{L}_{\mathrm{ex}} & \tilde{D} \\ \hline \tilde{H} & -\tilde{D}\mathcal{L}_{\mathrm{ex}} & \tilde{D} \end{array}\right].$$

It follows that

$$G_{\mathrm{FB2}}(s) = \mathcal{L}_{\mathrm{ex}} G_{\mathrm{FB1}}(s) \frac{\mathcal{L}_{\mathrm{ex}}}{s} = \left[\begin{array}{c|c} \mathcal{E} & \mathcal{F} \\ \hline \mathcal{H} & 0 \end{array}\right],$$

where

$$\mathcal{E} = \begin{bmatrix} \tilde{E} & -\tilde{F}\mathcal{L}_{\mathrm{ex}} & \tilde{F}\mathcal{L}_{\mathrm{ex}} \\ \tilde{H} & -\tilde{D}\mathcal{L}_{\mathrm{ex}} & \tilde{D}\mathcal{L}_{\mathrm{ex}} \\ 0 & 0 & 0 \end{bmatrix}, \ \mathcal{F} = \begin{bmatrix} 0 \\ 0 \\ I \end{bmatrix}, \mathcal{H} = \begin{bmatrix} \mathcal{L}_{\mathrm{ex}}\tilde{H} & -\mathcal{L}_{\mathrm{ex}}\tilde{D}\mathcal{L}_{\mathrm{ex}} & \mathcal{L}_{\mathrm{ex}}\tilde{D}\mathcal{L}_{\mathrm{ex}} \end{bmatrix}.$$

Note that we have

$$\mathrm{Ker}\,\mathcal{E} = \left\{ \begin{bmatrix} 0 & p & q \end{bmatrix}^\top \mid \mathcal{L}_{\mathrm{ex}}(p-q) = 0,\ p, q \in \mathbb{R}^N \right\},$$

which is equivalent to the eigenspace of $\mathcal{E}$ associated with the zero eigenvalue. Let $\mathcal{O}$ be the observability matrix of the pair $(\mathcal{E}, \mathcal{H})$. Then, it follows that $\mathrm{Ker}\,\mathcal{E}$ is a subset of $\mathrm{Ker}\,\mathcal{O}$, which is equivalent to the unobservable subspace of G_{FB2}. Since G_{FB1} is L_2-stable, we show that all modes associated with other than the zero eigenvalues of $\mathcal{E}$ is stable. This fact shows that G_{FB2} is L_2-stable for all n. Therefore, we show that $G_{\mathrm{NW}}(n)$ is L_2-stable for all n. □

As stated in Proposition 4, if the system g_j in (4.1) is output-strictly passive, the L_2-stability of $G_{\mathrm{NW}}(n)$ is always guaranteed independently of the number of nodes, i.e., Assumption 1 holds. Let us consider the case where g_j is given by a static system and a first-order system. Then, each node in (4.2) corresponds to a single integrator and a second-order oscillator, respectively. Note that both static system and first-order system are output-strictly passive. We see that a single integrator and a second-order oscillator is a special class of a cascade system composed of a single integrator and an output-strictly passive system.

In the following, we numerically and theoretically analyze the $\mathcal{H}_\infty$-norm of $G_{\mathrm{NW}}(n)$ regarding n as a parameter. In particular, from the viewpoint of the sparsity of the network, we find the external and internal network structures such that the $\mathcal{H}_\infty$-norm of $G_{\mathrm{NW}}(n)$ decreases. These analyses are the main contributions of this chapter.

4.3 Numerical Analysis: Relation between Disturbance Sensitivity and Sparsity of Network

In this section, numerical experiments are demonstrated in order to analyze the disturbance sensitivity of the homogeneous network system $G_{\mathrm{NW}}(n)$ in (4.7). The aim of this experiment is to observe the $\mathcal{H}_\infty$-norm of $G_{\mathrm{NW}}(n)$ from the following viewpoints: 1) the $\mathcal{H}_\infty$-norm of $G_{\mathrm{NW}}(n)$ as the number of nodes inside each cluster increases, 2) the relation between the $\mathcal{H}_\infty$-norm of $G_{\mathrm{NW}}(n)$ and the *sparsity* of the internal and external networks.

To demonstrate the experiment, we consider the network system $G_{\mathrm{NW}}(n)$ composed of 5 clusters, i.e, $N = 5$. In each cluster, the model order m was randomly selected from $\{1, 2, 3\}$. As stated in Proposition 4, Assumption 1 holds if g_j is output-strictly passive. On the basis of this fact, the model parameters A_j, B_j, C_j, and D_j were randomly determined such that g_j is output-strictly passive, which can be evaluated by, e.g., the Kalman-Yakubovich-Popov (KYP) lemma [60]. The internal and external network structures were assigned to the complete and path graph. This implies that there can be four combinations in the selection of the internal and external networks.

Figure 4.5 illustrates the value of n for each network pattern in Fig. 4.4 versus the $\mathcal{H}_\infty$-norm of $G_{\mathrm{NW}}(n)$. In Fig. 4.5, we first focus on the results of Patterns 1 and 2. The difference between Patterns 1 and 2 is just the internal network structure. As shown in Fig. 4.5, we see that in the case of Pattern 1, the $\mathcal{H}_\infty$-norm of $G_{\mathrm{NW}}(n)$ decreases with the increase of the value of n. On the other hand, in the case of Pattern 2, the $\mathcal{H}_\infty$-norm of $G_{\mathrm{NW}}(n)$ is invariant if n is greater than 2. This implies that if the internal network is given by the complete graph corresponding to the densest structure, the increase of the number of nodes inside each cluster plays an important role to reduce the disturbance sensitivity of $G_{\mathrm{NW}}(n)$.

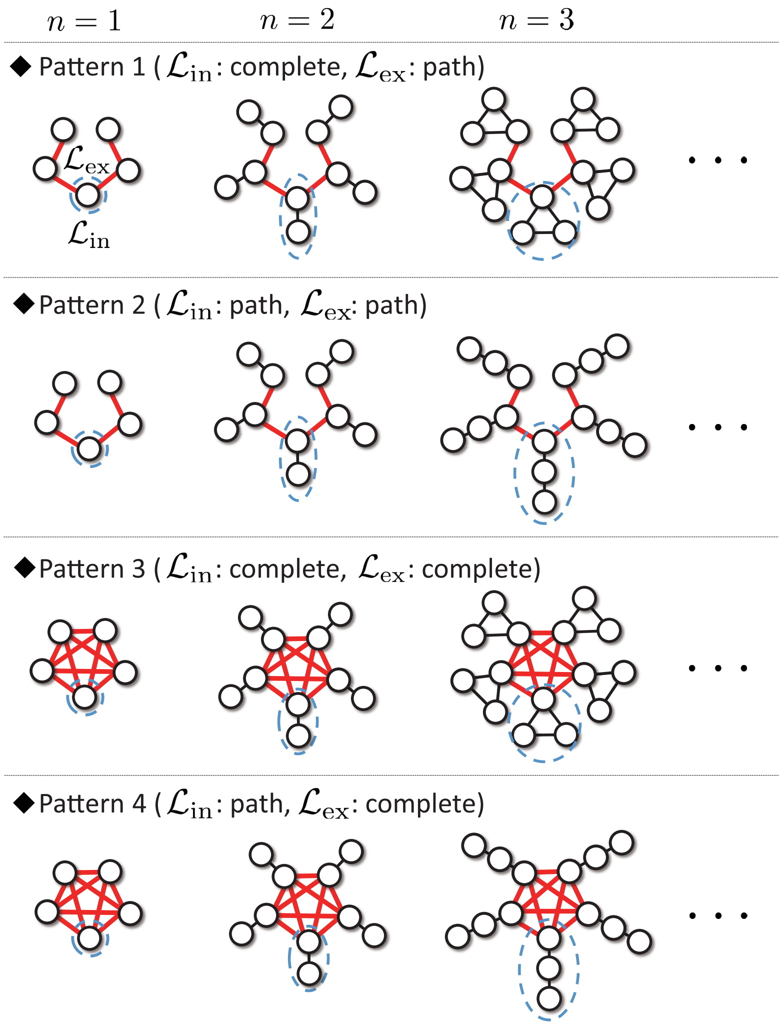

Figure 4.4: Overview of each node evolution for the homogeneous network system with $N = 5$ in four network structure patterns.

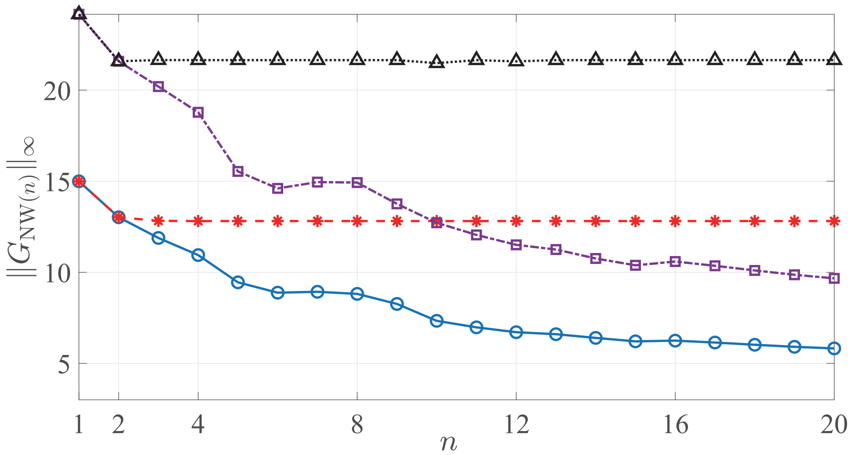

Figure 4.5: $\mathcal{H}_\infty$-norm of $G_{\mathrm{NW}}(n)$ versus the value of n in each pattern illustrated in Fig. 4.4

Next, we focus on the results of Patterns 1 and 3. The difference between Patterns 1 and 3 is just the external network structure. As shown in Fig. 4.5, we see that in the cases of both Patterns 1 and 3, the $\mathcal{H}_\infty$-norm of $G_{\mathrm{NW}}(n)$ decreases as the value of n increases, while the $\mathcal{H}_\infty$-norm of $G_{\mathrm{NW}}(n)$ in the case of Pattern 1 is smaller than that in the case of Pattern 3. This result suggests that the *sparse external network structure* contributes to reducing the disturbance sensitivity of $G_{\mathrm{NW}}(n)$. These observations conclude that the disturbance sensitivity of $G_{\mathrm{NW}}(n)$ tends to be reduced if the internal and external network structure are dense and sparse, respectively.

4.4 Main Result: Disturbance Sensitivity Analysis of Homogeneous Network systems

In this subsection, in order to theoretically support the finding observed from the experiment in Section 4.3, we analyze the disturbance sensitivity of homogeneous network systems in the limit of sufficiently large number of nodes. Then, we show that the minimum disturbance sensitivity level, evaluated by the maximum eigenvalue associated with the external network, is achieved if the internal network structure is given by the complete graph.

As a preliminary of the analysis, we consider decomposing the dynamics of the network system $G_{\mathrm{NW}}(n)$ into disjoint multi-dimensional modes. Let $G_{\mathrm{NW}}(n, s)$ be the transfer matrix of $G_{\mathrm{NW}}(n)$. The, we have

$$G_{\mathrm{NW}}(n,s) = \mathcal{C}(sI_{(m+1)nN} - \mathcal{A})^{-1}\mathcal{B} + \mathcal{D}.$$

Let us define an unitary matrix U such that $U^\top \mathcal{L}_{\mathrm{ex}} U = \Lambda$ holds where $\Lambda := \mathrm{diag}(\lambda_1, \lambda_2, \ldots, \lambda_N)$ with the eigenvalues λ_i of $\mathcal{L}_{\mathrm{ex}}$. Then, it follows that

$$\begin{aligned} G_{\mathrm{NW}}(n,s) &= U \left[\begin{array}{c|c} I_N \otimes E - \Lambda \otimes FH & \Lambda \otimes F \\ \hline -(\Lambda \otimes H) & \Lambda \end{array}\right] U^\top \\ &:= U \mathrm{diag}(\Sigma_1(n,s), \ldots, \Sigma_N(n,s)) U^\top, \end{aligned}$$

where $\Sigma_i(n,s), i \in \{1,2,\ldots,N\}$ is given by

$$\Sigma_i(n,s) = \left[\begin{array}{c|c} E - \lambda_i FH & \lambda_i F \\ \hline -\lambda_i H & \lambda_i \end{array}\right]. \tag{4.9}$$

It should be noted that, if E has one zero eigenvalue, the steady-state gain of $\Sigma_i(n,s)$ in (4.9) turns out to be zero as shown in the following lemma. The proof of this lemma is heavily related to the existence of the zero eigenvalue of E.

Lemma 5. *For any $\lambda_i \in \mathbb{C}$ and $n \in \{1,2,\ldots\}$, $\Sigma_i(n,s)$ in (4.9) satisfies*

$$\Sigma_i(n,0) = 0. \tag{4.10}$$

Proof. In the following, we show that (4.10) holds for both cases of $\lambda_i = 0$ and $\lambda_i \neq 0$. First, we suppose that $\lambda_i = 0$ holds. Then, it is straightforwardly shown that (4.10) holds because the coefficient matrices in terms of input and output are zero.

Next, we show that, for any nonzero λ_i, (4.10) holds. Letting $\Pi = \mathcal{L}_{\mathrm{in}} + \lambda_i e_1 e_1^\top$, we have

$$E - \lambda_i FH = \begin{bmatrix} A & B \\ -\Pi C & -\Pi D \end{bmatrix}.$$

Note that Π is nonsingular because $\mathrm{Ker}\,\mathcal{L}_{\mathrm{in}}$ and $\mathrm{Im}(e_1 e_1^\top)$ are not orthogonal. Using the fact that $-CA^{-1}B + D$ is nonsingular, we have

$$\begin{bmatrix} A & B \\ -\Pi C & -\Pi D \end{bmatrix}^{-1} = \begin{bmatrix} X_1 & A^{-1}B(-CA^{-1}B + D)^{-1}\Pi^{-1} \\ X_2 & -(-CA^{-1}B + D)^{-1}\Pi^{-1} \end{bmatrix},$$

where X_1 and X_2 are some nonsingular matrices with appropriate dimensions. Then, the steady-state gain of $\Sigma_i(n,s)$ can be reduced to

$$\begin{aligned}\Sigma_i(n,0) &= \lambda_i^2 H(E-\lambda_i FH)^{-1}F + \lambda_i \\ &= \lambda_i^2 e_1^\top \begin{bmatrix} C & D \end{bmatrix} \begin{bmatrix} A & B \\ -\Pi C & -\Pi D \end{bmatrix}^{-1} \begin{bmatrix} 0 \\ e_1 \end{bmatrix} + \lambda_i \\ &= -\lambda_i^2 e_1^\top \Pi^{-1} e_1 + \lambda_i.\end{aligned}$$

In the following, we show that $-\lambda_i^2 e_1^\top \Pi^{-1} e_1$ is equal to $-\lambda_i$. Note that $\mathrm{rank}(\Pi) = \mathrm{rank}(\mathcal{L}_{\mathrm{in}}) + 1$ holds because the graph Laplacian matrix $\mathcal{L}_{\mathrm{in}}$ has an eigenvector $\mathbf{1}_n$ corresponding to the zero eigenvalue. This condition enables us to apply Fact 6.4.2 in [59] to Π^{-1}. Let

$$P = I_n - \mathcal{L}_{\mathrm{in}}\mathcal{L}_{\mathrm{in}}^\dagger, \quad P^\dagger = I_n - \mathcal{L}_{\mathrm{in}}^\dagger \mathcal{L}_{\mathrm{in}},$$

where $\mathcal{L}_{\mathrm{in}}^\dagger$ is the generalized inverse of $\mathcal{L}_{\mathrm{in}}$. Noting that $P^\top P = P$ and $P^{\dagger\top} P^\dagger = P^\dagger$ hold, we have

$$\begin{aligned}\Pi^{-1} &= (\mathcal{L}_{\mathrm{in}} + \lambda_i e_1 e_1^\top)^{-1} \\ &= \mathcal{L}_{\mathrm{in}}^\dagger - \frac{\mathcal{L}_{\mathrm{in}}^\dagger e_1 e_1^\top P}{e_1^\top P e_1} - \frac{P^\dagger e_1 e_1^\top \mathcal{L}_{\mathrm{in}}^\dagger}{e_1^\top P^\dagger e_1} + (1+\lambda_i e_1^\top \mathcal{L}_{\mathrm{in}} e_1)\frac{P^\dagger e_1 e_1^\top P}{(\lambda_i e_1^\top P e_1)(e_1^\top P^\dagger e_1)}.\end{aligned}$$

This fact shows that $-\lambda_i^2 e_1^\top \Pi^{-1} e_1 = -\lambda_i$ holds. Then, we show that (4.10) holds. This completes the proof of Lemma 5. □

Lemma 5 shows that the steady-state gain of $\Sigma_i(n,s)$ is completely zero. In connection with the fact, we see that the steady-state gain of $G_{\mathrm{NW}}(n,s)$ is also completely zero. This implies that the network system completely suppresses an effect of the steady state disturbance. In order to analyze the $\mathcal{H}_\infty$-norm of $G_{\mathrm{NW}}(n)$ in the limit of a sufficiently large number of nodes, we provide the following lemma in terms of the eigenvalue and eigenvector associated with complete graph.

Lemma 6. *Suppose that $\mathcal{L}_{\mathrm{in}}$ is the graph Laplacian matrix that represents the complete graph, i.e., $\mathcal{L}_{\mathrm{in}} = nI_n - \mathbf{1}_n\mathbf{1}_n^\top$. Let ξ_j be the eigenvalue of $\Pi = \mathcal{L}_{\mathrm{in}} + \lambda_i e_1 e_1^\top$. Then, for any nonzero λ_i, the eigenvalue ξ_j satisfies*

$$\xi_j \in \{n+\mu(n), n, \varepsilon(n)\}, \tag{4.11}$$

where $\mu(n) \in \mathbb{R}$ and $\varepsilon(n) \in \mathbb{R}$ are constant values such that $\mu(n) + \varepsilon(n) = \lambda_i$ holds, and the algebraic multiplicity of $n + \mu(n)$ and $\varepsilon(n)$ are 1 and that of n is $n-2$. Furthermore, let $v_{\varepsilon(n)}$ be the eigenvector associated with $\varepsilon(n)$. Then, it holds that

$$\lim_{n\to\infty} \mu(n) = \lambda_i, \ \lim_{n\to\infty} \varepsilon(n) = 0, \ \lim_{n\to\infty} v_{\varepsilon(n)} = \frac{\mathbf{1}_n}{\sqrt{n}}. \tag{4.12}$$

Proof. First, we show that (4.11) holds. Suppose that $\mathcal{L}_{\text{in}} = nI_n - \mathbf{1}_n\mathbf{1}_n^\top$. Then, the eigenvalues of $\mathcal{L}_{\text{in}}$ are classified into n with the algebraic multiplicity $n-1$ and 0 with the algebraic multiplicity 1. In addition, the eigenspace of $\mathcal{L}_{\text{in}}$ associated with the eigenvalue n is described by $\overline{\operatorname{Ker}\mathcal{L}_{\text{in}}}$ in which $\operatorname{Ker}\mathcal{L}_{\text{in}}$ is equivalent to $\operatorname{span}(\mathbf{1}_n)$. Note that the eigenspace of Π associated with the eigenvalue n is described by $\overline{\operatorname{Ker}\mathcal{L}_{\text{in}}} \cap \operatorname{Ker} e_1e_1^\top$. From De Morgan's laws [55], we have

$$\begin{aligned}
\overline{\operatorname{Ker}\mathcal{L}_{\text{in}}} \cap \operatorname{Ker} e_1e_1^\top &= \overline{\operatorname{Ker}\mathcal{L}_{\text{in}} \cup \operatorname{Im} e_1e_1^\top} \\
&= \overline{\operatorname{Im}\mathbf{1}_n \cup \operatorname{Im}(e_1e_1^\top)} \\
&\subseteq \mathbb{R}^{n-2}.
\end{aligned}$$

We see that the eigenvalue n of Π has the algebraic multiplicity $n-2$. Since $\operatorname{trace}(\Pi) = n(n-1) + \lambda_i$ holds, the remaining two eigenvalues of Π are given by $n + \mu(n)$ and $\varepsilon(n)$ such that $\mu(n) + \varepsilon(n) = \lambda_i$ holds. Thus, we show that (4.11) holds.

Next, we show that (4.12) holds. Note that $\varepsilon(n)$ is the perturbed eigenvalue corresponding to the zero eigenvalue of $\mathcal{L}_{\text{in}}$. Then, the Taylor series expansions of $\varepsilon(n)$ and $v_{\varepsilon(n)}$ are given by

$$\begin{aligned}
\varepsilon(n) &= 0 + \left[\left.\frac{d\varepsilon(n)}{d\lambda_i}\right|_{\lambda_i=0} \right] \lambda_i + O(\lambda_i^2), \\
v_{\varepsilon(n)} &= \frac{\mathbf{1}_n}{\sqrt{n}} + \left[\left.\frac{dv_{\varepsilon(n)}}{d\lambda_i}\right|_{\lambda_i=0} \right] \lambda_i + O(\lambda_i^2).
\end{aligned}$$

On the basis of the proof of Proposition 10.3 in [61], the first derivatives are calculated as

$$\left.\frac{d\varepsilon(n)}{d\lambda_i}\right|_{\lambda_i=0} = \frac{1}{n}, \ \left.\frac{dv_{\varepsilon(n)}}{d\lambda_i}\right|_{\lambda_i=0} = \sum_{k=1}^{n-1} \frac{v_k^\top e_1e_1^\top \mathbf{1}_n}{n\sqrt{n}} v_k,$$

where v_k is a basis of the eigenspace associated with the eigenvalue n of $\mathcal{L}_{\text{in}}$ and $\|v_k\| = 1$ holds. Although the detailed derivation of more than 2nd-order terms of λ_i, denoted by $O(\lambda_i^2)$, are omitted in this thesis, $O(\lambda_i^2)$ can be written by $O(1/n^2)$. It follows that

$$\lim_{n\to\infty} \varepsilon(n) = 0, \ \lim_{n\to\infty} v_{\varepsilon(n)} = \frac{\mathbf{1}_n}{\sqrt{n}}.$$

Since $\mu(n) + \varepsilon(n)$ holds, we show that (4.12) holds. These completes the proof of Lemma 6 $\square$

Lemma 6 provides some properties of eigenvalue and eigenvector of Π that represents the perturbated complete graph. In particular, it provides eigenvalue and eigenvector of Π in the limit of sufficiently large number of n. As stated in Lemma 6, the eigenvalue of Π is classified into $n + \mu(n)$, n, and $\varepsilon(n)$. Then, it is shown that $\mu(n)$ goes to the perturbation λ_i as $n \to \infty$, while $\varepsilon(n)$ goes to zero as $n \to \infty$. This implies that one eigenvalue of Π goes to zero as $n \to \infty$, while the other eigenvalues go to infinity as $n \to \infty$. Furthermore, the eigenvalue corresponding to ε goes to $\mathbf{1}_n/\sqrt{n}$ as $n \to \infty$. This facts plays an important role to analyze the the $\mathcal{H}_\infty$-norm of $G_{\rm NW}(n)$ in the limit of a sufficiently large number of nodes. On the basis of Lemmas 5 and 6, we provide the $\mathcal{H}_\infty$-norm of $G_{\rm NW}(n)$ as $n \to \infty$.

Theorem 4. *Let Assumption 1 hold. In addition, suppose that $A_j = \bar{A}$, $B_j = \bar{B}$, $C_j = \bar{C}$, and $D_j = \bar{D}$ in (4.1) hold for some $\bar{A}$, $\bar{B}$, $\bar{C}$, and $\bar{D}$, and $\mathcal{L}_{\rm in} = nI_n - \mathbf{1}_n\mathbf{1}_n^\top$. Then, for any $\bar{A}$, $\bar{B}$, $\bar{C}$, and $\bar{D}$, we have*

$$\lim_{n\to\infty} \|G_{\rm NW}(n)\|_\infty = \bar{\lambda}(\mathcal{L}_{\rm ex}). \tag{4.13}$$

Proof. Suppose that $A_j = \bar{A}$, $B_j = \bar{B}$, $C_j = \bar{C}$, $D_j = \bar{D}$ hold for some $\bar{A}$, $\bar{B}$, $\bar{C}$, and $\bar{D}$. In connection with the fact, it is shown that $A = I_n \otimes \bar{A}$, $B = I_n \otimes \bar{B}$, $C = I_n \otimes \bar{C}$, and $D = I_n \otimes \bar{D}$ hold. As a preliminary of the proof of Theorem 4, let us decompose the dynamics of $\Sigma_i(n,s)$ in (4.9) into disjoint modes in a similar manner to the derivation of $\Sigma_i(n,s)$. We define V as an unitary matrix such that $V^\top \Pi V = \Xi$ holds where $\Xi = \mathrm{diag}(\xi_1, \xi_2, \ldots, \xi_n)$ with the eigenvalue of ξ_j. Then, it is shown that

$$\begin{bmatrix} V^\top \otimes I_m & 0 \\ 0 & V^\top \end{bmatrix} (E - \lambda_i FH) \begin{bmatrix} V \otimes I_m & 0 \\ 0 & V \end{bmatrix} = \begin{bmatrix} I_n \otimes \bar{A} & I_n \otimes \bar{B} \\ -\Xi \otimes \bar{C} & \Xi \otimes \bar{D} \end{bmatrix}.$$

On the basis of this fact, we obtain $\Sigma_i(n,s)$ as

$$\begin{aligned} \Sigma_i(n,s) &= -\lambda_i^2 H(sI_{(m+1)n} - E + \lambda_i FH)^{-1}F + \lambda_i \\ &= -\lambda_i^2 e_1^\top V \mathrm{diag}(\sigma(s,\xi_1), \ldots, \sigma(s,\xi_n)) V^\top e_1 + \lambda_i, \end{aligned} \tag{4.14}$$

where a state space realization of $\sigma(s,\xi_j)$ is given by

$$\sigma(s,\xi_j) = \left[\begin{array}{cc|c} \bar{A} & \bar{B} & 0 \\ -\xi_j\bar{C} & -\xi_j\bar{D} & 1 \\ \hline \bar{C} & \bar{D} & 0 \end{array}\right].$$

The above mode decomposition shows that (4.13) holds. Let us consider that the realization of $g_j(s)$ in (4.1) is given by the controllable canonical form, i.e., $\bar{A}$, $\bar{B}$, and $\bar{C}$ are given by

$$\bar{A} = \begin{bmatrix} 0 & 1 & \cdots & 0 \\ \vdots & \vdots & \ddots & \vdots \\ 0 & 0 & \cdots & 1 \\ -\alpha_0 & -\alpha_1 & \cdots & -\alpha_{m-1} \end{bmatrix},\quad \bar{B} = \begin{bmatrix} 0 \\ \vdots \\ 0 \\ 1 \end{bmatrix},\quad \bar{C} = \begin{bmatrix} \beta_0 & \beta_1 & \cdots & \beta_{m-1} \end{bmatrix},$$

where $\alpha_k, k \in \{1,2,\dots,m-1\}$ and $\beta_k, k \in \{1,2,\dots,m-1\}$ are the model parameters of $g_j(s)$. Then, $\sigma(s,\xi_j)$ can be written as

$$\sigma(s,\xi_j) = \frac{f(s)}{h(s,\xi_j)},$$

where $f(s)$ and $h(s,\xi_j)$ are given by

$$f(s) := \bar{D}s^m + (\beta_{m-1} + \alpha_{m-1}\bar{D})s^{m-1} + \cdots + (\beta_1 + \alpha_1\bar{D})s + \beta_0 + \alpha_0\bar{D} \tag{4.15}$$

$$\begin{aligned} h(s,\xi_j) := {} & s^{m+1} + (\alpha_{m-1} + \xi_j\bar{D})s^m + (\alpha_{m-2} + \xi_j\beta_{m-1} + \xi_j\alpha_{m-1}\bar{D})s^{m-1} + \cdots \\ & + (\alpha_0 + \xi_j\beta_1 + \xi_j\alpha_1\bar{D})s + \xi_j\beta_0 + \xi_j\alpha_0\bar{D}. \end{aligned} \tag{4.16}$$

Suppose that $\mathcal{L}_{\mathrm{in}} = nI_n - \mathbf{1}_n\mathbf{1}_n^\top$ holds. This implies that the internal network structure of each node is given by the complete graph. Recall that $\Pi = \mathcal{L}_{\mathrm{in}} + \lambda_i e_1 e_1^\top$. Then, as stated in Lemma 6, the eigenvalues of Π satisfy $\xi_j \in \{n+\mu(n), n, \varepsilon(n)\}$ such that $\mu(n)+\varepsilon(n) = \lambda_i$ holds where the algebraic multiplicity of $n+\mu(n)$ and $\varepsilon(n)$ are 1 and that of n is $n-2$. In addition, the limits of $\mu(n)$ and $\varepsilon(n)$ are given by

$$\lim_{n\to\infty} \mu(n) = \lambda_i, \quad \lim_{n\to\infty} \varepsilon(n) = 0.$$

This implies that one eigenvalue of Π goes to zero as $n \to \infty$, while the other eigenvalues go to infinity as $n \to \infty$. Accordingly, we see that, in $\Sigma_i(n,s)$, the high frequency modes corresponding to the eigenvalues n and $n+\mu(n)$ decay, while only the low frequency mode corresponding to the eigenvalue $\varepsilon(n)$ remains as $n \to \infty$. Furthermore, as stated in Lemma 6, the eigenvector corresponding to $\varepsilon(n)$ goes to $\mathbf{1}_n/\sqrt{n}$ as $n \to \infty$. Since $\Sigma_i(n, s)$ is given by the linear combination of $\sigma_j(s)$, $\Sigma_i(n, s)$ as $n \to \infty$ can be reduced to

$$\lim_{n\to\infty} \Sigma_i(n, s) = \lim_{n\to\infty} \frac{\lambda_i}{n}\sigma(s, \varepsilon(n)) = \lim_{n\to\infty} -\frac{\lambda_i^2 f(s)}{nh(s, \varepsilon(n))} + \lambda_i, \tag{4.17}$$

where $f(s)$ and $h(s)$ are given by (4.15) and (4.16). Note that, as shown in Lemma 5, for any $\lambda_i \in \mathbb{C}$, $\Sigma_i(n, 0) = 0$ holds. Then, if $n \to \infty$ $\Sigma_i(n, s)$, it holds that

$$\lim_{n\to\infty} \Sigma_i(n, 0) = \lim_{n\to\infty} \lambda_i \left(1 - \frac{\lambda_i}{n\varepsilon(n)}\right) = 0.$$

This implies that $n\varepsilon(n)$ must go to λ_i as $n \to \infty$ if $\Sigma_i(n, 0) = 0$ holds. On the basis of this fact, we have

$$\lim_{n\to\infty} \Sigma_i(n, s) = \begin{cases} \lambda_i, & s \neq 0 \\ 0, & s = 0. \end{cases} \tag{4.18}$$

Noting that $U\Lambda U^\top = \mathcal{L}_{\rm ex}$ holds, it is shown that (4.13) holds. This completes the proof of Theorem 4. □

Theorem 4 shows the fact on the external and internal network structures that the disturbance sensitivity of $G_{\rm NW}(n)$, in which each cluster has identical node, is reduced. This is our theoretical contribution. In the following, we remark that the value of $\bar{\lambda}(\mathcal{L}_{\rm ex})$ corresponds to the minimum disturbance sensitivity level of $G_{\rm NW}(n)$. This is because the network system $G_{\rm NW}(n)$ with any internal and external networks satisfies

$$\|G_{\rm NW}(n)\|_\infty \geq \bar{\lambda}(\mathcal{L}_{\rm ex}) \tag{4.19}$$

for all $n \in \{1, 2, \ldots\}$. The inequality (4.19) is derived because for any internal and external networks $G_{\rm NW}(n, s)$ satisfies

$$\lim_{s\to\infty} G_{\rm NW}(n, s) = \mathcal{L}_{\rm ex}$$

for all n. Suppose that $\mathcal{L}_{\rm in} = nI_n - \mathbf{1}_n\mathbf{1}_n^\top$ holds; in other words the internal network structure in all clusters are given by the complete graph corresponding to the densest internal network structure. As stated in Theorem 4, as the value of n becomes sufficiently large, the $\mathcal{H}_\infty$-norm of $G_{\rm NW}(n)$ can be guaranteed to converge to $\bar{\lambda}(\mathcal{L}_{\rm ex})$. Noting that $\bar{\lambda}(\mathcal{L}_{\rm ex})$ is equivalent to the lower bound in (4.19), it is shown that in the limit of sufficiently large number of nodes, the minimum disturbance sensitivity level is acquired in the network system $G_{\mathrm{NW}}(n)$ if the internal network structure is the densest. Furthermore, it should be emphasized here that if the external network structure is sparser, the value of $\bar{\lambda}(\mathcal{L}_{\mathrm{ex}})$ tends to be smaller. This implies that the *sparsity* of the external network contributes to reduce the disturbance sensitivity of $G_{\mathrm{NW}}(n)$ as $n \to \infty$.

Theorem 4 is actually compatible with the numerical experiment shown in Fig. 4.5. Let us focus on Patterns 1 and 3 in which the internal network structure is given by the complete graph. Although the analysis of the network system involving identical nodes is provided by Theorem 4, we see that the $\mathcal{H}_\infty$-norm of $G_{\mathrm{NW}}(n)$ in both patterns tends to converge to $\bar{\lambda}(\mathcal{L}_{\mathrm{ex}})$ with the increase of the value of n. Through the numerical experiment in Section 4.3 and the theoretical result in this section, we conclude that the *sparse external network* and the *dense internal network* play an important role to reduce the disturbance sensitivity of the evolving network system.

4.5 Chapter Summary

This chapter addressed the disturbance sensitivity analysis of the homogeneous network systems, where identical clusters of nodes being not necessarily identical are interconnected. In particular, we described each node as a dynamical system with a single integrator, which can express a general system including, e.g., a single integrator and a second-order oscillator. In this analysis, we focused on external and internal network structures: the network structure among clusters and the network structure among nodes inside each cluster. Then, the disturbance sensitivity of the overall network system, in which input and output ports are assigned at interconnection links among boundary nodes, was analyzed from viewpoint of the sparsity of the external and internal networks as well as the number of nodes. First, we numerically demonstrated that, as the number of nodes increases, the $\mathcal{H}_\infty$-norm of the network system tends to decrease if the external network structure is sparse and the internal network structure is dense. Furthermore, to support this finding, we assumed that all nodes inside each cluster are identical. Then, we have theoretically proven that in the limit of sufficiently large number of nodes, the minimum disturbance sensitivity level, evaluated by the maximum eigenvalue associated with the external network, is achieved if the internal network is the complete graph.

Chapter 5

Conclusion

5.1 Summary of Results

This thesis summarized the line of work on the performance analysis of the evolving dynamical network system toward the establishment of its design strategy. Summaries in individual chapters are given as follows:

First, in Chapter 2, the localizability index is proposed for the feedback system to which the retrofit controller is implemented. The localizability index was defined as the $\mathcal{H}_\infty$-norm of the error system between the control system with and without the environment. The proposed index measured how much the control performance of the local system is kept invariant with respect to the variation of the environment. Then, it was shown that the estimation of the localizability index requires only the model parameters of the local system in the sense of the upper bound. By using an example of PV-integrated power systems, the retrofit controller placement problem was analyzed from the proposed localizability index. In Chapter 3 and 4, the performance improvement problem for the evolving network system was addressed. In Chapter 3, we considered the feedback system composed of two passive subsystems that is characterized by two matrix parameters, as referred to as (Q, R)-passivity. In particular, we derived conditions on the parameters in the model sets describing subsystems to achieve the performance improvement; the L_2-gain of the model set describing the feedback system is strictly less than that describing the disconnected subsystem. Furthermore, the performance improvement analysis of the feedback system was extended to those of an iterative feedback system, which is constructed by repetitive feedback connection of multiple subsystems with a decentralized structure. Then, we derived a condition or port selection in the baseline system such that the performance improvement is achieved. Finally, the frequency control performance analysis of the power system was illustrated based on the model-set-based analysis, in particular, the viewpoint of the port-Hamiltonian systems. Chapter 4 addressed the disturbance sensitivity analysis of the homogeneous network systems, which is composed of identical clusters of nodes being not necessarily identical are interconnected. In particular, each node description was employed as a cascade system composed of dynamical component and a single integrator. This description was general in the sense of expressing a single integrator and a second-order oscillator. First, it was numerically shown, as the number of nodes increases, the disturbance sensitivity of the network system, evaluated by $\mathcal{H}_\infty$-norm, tends to reduce if the external and internal network structures are sparse and dense, respectively. Furthermore, we assumed that all nodes inside each cluster are identical. Then, we have proven that the internal network contributes to achieve the minimum disturbance sensitivity level, evaluated by the maximum eigenvalue associated with the external network, in the limit of sufficiently large number of nodes.

5.2 Future Works

In Chapter 2, the model of the environment in the network system is not assumed to be available for the estimation of the localizability. However, under the assumption of obtaining the interconnection signal from the environment, the model of the environment can be identified by using some closed-loop identification techniques. On possible way to reduce the conservativeness in the evaluation is that the identified environment model is utilized for the estimation of the localizability. In addition, the performance improvement problem for the homogeneous network system addressed in Chapter 4 will be extended to that for heterogeneous network systems. In particular, the idea of the model-based-analysis addressed in Chapter 3 will be integrated into the discussion in Chapter 4. Finally, a design strategy will be developed for evolving network systems based on the analysis in this thesis.

Bibliography

[1] F. Dörfler and F. Bullo, "Synchronization in complex networks of phase oscillators: A survey," *Automatica*, vol. 50, no. 6, pp. 1539–1564, 2014.

[2] C. Favaretto, A. Cenedese, and F. Pasqualetti, "Cluster synchronization in networks of kuramoto oscillators," *IFAC-PapersOnLine*, vol. 50, no. 1, pp. 2433–2438, 2017.

[3] T. Menara, G. Baggio, D. S. Bassett, and F. Pasqualetti, "Exact and approximate stability conditions for cluster synchronization of kuramoto oscillators," in *Procindigs of American Control Conference*, 2019.

[4] T. Menara, G. Baggio, D. Bassett, and F. Pasqualetti, "Stability conditions for cluster synchronization in networks of heterogeneous kuramoto oscillators," *IEEE Transactions on Control of Network Systems*, 2019.

[5] D. Zelazo, S. Schuler, and F. Allgöwer, "Performance and design of cycles in consensus networks," *Systems & Control Letters*, vol. 62, no. 1, pp. 85–96, 2013.

[6] M. Siami and N. Motee, "Fundamental limits and tradeoffs on disturbance propagation in linear dynamical networks," *IEEE Transactions on Automatic Control*, vol. 61, no. 12, pp. 4055–4062, 2016.

[7] Y. Ghaedsharaf and N. Motee, "Performance improvement in time-delay linear consensus networks," in *Proceedings of 2017 American Control Conference*, 2017, pp. 2345–2350.

[8] M. Siami and N. Motee, "Growing linear dynamical networks endowed by spectral systemic performance measures," *IEEE Transactions on Automatic Control*, vol. 63, no. 7, pp. 2091–2106, 2017.

[9] M. Pirani, H. Sandberg, and K. H. Johansson, "A graph-theoretic approach to the h_∞ performance of dynamical systems on directed and undirected networks," *arXiv preprint arXiv:1804.10483*, 2018.

[10] H. G. Oral, E. Mallada, and D. F. Gayme, “Performance of first and second order linear networked systems over digraphs,” in *Proceedings of 56th IEEE Conference on Decision and Control*, 2017, pp. 1688–1694.

[11] T. W. Grunberg and D. F. Gayme, “Performance measures for linear oscillator networks over arbitrary graphs,” *IEEE Transactions on Control of Network Systems*, vol. 5, no. 1, pp. 456–468, 2016.

[12] C. Ji and D. F. Gayme, “Collision potential analysis in first and second order integrator networks over strongly connected digraphs,” in *Proceedings of 57th IEEE Conference on Decision and Control*, 2018, pp. 1251–1257.

[13] X.-L. Tan and M. Ikeda, “Decentralized stabilization for expanding construction of large-scale systems,” *IEEE Transactions on Automatic Control*, vol. 35, no. 6, pp. 644–651, 1990.

[14] C. Langbort, R. S. Chandra, and R. D’Andrea, “Distributed control design for systems interconnected over an arbitrary graph,” *IEEE Transactions on Automatic Control*, vol. 49, no. 9, pp. 1502–1519, 2004.

[15] M. Rotkowitz and S. Lall, “A characterization of convex problems in decentralized control,” *IEEE transactions on Automatic Control*, vol. 50, no. 12, pp. 1984–1996, 2005.

[16] L. Lessard and S. Lall, “Convexity of decentralized controller synthesis,” *IEEE Transactions on Automatic Control*, vol. 61, no. 10, pp. 3122–3127, 2015.

[17] C. Langbort and J.-C. Delvenne, “Distributed design methods for linear quadratic control and their limitations,” *IEEE Transactions on Automatic Control*, vol. 55, no. 9, pp. 2085–2093, 2010.

[18] Z. Qu and M. A. Simaan, “Modularized design for cooperative control and plug-and-play operation of networked heterogeneous systems,” *Automatica*, vol. 50, no. 9, pp. 2405–2414, 2014.

[19] J. Stoustrup, “Plug & play control: Control technology towards new challenges,” *European Journal of Control*, vol. 15, no. 3, pp. 311–330, 2009.

[20] B. Goodwine and P. Antsaklis, “Multi-agent compositional stability exploiting system symmetries,” *Automatica*, vol. 49, no. 11, pp. 3158–3166, 2013.

[21] D. Hill and P. Moylan, "Connections between finite-gain and asymptotic stability," *IEEE Transactions on Automatic Control*, vol. 25, no. 5, pp. 931–936, 1980.

[22] B. Brogliato, R. Lozano, B. Maschke, and O. Egeland, *Dissipative Systems Analysis and Control: Theory and Applications.* Springer, 2006.

[23] A. J. van der Schaft, *L2-gain and passivity techniques in nonlinear control.* Springer, 2000, vol. 2.

[24] G. Zames, "On the input-output stability of time-varying nonlinear feedback systems part I: Conditions derived using concepts of loop gain, conicity, and positivity," *IEEE Transactions on Automatic Control*, vol. 11, no. 2, pp. 228–238, 1966.

[25] H. Bai, M. Arcak, and J. Wen, *Cooperative Control Design: A Systematic, Passivity-Based Approach.* Springer Science & Business Media, 2011.

[26] M. Bürger, D. Zelazo, and F. Allgöwer, "Duality and network theory in passivity-based cooperative control," *Automatica*, vol. 50, no. 8, pp. 2051–2061, 2014.

[27] T. Hatanaka, N. Chopra, M. Fujita, and M. W. Spong, *Passivity-Based Control and Estimation in Networked Robotics.* Springer, 2015.

[28] M. Arcak, C. Meissen, and A. Packard, *Networks of Dissipative Systems: Compositional Certification of Stability, Performance, and Safety.* Springer, 2016.

[29] J.-L. Wang, H.-N. Wu, and T. Huang, "Passivity-based synchronization of a class of complex dynamical networks with time-varying delay," *Automatica*, vol. 56, pp. 105–112, 2015.

[30] S. Fiaz, D. Zonetti, R. Ortega, J. M. Scherpen, and A. van Der Schaft, "A port-hamiltonian approach to power network modeling and analysis," *European Journal of Control*, vol. 19, no. 6, pp. 477–485, 2013.

[31] T. Stegink, C. De Persis, and A. van der Schaft, "A unifying energy-based approach to stability of power grids with market dynamics," *IEEE Transactions on Automatic Control*, vol. 62, no. 6, pp. 2612–2622, 2017.

[32] J. P. Koeln and A. G. Alleyne, "Stability of decentralized model predictive control of graph-based power flow systems via passivity," *Automatica*, vol. 82, pp. 29–34, 2017.

[33] M. Arcak and E. Sontag, "A passivity-based stability criterion for a class of biochemical reaction networks," *Mathematical Biosciences and Engineering*, vol. 5, no. 1, p. 1, 2008.

[34] F. Farokhi and K. H. Johansson, "Optimal control design under limited model information for discrete-time linear systems with stochastically-varying parameters," *IEEE Transactions on Automatic Control*, vol. 60, no. 3, pp. 684–699, 2014.

[35] A. S. R. Ferreira, C. Meissen, M. Arcak, and A. Packard, "Symmetry reduction for performance certification of interconnected systems," *IEEE Transactions on Control of Network Systems*, vol. 5, no. 1, pp. 525–535, 2016.

[36] F. Zhu, M. Xia, and P. J. Antsaklis, "On passivity analysis and passivation of event-triggered feedback systems using passivity indices," *IEEE Transactions on Automatic Control*, vol. 62, no. 3, pp. 1397–1402, 2017.

[37] M. Xia, P. J. Antsaklis, V. Gupta, and F. Zhu, "Passivity and dissipativity analysis of a system and its approximation," *IEEE Transactions on Automatic Control*, vol. 62, no. 2, pp. 620–635, 2017.

[38] K. Zhou, J. C. Doyle, and K. Glover, *Robust and Optimal Control.* New Jersey: Prentice hall, 1996.

[39] T. Ishizaki, T. Sadamoto, J.-i. Imura, H. Sandberg, and K. H. Johansson, "Retrofit control: Localization of controller design and implementation," *Automatica*, vol. 95, pp. 336–346, 2018.

[40] H. Sasahara, T. Ishizaki, M. Inoue, T. Sadamoto, and J.-i. Irnura, "A characterization of all retrofit controllers," in *Proceedings of 2018 Annual American Control Conference*, 2018, pp. 6194–6199.

[41] M. Inoue, T. Ishizaki, and M. Suzumura, "Parametrization of all retrofit controllers toward open control-systems," in *Proceedings of 2018 European Control Conference*, 2018, pp. 715–720.

[42] N. Sakamoto and M. Suzuki, "γ-passive system and its phase property and synthesis," *IEEE Transactions on Automatic Control*, vol. 41, no. 6, pp. 859–865, 1996.

[43] M. Araki and B. Kondo, "Stability and transient behavior of composite nonlinear systems," *IEEE Transactions on Automatic Control*, vol. 17, no. 4, pp. 537–541, 1972.

[44] K. Zhou, J. C. Doyle, K. Glover *et al.*, *Robust and optimal control.* Prentice hall New Jersey, 1996, vol. 40.

[45] The Institute of Electrical Engineers of Japan, "Japanese power system model", [online]. Available: http://denki.iee.jp/pes/?page_id=141.

[46] K. Urata, T. Ishizaki, and J.-i. Imura, “Quantitative analysis of controller design localizability,” *Transactions of the Society of Instrument and Control Engineers (in japanese)*, vol. 55, pp. 148–155, 2019.

[47] T. Ishizaki, T. Kawaguchi, H. Sasahara, and J.-i. Imura, “Retrofit control with approximate environment modeling,” *Automatica*, vol. 107, pp. 442–453, 2019.

[48] M. Mesbahi and M. Egerstedt, *Graph Theoretic Methods in Multiagent Networks.* Princeton University Press, 2010.

[49] P. M. Anderson and M. Mirheydar, “A low-order system frequency response model,” *IEEE Transactions on Power Systems*, vol. 5, no. 3, pp. 720–729, 1990.

[50] K. Urata, M. Inoue, T. Ishizaki, and J.-i. Imura, “Performance improvement via iterative connection of passive systems,” *IEEE Transactions on Automatic Control*, 2019.

[51] K. Urata and M. Inoue, “Dissipativity reinforcement in feedback systems and its application to expanding power systems,” *International Journal of Robust and Nonlinear Control*, vol. 28, no. 5, pp. 1528–1546, 2018.

[52] P. J. Moylan and D. J. Hill, “Stability criteria for large-scale systems,” *IEEE Transactions on Automatic Control*, vol. 23, no. 2, pp. 143–149, 1978.

[53] J. C. Willems, “Dissipative dynamical systems part I: General theory,” *Archive for Rational Mechanics and Analysis*, vol. 45, no. 5, pp. 321–351, 1972.

[54] R. Horn and C. Johnson, *Matrix Analysis.* Cambridge University Press, 2012.

[55] R. A. Horn and C. R. Johnson, *Matrix analysis.* Cambridge university press, 2012.

[56] P. Kundur, N. J. Balu, and M. G. Lauby, *Power system stability and control.* McGraw-hill New York, 1994, vol. 7.

[57] J. Machowski, J. Bialek, and J. R. Bumby, *Power System Dynamics and Stability.* John Wiley & Sons, 1997.

[58] A. van der Schaft and D. Jeltsema, “Port-hamiltonian systems theory: An introductory overview,” *Foundations and Trends® in Systems and Control*, vol. 1, no. 2-3, pp. 173–378, 2014.

[59] D. S. Bernstein, *Matrix mathematics: theory, facts, and formulas.* Princeton university press, 2009.

[60] A. Rantzer, “On the Kalman-Yakubovich-Popov lemma,” *Systems & Control Letters*, vol. 28, no. 1, pp. 7–10, 1996.

[61] A. C. Antoulas, *Approximation of large-scale dynamical systems.* Siam, 2005, vol. 6.

Acknowledgement

First and foremost, I sincerely appreciate my supervisor Jun-ichi Imura for his guidance and support and for providing me this precious study opportunity as a doctoral student in his laboratory. Although he had to deal with many tasks as vice-president in Tokyo Tech., he took his valuable time out from his busy schedule to give me insightful suggestions and proper advices. Thanks to such suggestions and advices, I deeply feel that I achieve some results that have been accepted by many high-level international conferences and journals. I truly appreciate that he gave me the opportunity to pursue my own study and other projects.

I am deeply grateful to Assistant Professor Takayuki Ishizaki for his enthusiastic support, proper advice, and invaluable discussion that not only reveal the weakpoint in my study but make my research of great achievement. If he didn't give me supports and widespread advices from mathematics to scientific writing and presentation, I don't get any results during the PhD course.

I am also very grateful to Associate Professor Tomohisa Hayakawa, Professor Kazuhiro Nakadai, Associate Professor Kenji Nishida, Assistant Professor Katsutoshi Itoyama in Tokyo Institute of Technology, Assistant Professor Tomonori Sadamoto in the University of Electro-Communications, and Dr. Takahiro Kawaguchi in Tokyo Institute of Technology for valuable comments and suggestions. I am indebted to my previous supervisors, Professor Shuichi Adachi in Keio University and Assistant Professor Masaki Inoue in Keio University who taught me the fundamentals of scientific research. In particular, Dr. Masaki cared about the progress of my research and gave me many encourage comments and proper advices for my research when we met at a international conference. If he hadn't recommend to proceed to the PhD course at another university, I wouldn't be I am today.

I am very grateful to Noriko Sugimoto and Akiho Setoguchi for their support of my life in the laboratory. Moreover, I thank current and past members of Imura, Hayakawa and Nakadai laboratories for many great discussions and all the good times. Finally, I sincerely appreciate my family for supporting my daily life.

Kengo Urata, Tokyo Institute of Technology

List of Publications

Journal Papers

- Kengo Urata, Masaki Inoue, Takayuki Ishizaki, Jun-ichi Imura, "Performance improvement via iterative connection of passive systems," *IEEE Transactions on Automatic Control,* 2020. (accepted for publication)

- Kengo Urata, Takayuki Ishizaki, Jun-ichi Imura, "Quantitative analysis of controller design localizability," *Transactions of the Society of Instrument and Control Engineers,* Vol. 55, No. 3, pp. 148–155, 2018. (in Japanese)

Refereed International Conference Papers

- Kengo Urata, Takayuki Ishizaki, Jun-ichi, Imura, "Disturbance sensitivity analysis of evolving network systems from viewpoint of network structure," in *Proceedings of IEEE Conference on Decision and Control,* 2019.

- Kengo Urata, Takayuki Ishizaki, Jun-ichi Imura, "Quantitative analysis of controller design localizability," in *Proceedings of The 23rd International Symposium on Mathematical Theory of Network and Systems*, 2018.